Idealistic views of an elementary particle reaction

$$e^+ + e^- \to Z^0 \to q\bar{q}$$
$$(+\,\text{hadronization})$$

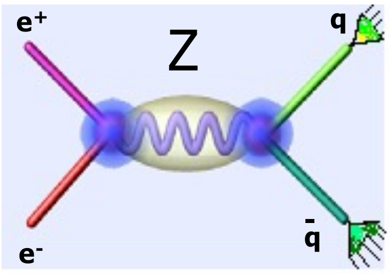

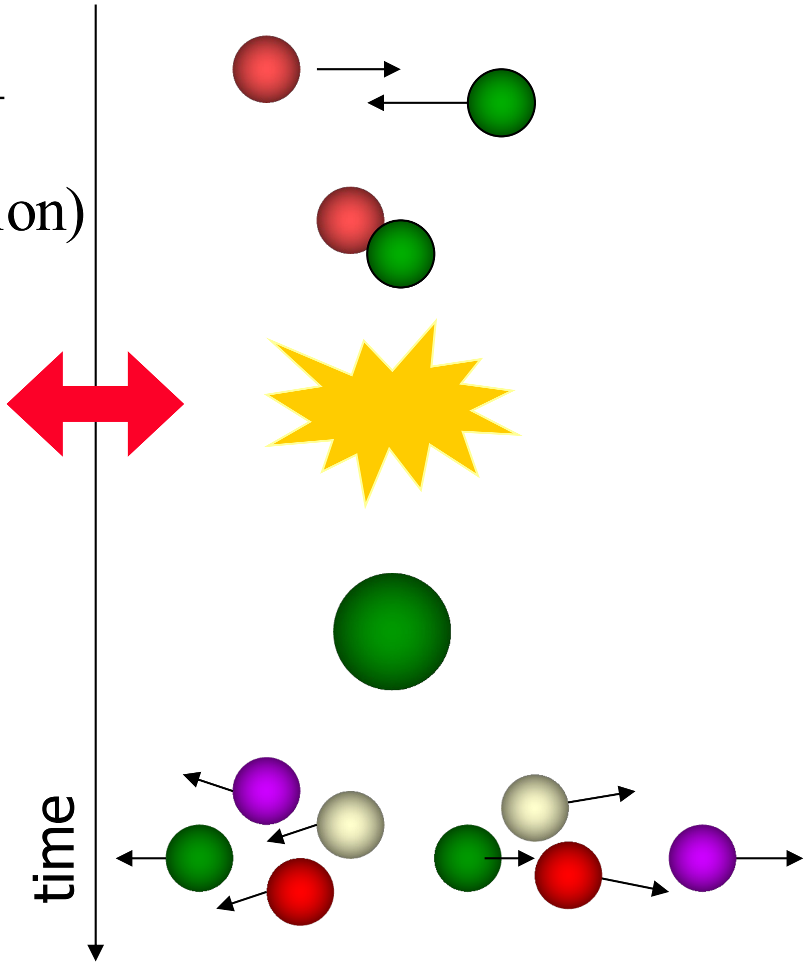

- Usually ‘detect’ only end products, not reaction itself.
- To reconstruct reaction mechanism & involved particles, need maximum info on end products (particle type, momentum, energy, trajectory ...)

Interactions of different types of particles with matter

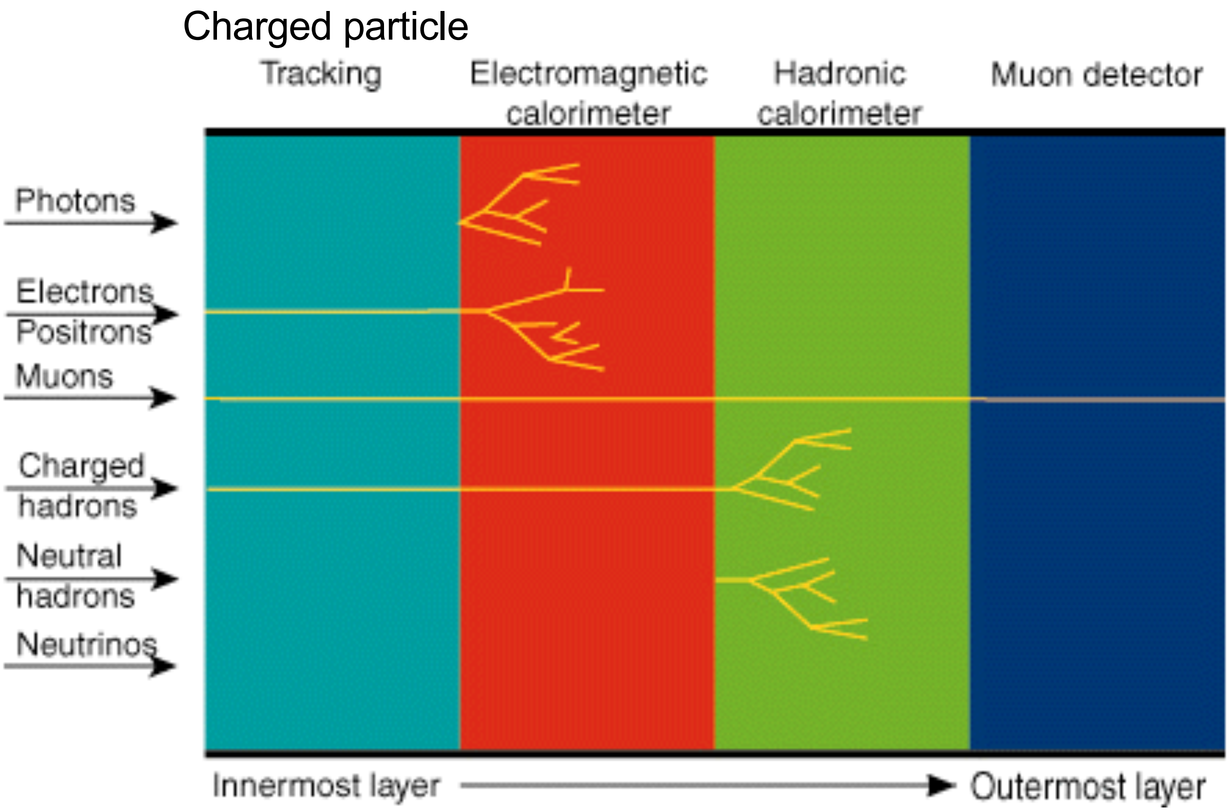

Interaction of radiation with matter basis of detectors

- Detector type presentation will be purpose driven e.g. what they are supposed to do (track particles, measure energy, identify particle type …) !
- Particle interaction with matter explained along side to better connect detector ⇔ particle interaction.

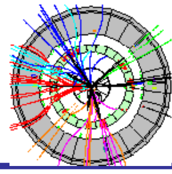

Detector type selection based on several points:

- primary purpose of detector (measure, count, veto)?
- what needs to be measured & with which resolution (point, time, energy, momentum, velocity, etc ...)?
- what radiation/particle rate has detector to sustain?
- what is an acceptable dead time? dead-time-less?
- does environment limit choice somehow (limited space?, magnetic field?, restriction on output size?, etc…)
- area to be covered ↔ cost ?

Table 35.1: Typical resolutions and deadtimes of common charged particle detectors. Revised November 2021.

Detector Type	Intrinsinc Spatial Resolution (rms)	Time Resolution	Dead Time
Resistive plate chamber	50μm	50–1000 ps*	10 ns†
Liquid argon TPC	0.5–1 mm‡	0.01-1 μs§	—¶
Scintillation tracker	$\sim$100 μm	100 ps/n$^{\Vert}$	10 ns
Bubble chamber	10–150 μm	1 ms	50 ms**
Wire chambers (proportional and drift chambers)	50–100 μm	5–10 ns††	2–200 ns‡‡
Micro-pattern gas detect.	30–40 μm	5–10 ns††	2–200 ns‡‡
Silicon strips/pixels	$\lesssim 10\,\mu$m§§	few ns¶¶ ‡‡	$\lesssim$ 50 ns‡‡

*LHC: $\sim$ 2mm gap, $\sim$1ns. HL-LHC: $\sim$ 1mm gap, $\sim$350ps. Timing RPC: $\sim$50ps
†Limited by amplifier and discriminator bandwidth, usually around 100MHz
‡Detector geometry dependent
§Using the scintillation signal
¶No deadtime for medium
$^{\Vert}$$n$ = index of refraction.
**Multiple pulsing time.
††For fast particles
‡‡Depending/limited by the amplifying electronics [8]
§§Depending on electrode pitch, best values around 2–4 μm have been achieved
¶¶Resolutions $<$ 100 ps are reached in dedicated pixel developments

pdg.lbl.gov

Evolution of detector techniques due to :

- performant production techniques & electronics
- current mode operation (measuring average current) ⇒ pulse mode operation (current ⇒voltage)

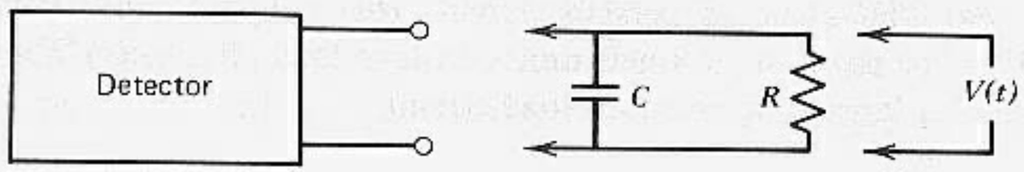

Knoll

If time constant (= RC) of circuit large then voltage ∝ charge ⇒ measurement of the deposited energy

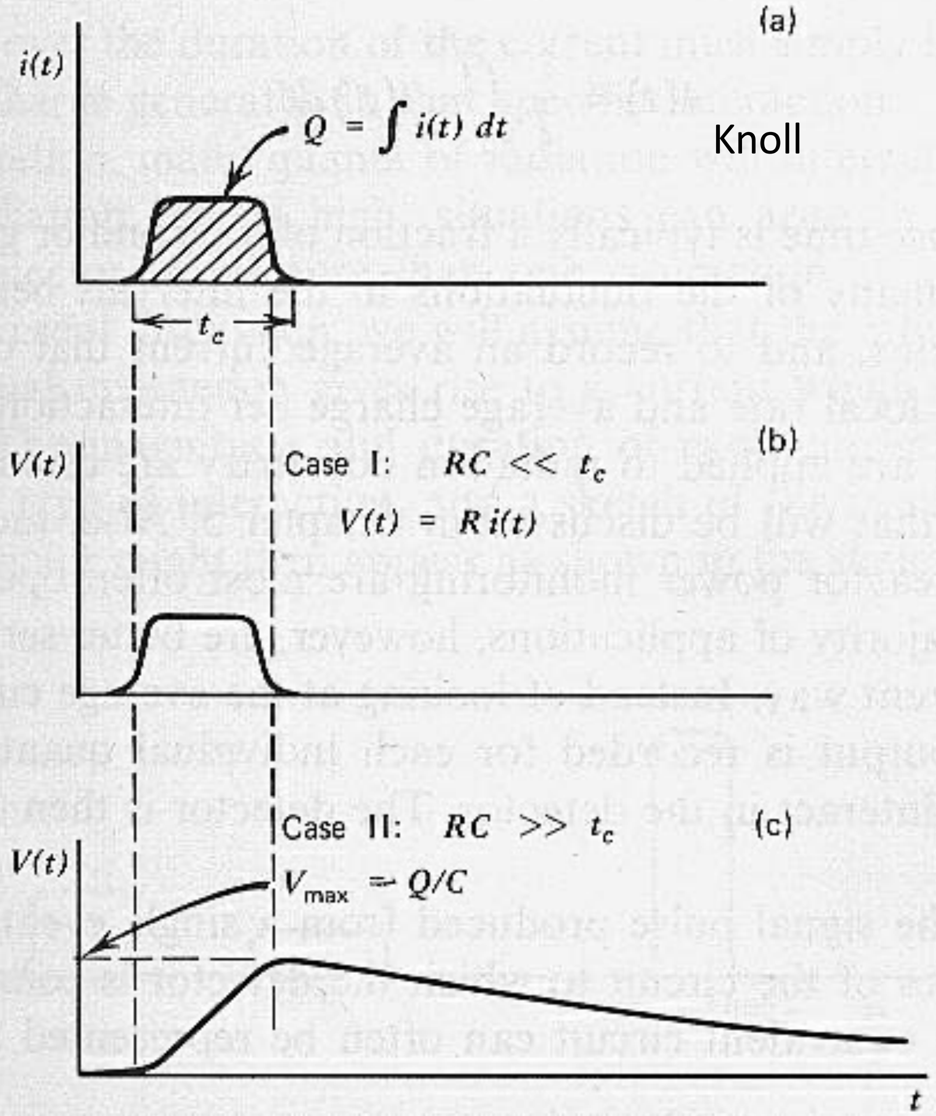

Knoll

Position sensitive detectors &tracking

Momentum measurement

Multiple scattering

Bethe-Bloch formula / Landau tails

Ionization of gases

Wire chambers

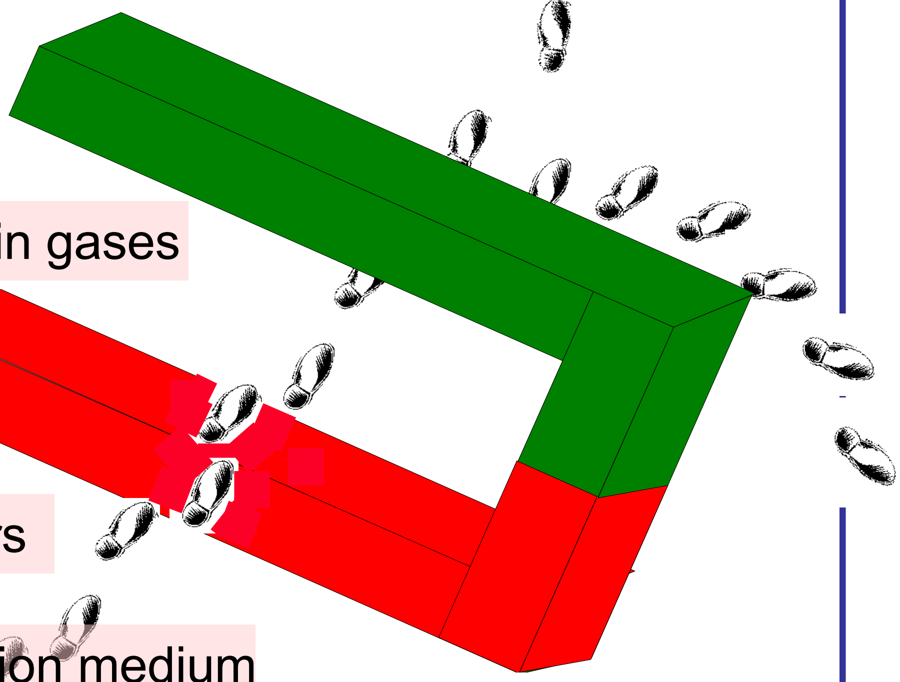

Drift and diffusion in gases

Drift chambers

Micro gas detectors

Silicon as a detection medium

Silicon detectors strips/pixels

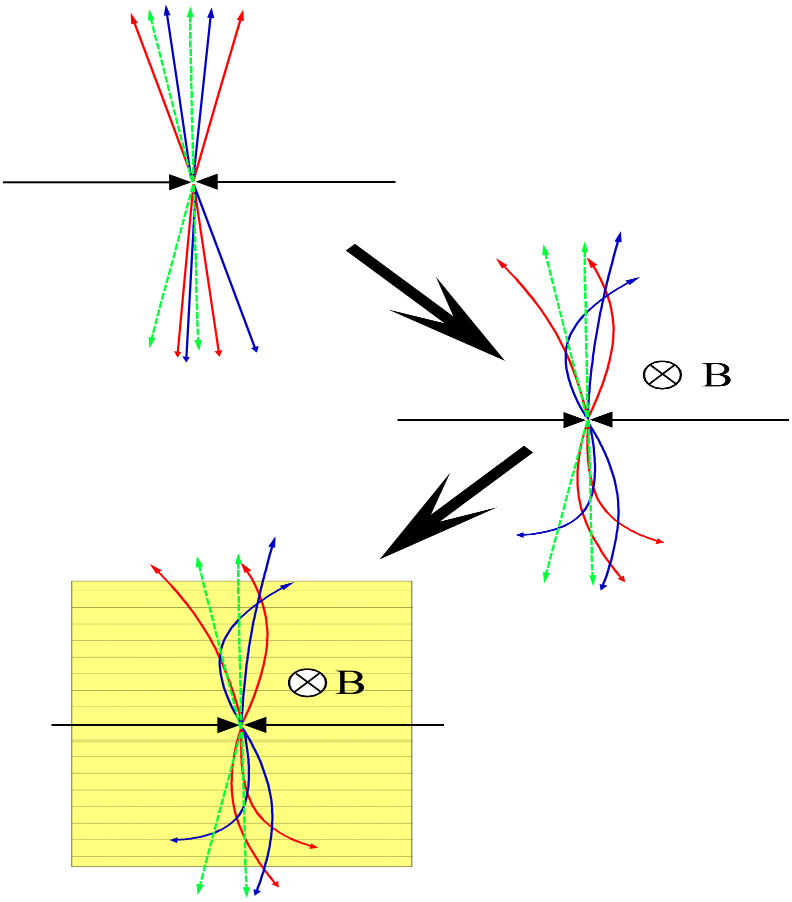

(E.Wilson)

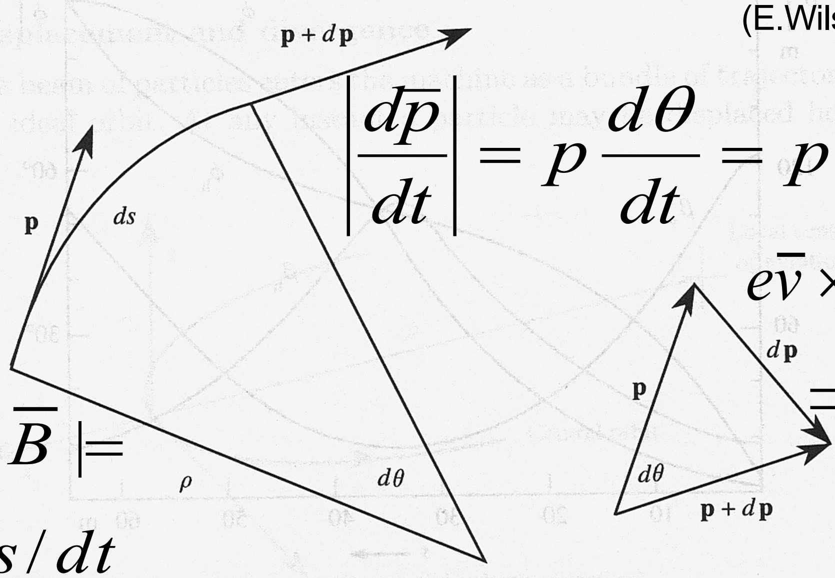

$$\left|\frac{d\bar{p}}{dt}\right| = p\,\frac{d\theta}{dt} = p/\rho\cdot ds/dt$$

$$e\bar{v}\times\bar{B} = d\bar{p}/dt$$

$$\Rightarrow B\rho = p/e$$

$$e\,|\bar{v}\times\bar{B}\,| = eB\cdot ds/dt$$

Fig. 2.3 Vector diagram showing differential changes in momentum for a particle trajectory.

magnetic rigidity: $B\rho[\mathrm{Tm}] = 3.3356\,p[\mathrm{GeV}]$

Momentum measurement

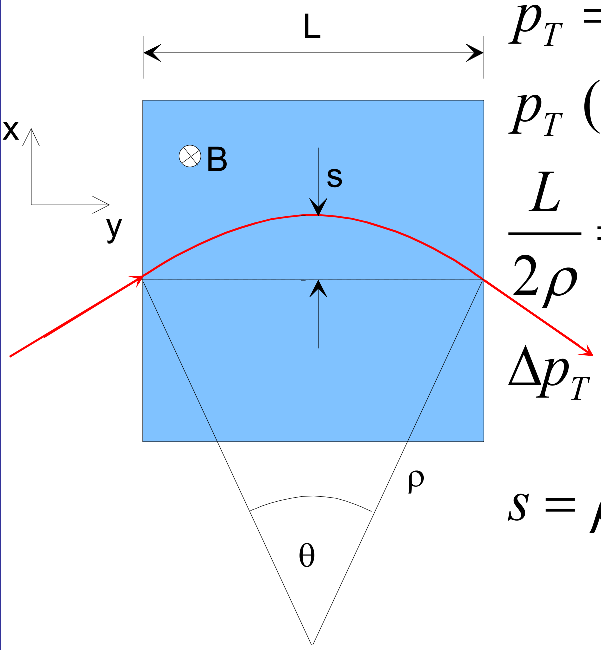

$$p_T = qB\rho$$

$$p_T\ (\mathrm{GeV/c}) = 0.3B\rho \quad (\mathrm{T\cdot m})$$

$$\frac{L}{2\rho} = \sin\theta/2 \approx \theta/2 \ \rightarrow\ \theta \approx \frac{0.3L\cdot B}{p_T}$$

$$\Delta p_T = p_T \sin\theta \approx 0.3L\cdot B$$

$$s = \rho\left(1-\cos\theta/2\right) \approx \rho\frac{\theta^2}{8} \approx \frac{0.3}{8}\frac{L^2B}{p_T}$$

sagitta s determined by 3 measurements with error $\sigma(x)$:

$$s = x_2 - \frac{x_1+x_3}{2} \Rightarrow \left.\frac{\sigma(p_T)}{p_T}\right|^{meas.} = \frac{\sigma(s)}{s} = \frac{\sqrt{\frac{3}{2}}\sigma(x)}{s} = \frac{\sqrt{\frac{3}{2}}\sigma(x)\cdot 8p_T}{0.3\cdot BL^2}$$

for N equidistant measurements, one obtains

(R.L. Gluckstern, Nuclear Instruments & Methods 24 (1963) 381)

$$\left.\frac{\sigma(p_T)}{p_T}\right|^{\mathrm{meas}} = \frac{\sigma(x)\cdot p_T}{0.3\cdot BL^2}\sqrt{720/(N+4)} \quad (\text{for } N \geq 10)$$

For example: L = 1 m, B = 1.4 T, σ(x) = 175 μm, N = 15

$$\left.\frac{\sigma(p_T)}{p_T}\right|^{\mathrm{meas}} \approx 0.26\,\%\cdot p_T \quad (s \approx 5.25 \text{ cm} / p_T\,[\mathrm{GeV}])$$

NB! $\left.\frac{\sigma(p_T)}{p_T^2}\right|^{\mathrm{meas}} =$ constant (at least for large p_T)

Elastic scattering

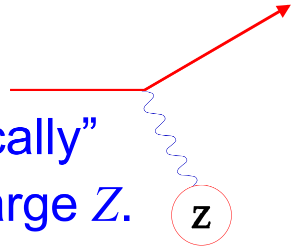

Incoming particle (charge z) interacts "elastically" (no momentum transfer) with target nuclei of charge Z.
cross section for this electromagnetic process

$$\frac{d\sigma}{d\Omega} = \frac{\alpha^2 z^2 Z}{4p^2\beta^2}\frac{1}{\sin^4\theta/2}(1-\beta\sin^2(\theta/2))$$

classical → relativistic
Rutherford → Mott

- average scattering angle $\langle\theta\rangle = 0$
- cross section for $\theta \to 0$ infinite !!
- causes a change of particle direction !!

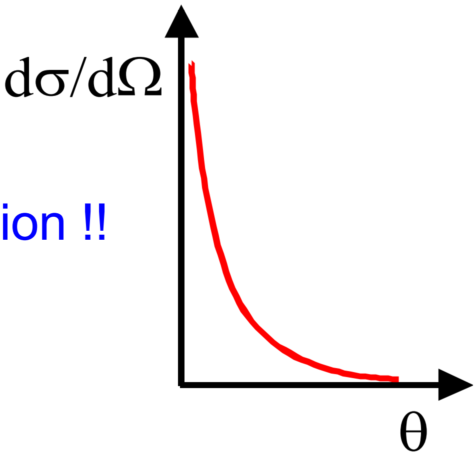

Multiple Scattering

sufficiently thick material layer →
particle undergoes many scatterings: **multiple scattering**

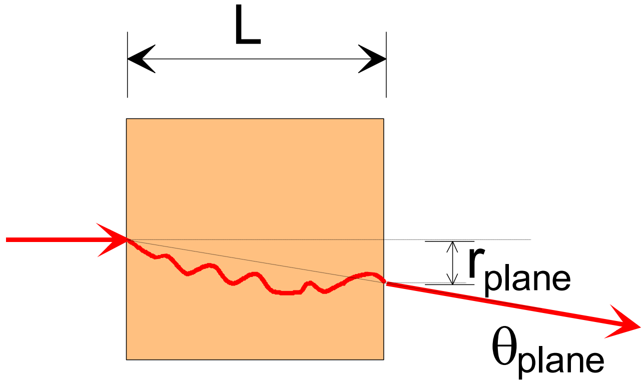

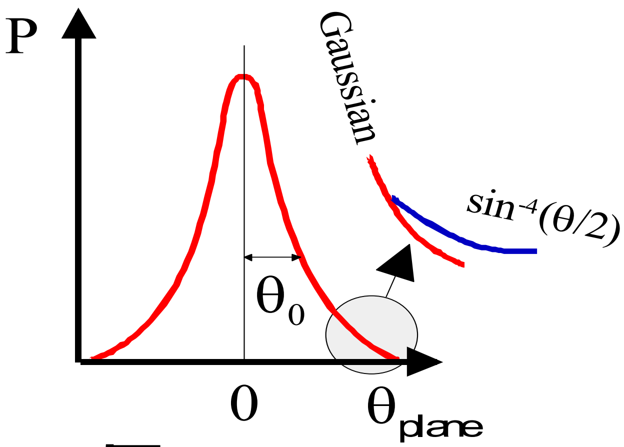

"Highland" formula:

Approximation $$\theta_0 = \frac{13.6\text{ MeV}}{\beta c p}\, z\sqrt{\frac{L}{X_0}}\left[1 + 0.038\ln\left(\frac{L z^2}{X_0\beta^2}\right)\right]$$

X_0 = radiation length of medium (definition later)
(accuracy ≤ 11% for $10^{-3} < L/X_0 < 100$)

$$\theta_0 = \theta_{\text{plane}}^{\text{RMS}} = \sqrt{V[\theta]} = \theta_{\text{space}}^{\text{RMS}}/\sqrt{2}$$

distribution sufficiently described by a Gaussian though tails shows $\sin^{-4}\theta/2$ behaviour (”Moliere” distribution). approximative formula assumes Gaussian distribution.

Back to momentum measurements:
contribution from multiple scattering ($\beta = 1$ & $z = 1$)

$$\Delta p^{MS} = p\sin\theta_0 \approx p \cdot 0.0136\frac{1}{p}\sqrt{\frac{L}{X_0}} \quad \text{[in GeV]}$$

$$\left.\frac{\sigma(p)}{p_T}\right|^{MS} = \frac{\Delta p^{MS}}{\Delta p_T} = \frac{0.0136\sqrt{L/X_0}}{0.3BL} = 0.045\frac{1}{B\sqrt{LX_0}}$$

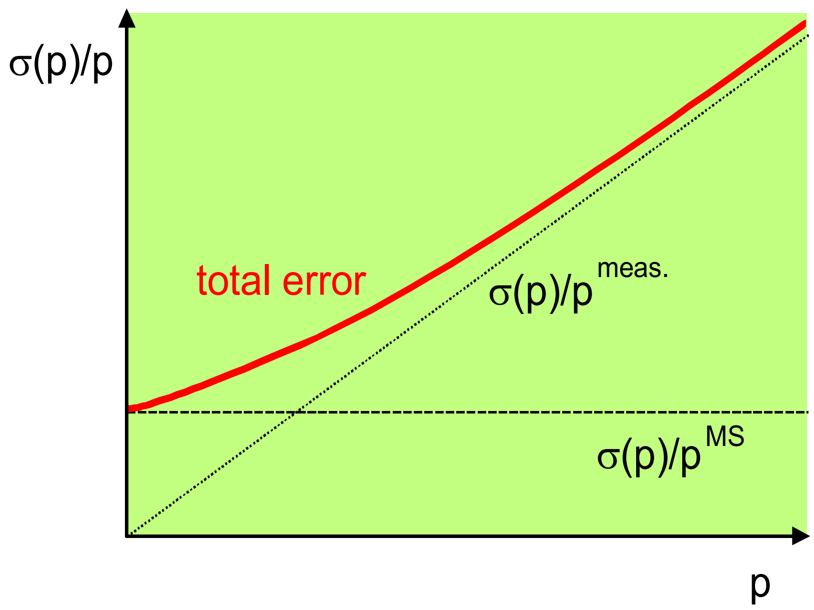

independent of p !

For example: Ar (X_0 = 110 m), L = 1 m, B = 1.4 T

$$\left.\frac{\sigma(p)}{p_T}\right|^{MS} \approx 0.3\ \%$$

Momentum measurement in experiments with solenoid magnet:

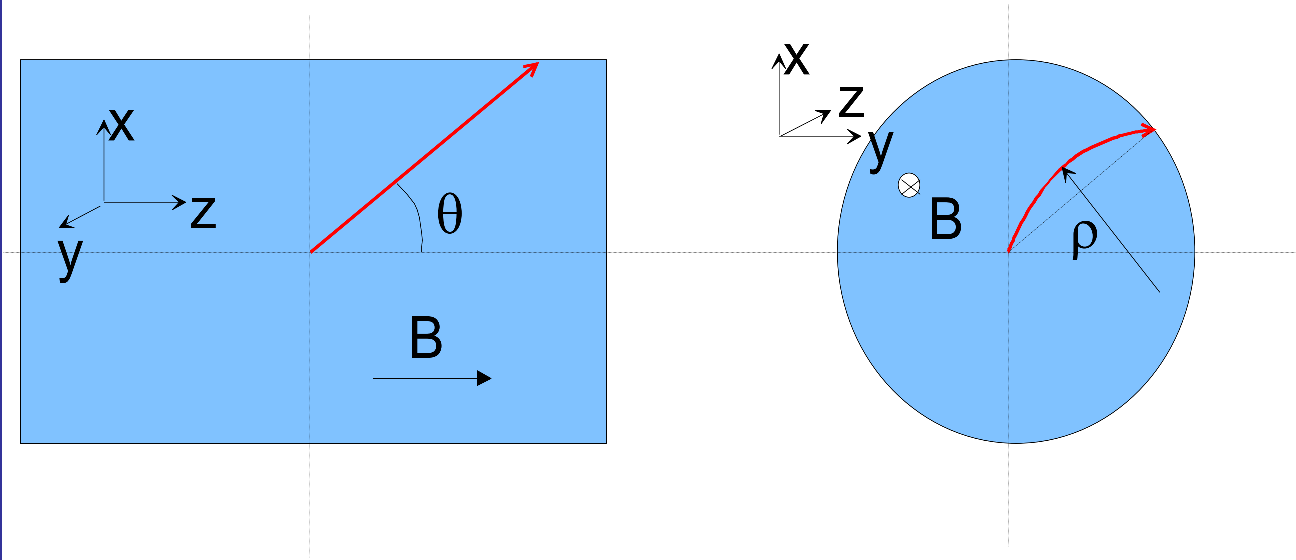

$$p_T = p\sin\theta$$

polar angle determined from a straight line fit $R = R(z)$

N equidistant points with error $\sigma(z)$

$$\left.\sigma(\theta)\right|^{meas.} = \frac{\sigma(z)}{L}\sqrt{12(N-1)/(N(N+1))}$$

\+ multiple scattering contribution….

mostly rather small

In most practical cases: $\dfrac{\sigma(p)}{p} \approx \dfrac{\sigma(p_T)}{p_T}$

In summary: $$\boxed{\left.\frac{\sigma(p)}{p}\right|^{\text{meas}} \propto \frac{\sigma(x)\cdot p_T}{BL^2}\frac{1}{\sqrt{N}}}$$

Position resolution of particle impact point.

One or several sensitive detector elements (e.g. wire in a wire chamber or strip in a silicon strip detector) will see the signal from particle passage depending on orientation of particle with respect to the plane of detector elements.

Let d be the spacing of detector elements. Position of particle impact point on the plane of detector elements then given with a precision of:

$$\sigma_{position} \leq \frac{d}{\sqrt{12}}$$

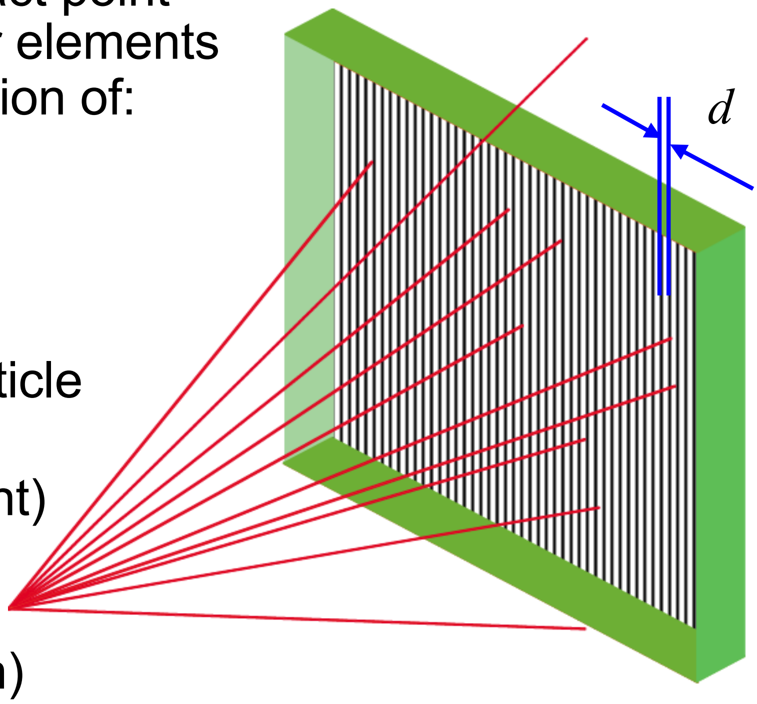

For binary readout (i.e. knowledge whether particle gave signal or not on a specific detector element) equal sign valid. For analog readout (i.e. pulse height information) position resolution is better. The theoretical lower limit is:

$$\sigma_{position} \approx \frac{d}{2\sqrt{12}} \approx \frac{d}{7}$$

assuming particle next to a wire only fires this wire & a particle passing between two wires fires only 2 wires.

NB! other effects like e.g. electronics noise or charge diffusion can deteriorate initial resolution significantly.

Further reading: R. Frühwirth et al., Data Analysis Techniques for High-Energy Physics

Detection of charged particles

How do they loose energy in matter ?

- Discrete collisions with atomic electrons of material

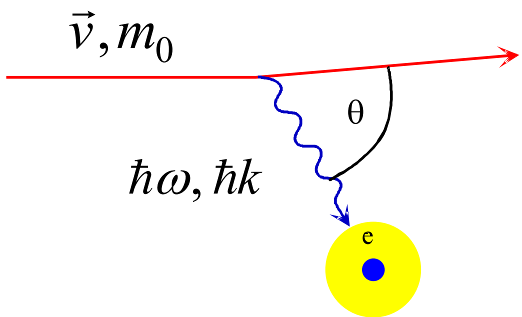

$$\left\langle \frac{dE}{dx} \right\rangle = -\int_0^\infty n_e E \frac{d\sigma}{dE} \hbar \, d\omega$$

n_e : electron density

Collisions with nuclei not important since average energy loss inversely proportional to target mass ($m_e << m_N$).

classical derivation of energy loss given in W.R. Leo: Techniques for nuclear & particle physics experiments (Springer 1987) p. 22-23.

- If energy transfer big enough ⇨ **ionization,** otherwise **excitation.**

<u>Ionization & excitation basis for particle measurements</u>

Instead of ionizing atom, under certain conditions photon can also escape material (marginal source of energy loss)

⇨ Emission of **Cherenkov** or **Transition** radiation. utilized for particle identification (see later).

NB! electrons have to be treated separately since then $m_{projectile} = m_{target}$ making assumptions made in extraction of upcoming formulas not valid anymore. For electrons also photon emission via "bremsstrahlung" is a significant source of energy loss (see electromagnetic shower discussion)

Average differential energy loss $\left\langle \frac{dE}{dx} \right\rangle$

Ionisation only $\rightarrow$ Bethe - Bloch formula

$$\left\langle \frac{dE}{dx} \right\rangle \approx -\frac{4\pi\alpha^2(\hbar c)^2}{m_e c^2 \beta^2} n_e z^2 \left[\ln \frac{2m_e c^2 \gamma^2 \beta^2}{I} - \beta^2 - \frac{\delta}{2} \right]$$

- dE/dx ("stopping power") in [MeV g^{-1} cm^2]
- dE/dx depends only on β, independent of $m_{\text{projectile}}$
- Formula takes into account energy transfers

$$I \le dE \le T^{\max} \approx 2m_e c^2 \beta^2 \gamma^2 \ (\text{valid if } 2\gamma m_e \le m_{\text{projectile}})$$

I : mean excitation potential

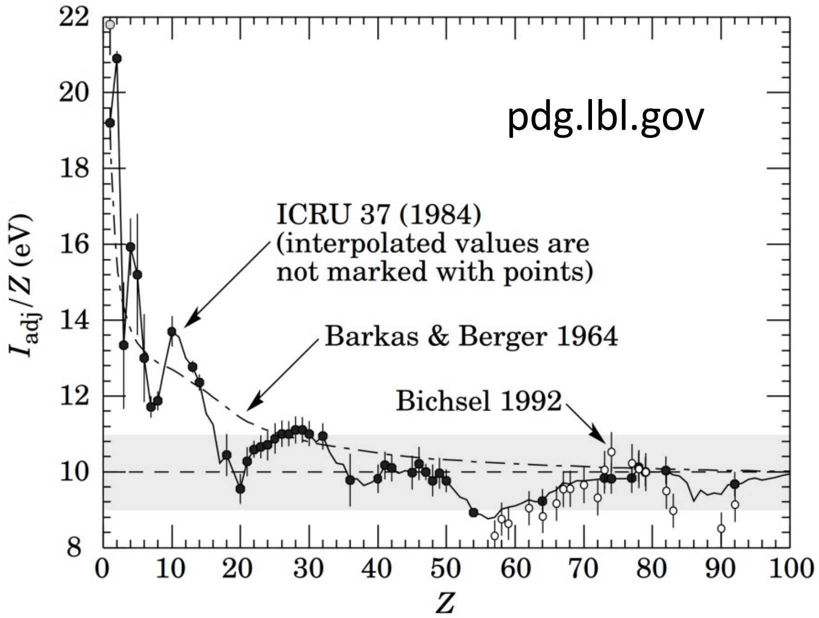

$I \approx 16 \cdot Z^{0.9}$ [eV]

- electron density of material $n_e = N_A \, Z / A$
- Bethe-Bloch only valid for "heavy" particles ($m \ge m_\mu$).

Bethe-Bloch formula

$$\left\langle \frac{dE}{dx} \right\rangle \approx -\frac{4\pi\alpha^2(\hbar c)^2}{m_e c^2 \beta^2} n_e z^2 \left[\ln \frac{2 m_e c^2 \gamma^2 \beta^2}{I} - \beta^2 - \frac{\delta}{2} \right]$$

Z/A does not differ much for various elements, except for hydrogen (H_2)!

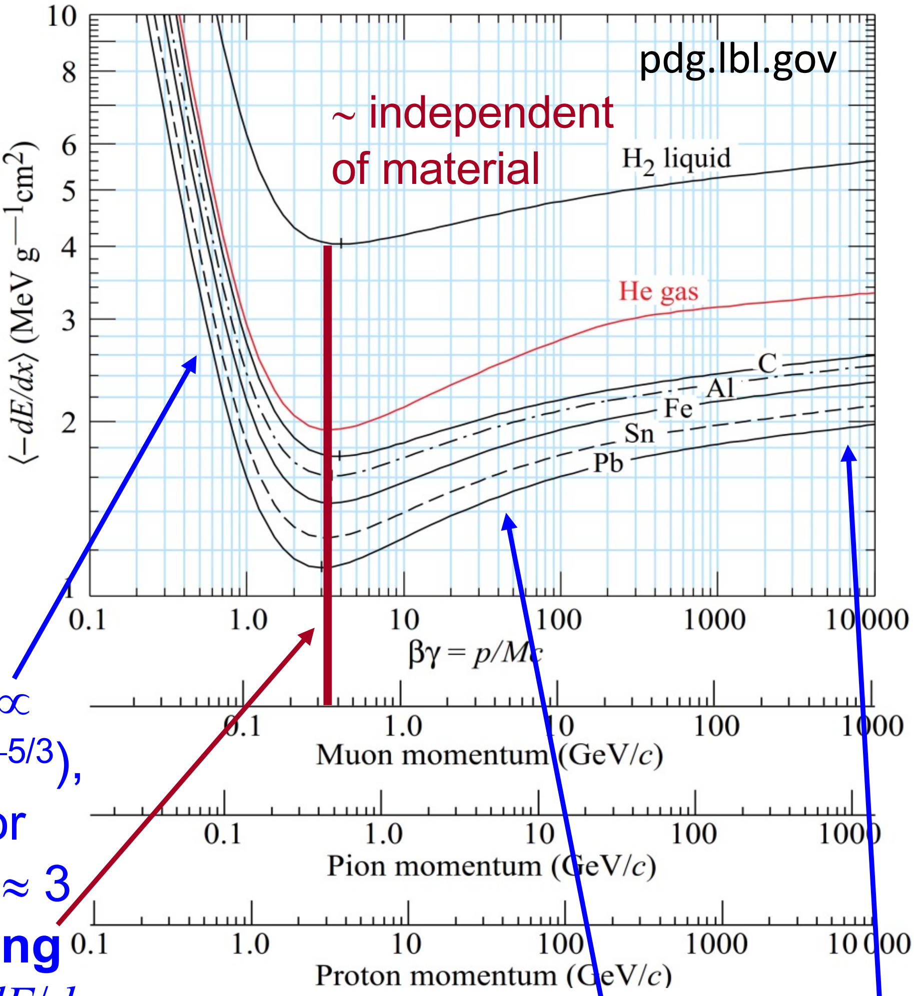

- dE/dx first falls $\propto 1/\beta^2$ (precisely $\beta^{-5/3}$), kinematical factor
- minimum at $\beta\gamma \approx 3$ **minimum ionizing particle** (MIP), $dE/dx \approx$ 1–2 MeV g^{-1} cm^2)
- then again rising due to ln γ^2 term, **relativistic rise**, due to relativistic expansion of transverse electric field → significant contributions from more distant collisions.
- relativistic rise cancelled at high γ by "**density effect**", polarization of medium screens more distant atoms. parameterized by δ (material dependent) → Fermi plateau

For more details see e.g. J.D. Jackson, Classical electrodynamics, section 13

dE/dx measurement in the CMS Tracker

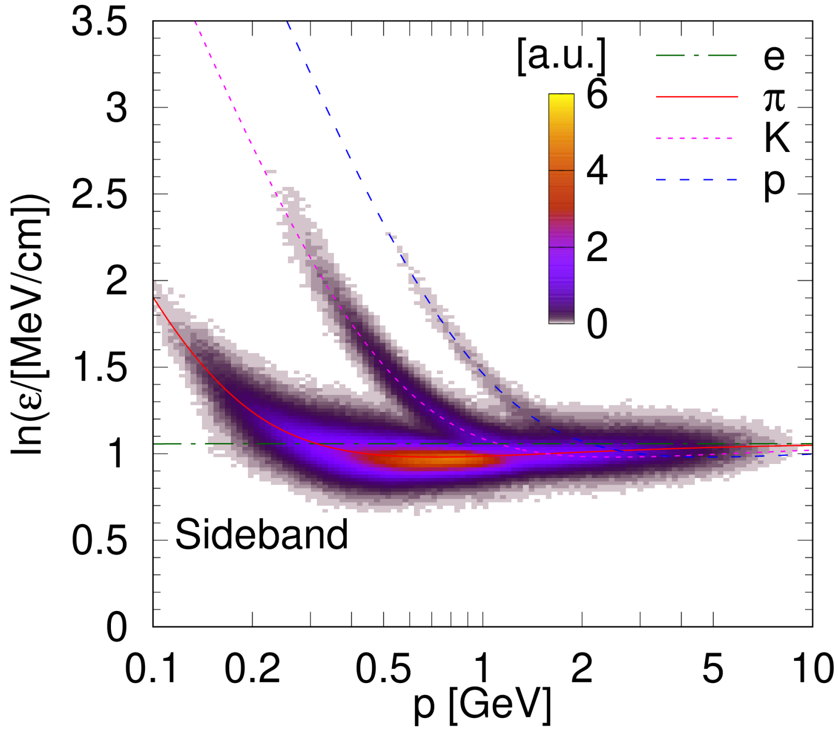

Range of particles in matter

$R \propto E_{\text{kinetic}}^2 / Z^2$

Range approximately proportional to kinetic energy square at low energy & approximately proportional to the kinetic energy at high energy where the dE/dx is about constant.

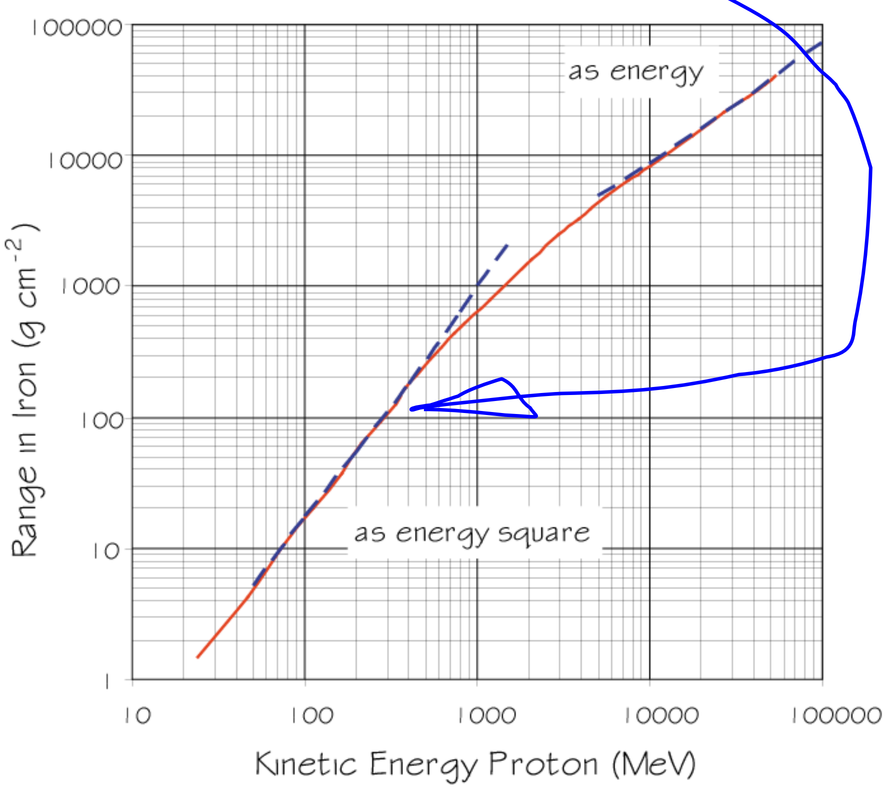

Real detectors (limited sampling) do not measure <dE/dx>, but energy ΔE deposited in a layer of finite thickness δx.

For thin layers (& low density materials):
- few collisions, some high energy transfers ("δ–electrons")
- energy loss distribution, "Landau" distribution, show large fluctuations towards high losses due to these δ–electrons

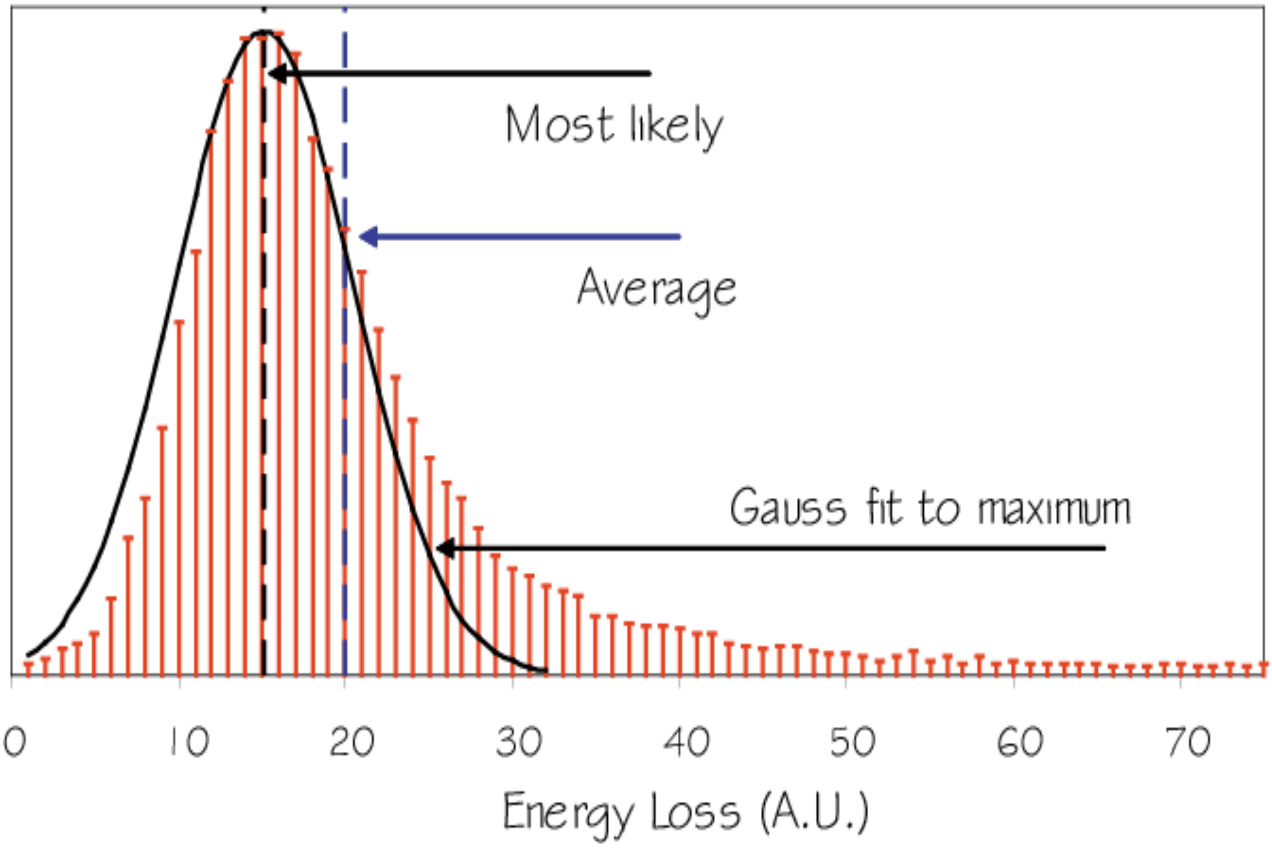

δ-electrons leads to broadening of area, where charge is deposited $\Rightarrow$ worse spatial resolution for such particles.

For thick layers & high density materials:
$\rightarrow$ many collisions.
$\rightarrow$ (more) Gaussian(-like) distribution of energy loss.

Primary & total ionization

Fast charged particles ionize the atoms of a gas.

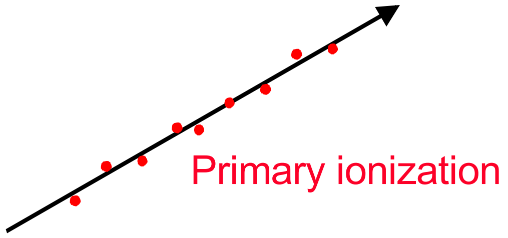

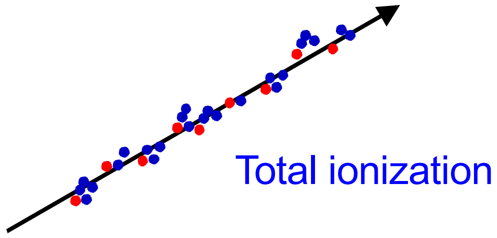

Often the resulting primary electron will have enough kinetic energy to ionize other atoms.

$$n_{total} = \frac{\Delta E}{W_i} = \frac{\frac{dE}{dx}\Delta x}{W_i}$$

total number of created electron–ion pairs.
ΔE = total energy loss
W_i = effective <energy loss>/pair

$$n_{total} \approx 2\ldots4 \cdot n_{primary}$$

Number of primary electron-ion pairs in frequently used (detector) gases

$\bar{Z}$

$$n_{total}/\mathrm{cm} \approx 4\ldots6 \cdot Z$$

~ 100 pairs/cm in Ar
~ 50 pairs/cm in CH_4
~ 310 pairs/cm in Xe

Ideal detector gas: high density, low W_i & chemically "inactive"

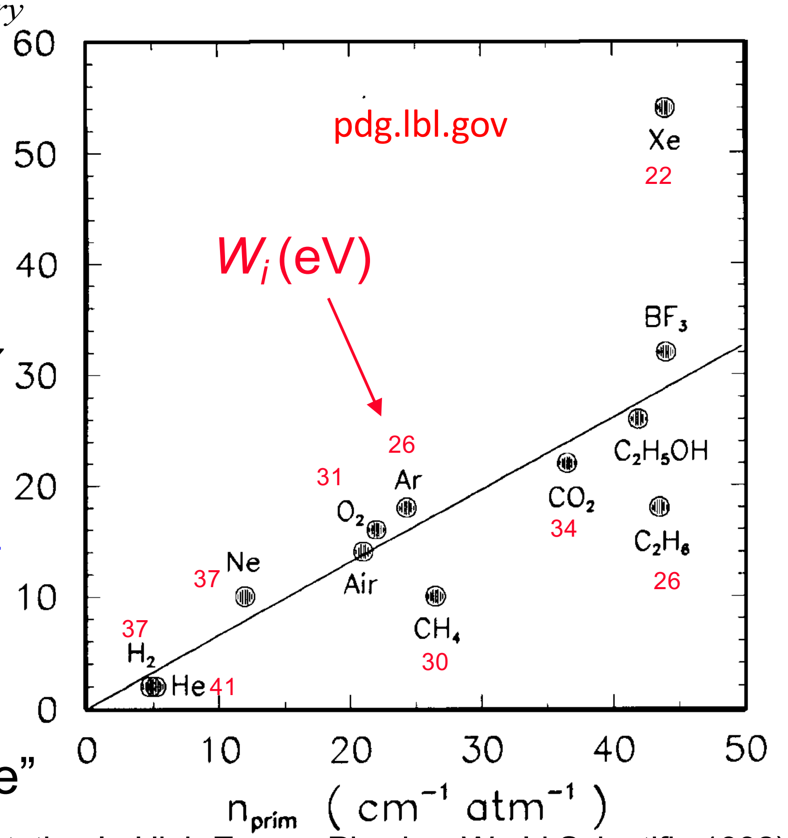

(Lohse and Witzeling, Instrumentation In High Energy Physics, World Scientific, 1992)

≈ 100 electron-ion pairs are not easy to detect!

Electronic noise of amplifiers ≈ few hundred e⁻ (ENC) !

Need to increase the number of electron-ion pairs.

Gas amplification

Cylindrical field geometry (simplest) ⇒ **proportional chamber / straw (drift) tube detector**

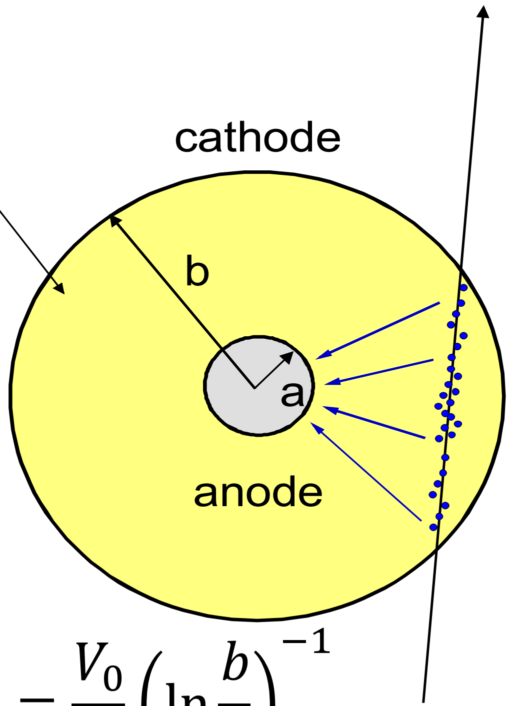

$$\varepsilon(r) = \frac{V_0}{r}\left(\ln\frac{b}{a}\right)^{-1}$$

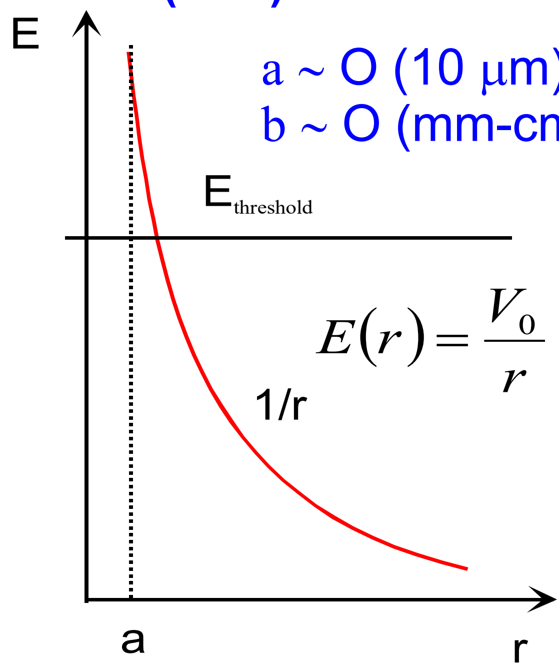

$a \sim O$ (10 μm)
$b \sim O$ (mm-cm)

$$E(r) = \frac{V_0}{r}$$

Electrons drift towards anode wire (≈ stop & go, see later).

Close to anode wire electric field sufficiently high (~MV/m) so that electrons gain enough energy for further ionization →

exponential increase of number of electron-ion pairs.

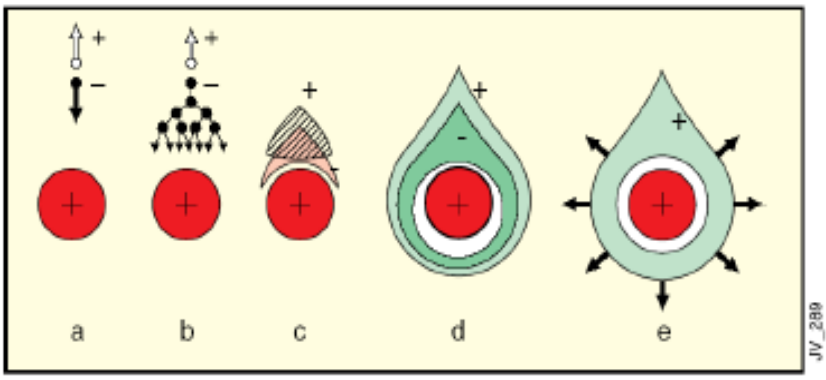

From ionisation to gas amplification.

Let $1/\alpha$ be the mean free path between each ionization

$$\alpha = \alpha\,(\varepsilon, \text{density, gas type})$$

density → temperature, pressure

$\varepsilon \rightarrow \varepsilon = \varepsilon(r)$

gas amplification: $M = n / n_0 = \exp\left(\int_a^b \alpha(r)dr \right)$

Korff's approximation: $\alpha = p \times A \exp\left(- Bp / \varepsilon \right)$

Where A & B gas dependent constants and p pressure.

$$\frac{\varepsilon}{V_0} = \frac{1}{r}\left(\ln \frac{b}{a} \right)^{-1} \Rightarrow M = \exp\left[\frac{AV_0}{B}\left(\ln \frac{b}{a} \right)^{-1} e^{-\frac{Bpa \ln \frac{b}{a}}{V_0}} \right]$$

(F. Sauli)

$$M = e^{\int_a^b \alpha(r)dr}$$

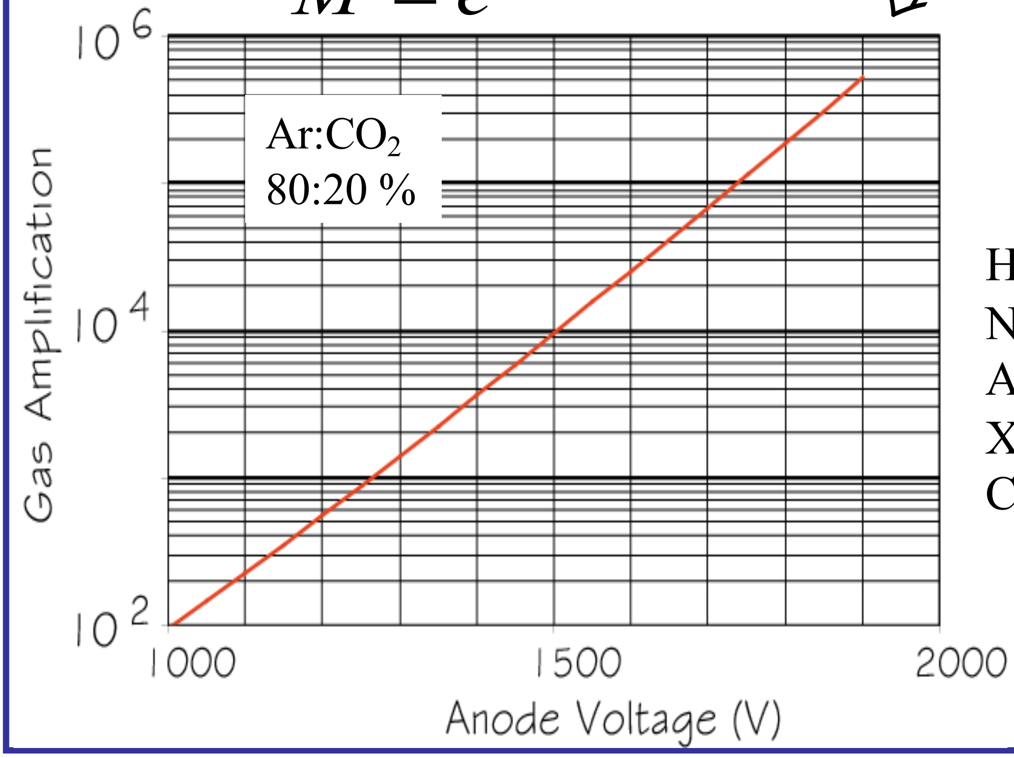

	A	B
	1/Torr·cm	V/Torr· cm
He	3	34
Ne	4	100
Ar	14	180
Xe	26	350
CO_2	20	466

Choice of gas:

Dense noble gases. Energy dissipation mainly by ionization! High specific ionization.

De-excitation of noble gases only possible via emission of photons, e.g. 11.6 eV for Argon.

Above ionization threshold of metals, e.g. Copper 7.7 eV.

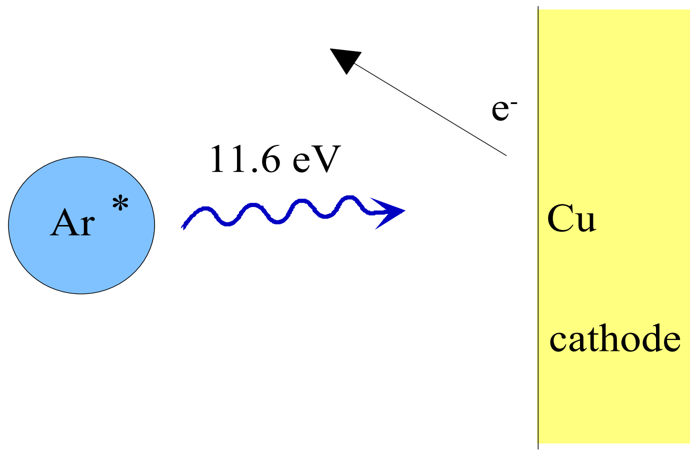

→ new avalanches → permanent discharges !

Solution: Add poly-atomic gases such as methane as quenchers.

Absorption of photons in a large energy range (many vibrational & rotational energy levels).

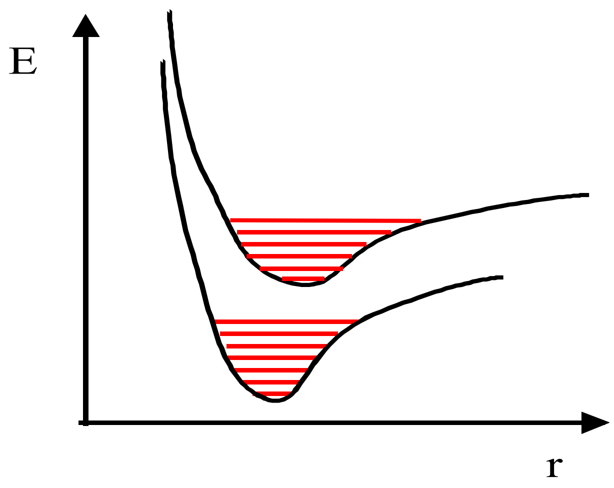

Energy dissipation by collisions or dissociation into smaller molecules.

(F. Sauli, CERN 77-09)

Signal formation

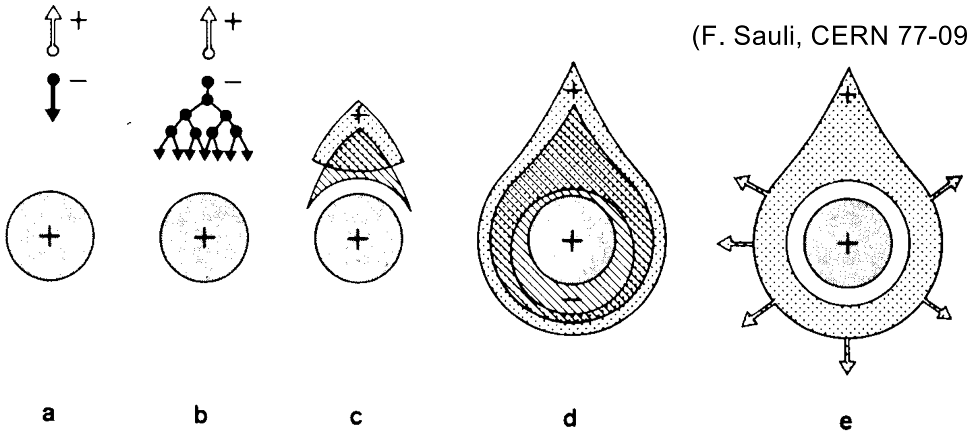

Avalanche formation: within a few wire radii & t < 1 ns!
(assume all charge created a small distance λ from anode)

Signal induction both on anode & cathode due to moving charges (both electrons & ions).

$$dV = \frac{Q}{lCV_0}\frac{dV}{dr}dr \Rightarrow$$

$$V_{electrons}^{signal} = -\frac{Q}{2\pi\varepsilon_0 Cl}\ln\frac{r_0+\lambda}{r_0} \quad \& \quad V_{ions}^{signal} = +\frac{Q}{2\pi\varepsilon_0 Cl}\ln\frac{R}{r_0+\lambda}$$

(lC = total capacitance of wire, r_0 (R) = anode (cathode) radius)

Electrons collected by anode wire, i.e. *dr* small (few μm).
Electrons contribute very little to detected signal (~ 1 %).

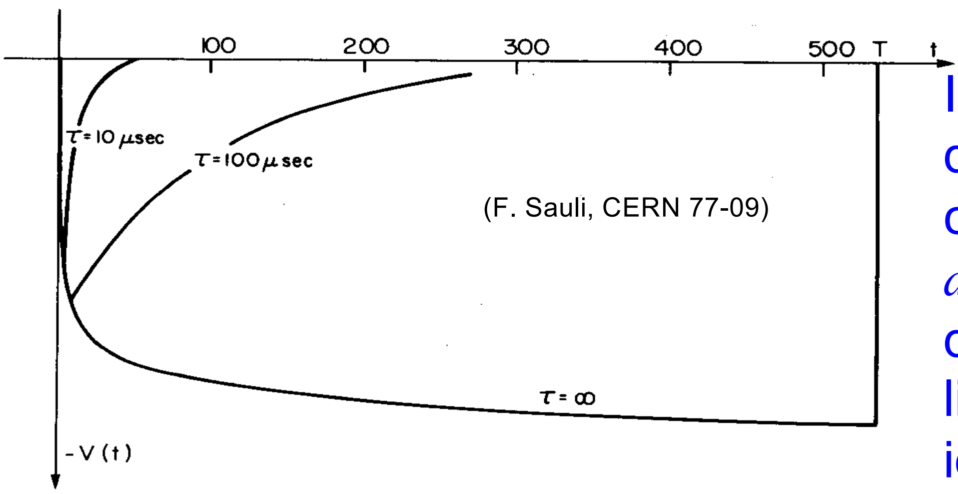

Ions have to drift back to cathode, i.e. dr big. Signal duration limited by total ion drift time !!

Need electronic signal differentiation to limit dead time.

Operation modes:

- Ionization mode: full charge collection, but no charge multiplication.
- Proportional mode: above threshold voltage multiplication starts. detected signal proportional to original ionization → energy measurement (dE/dx), secondary avalanches have to be quenched. Gain $10^4 - 10^6$.
- Limited Proportional → Saturated → Streamer mode: strong photo-emission leading to secondary avalanches, merging with the original avalanche. requires strong quenchers or pulsed HV. High gain(10^{10}), large signals → simple electronics.
- Geiger mode: massive photo emission. full length of anode wire affected. Stop discharges by cutting down HV. Strong quenchers needed as well.

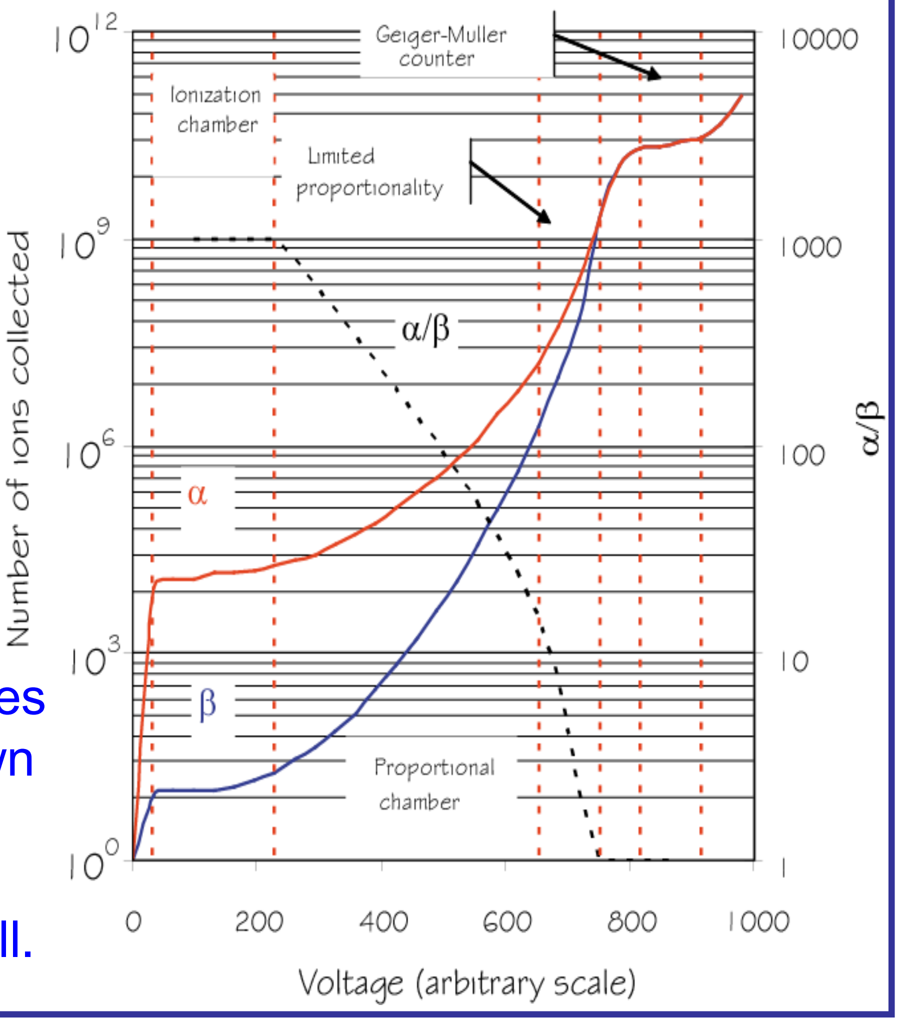

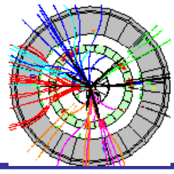

Multi wire proportional chamber (MWPC)

(G. Charpak et al. 1968, Nobel prize 1992)

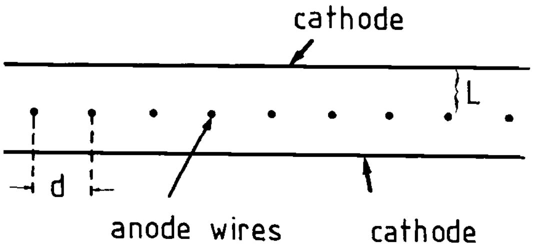

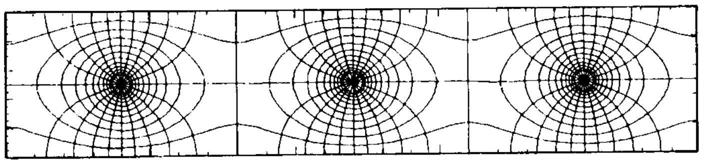

field lines & equipotentials around anode wires

Capacitive coupling of non-screened parallel wires? Negative signals on all wires? Compensated by positive signal induction from ion avalanche.

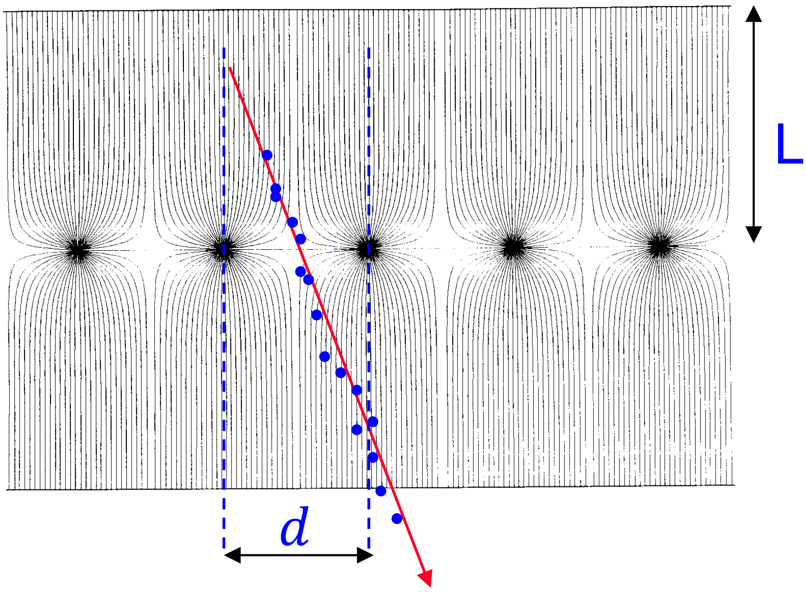

Typical parameters:
L = O (cm),
d = O (mm),
r_{wire}= O (10 μm)

Normally digital readout: spatial resolution limited to $\sigma_x \approx \frac{d}{\sqrt{12}}$ (d = 1 mm, σ_x = 300 μm)

Address of fired wire(s) give only 1-dimensional info.

A 'derivative'

- Resistive plate chambers (RPC)

No wires !

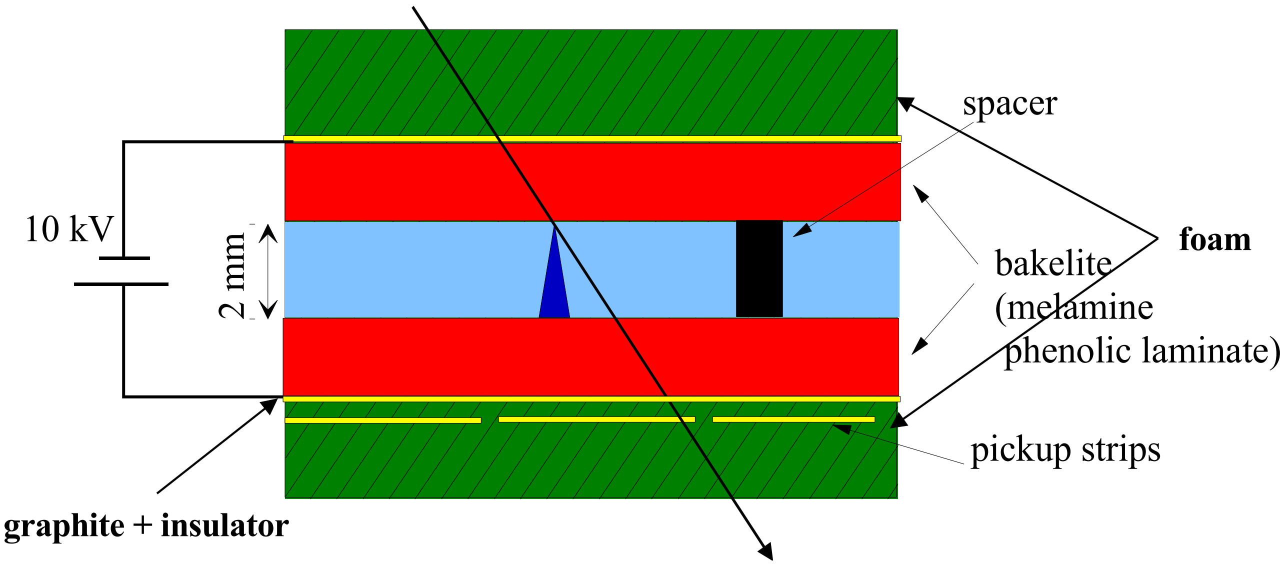

Gas: $C_2F_4H_2$, (C_2F_5H) + few % isobutane

(ATLAS, A. Di Ciaccio, NIM A 384 (1996) 222)

Time dispersion ≈ 1..2 ns → suited as trigger chamber
Rate capability ≈ 1 kHz / cm^2, efficiency ≥ 90 %

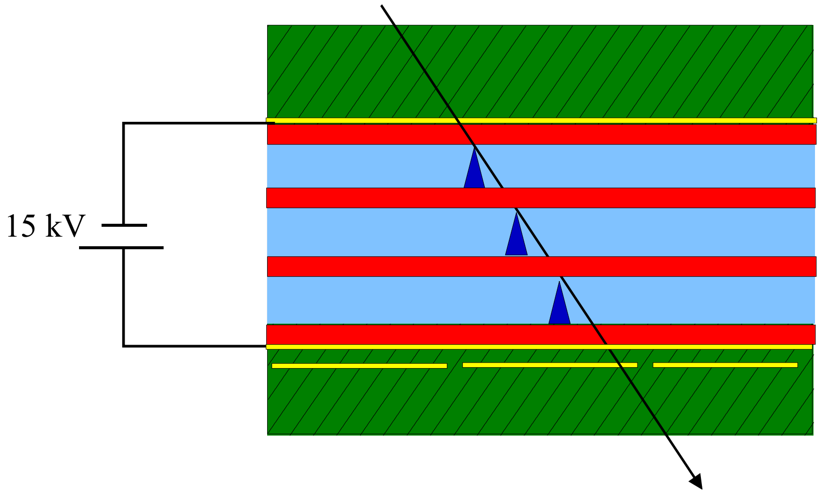

Double & multi-gap geometries → improve timing & efficiency

comparatively cheap ⇒ large-area coverage
operation close to streamer mode (to get sufficient signal)
used by all LHC experiments for triggering on muons !!

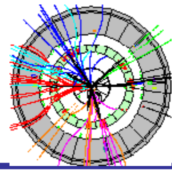

Muon/tracking chambers at LHC

LHCb OUTER TRACKER

SINGLE WIRE PROPORTIONAL CHAMBERS

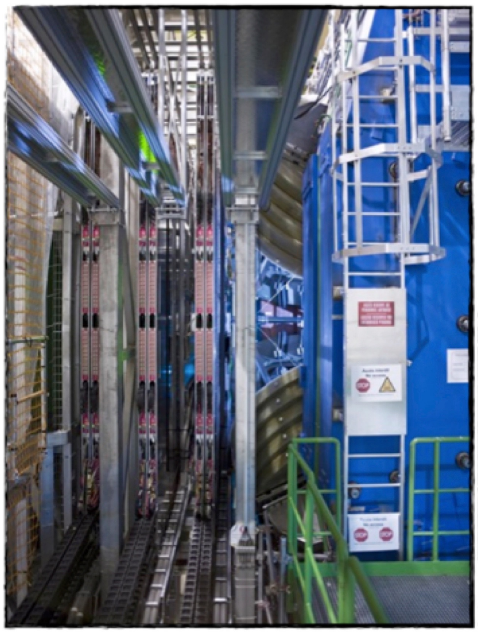

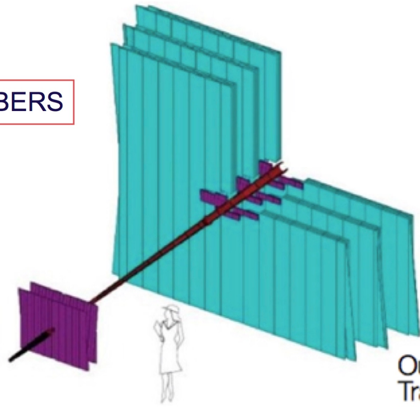

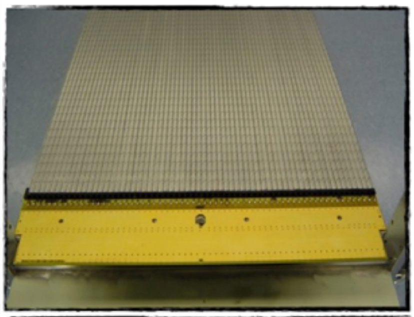

Straw Tubes
[double layers]

3 Chambers
[4 layers á 18 modules]

Cathode Strip Chambers (CSC)

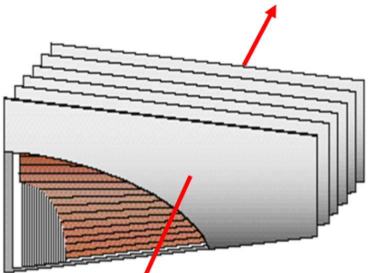

used for muon chambers @ LHC

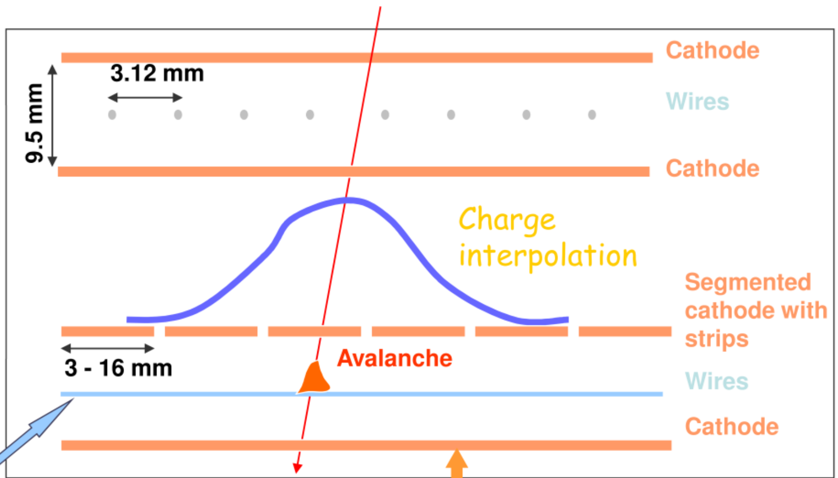

ANODE WIRES
Spatial resolution ~mm,
Time resolution (~4 ns)

CATHODE STIPS
Spatial resolution ~ 100 μm
Timing resolution (t_D~100 ns)

K.Hoepfner, RWTH Aachen   Cern ACT Lecture: Muon Systems, May 2011

Faster and more precision ? → smaller structures

Micro-Pattern Gas Detectors (MPGD)

MWPC (Multi Wire Proportional Chamber)

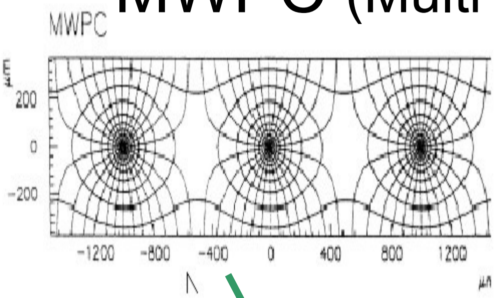

The “daddy” of proportional counters

Photolithographic techniques

MSGC (Micro Strip Gas Chambers)

A. Oed, NIM. A 263 (1988) 351;
A. Barr et al., NPB 61 (1988) 264.

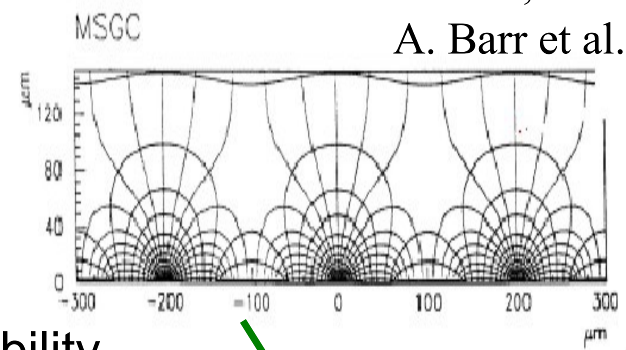

- Spatial resolution
- Rate capability

advanced PCB technology
(Printed Circuit Board)

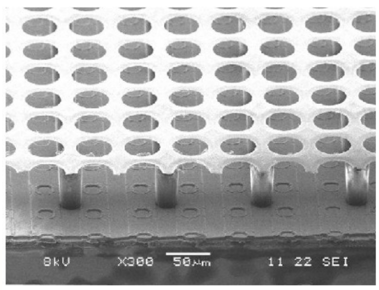

GEM

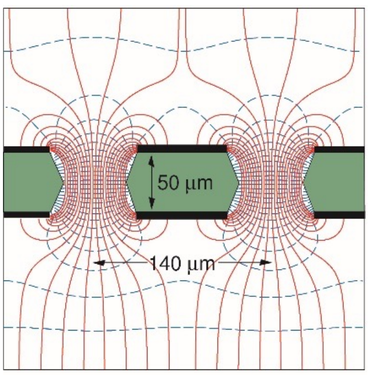

MicroMegas

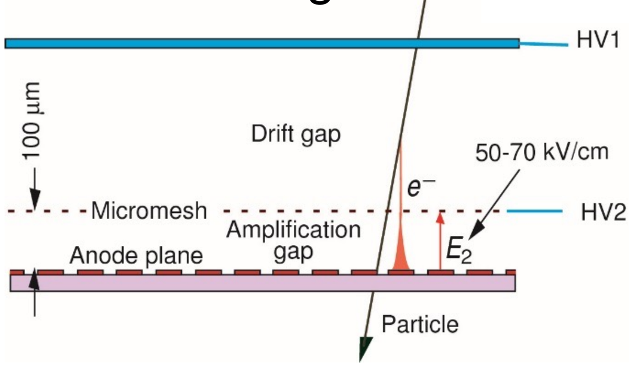

Y. Giomataris et al., NIM A 376 (1996) 29.

- **Common advantages of MPGD family:**
  - **Good efficiency ⇨ 99% efficiency in GEMs for a multiplication of 6500**
  - **Good spatial resolution**
    ⇨ MicroMegas ~10 μm
  - **Good gain at high rate**
    GEM's > MHz/mm²
  - **Good energy resolution and gain stability**
  - **Good time resolution**
    even down to ~25 ps for MicroMegas (PICOSEC)
  - **With careful design & production also good aging rate achievable**

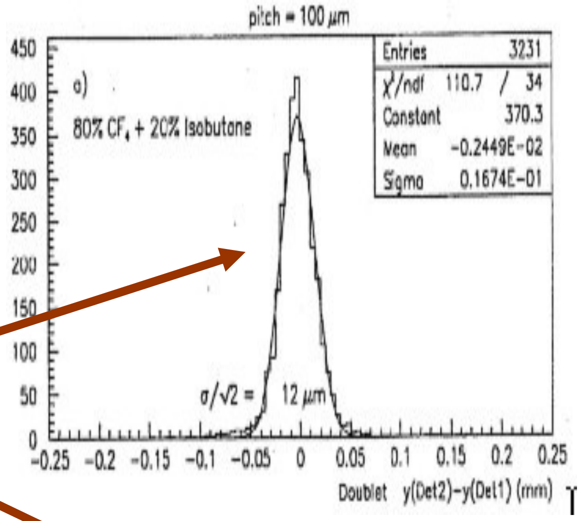

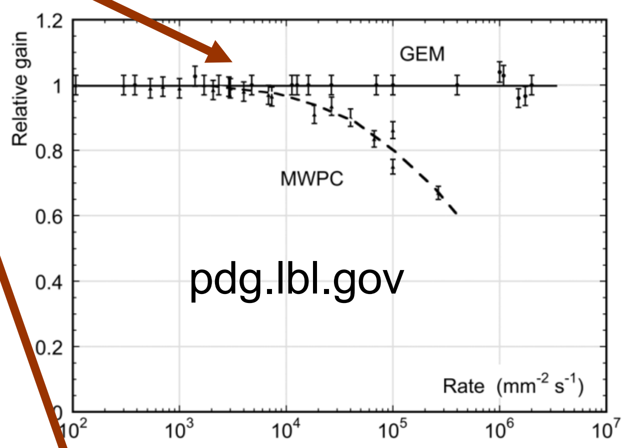

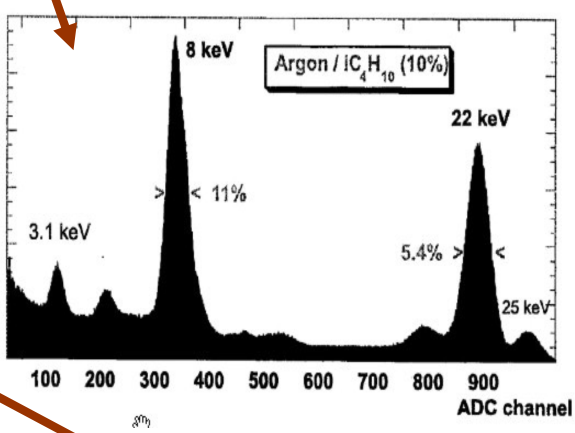

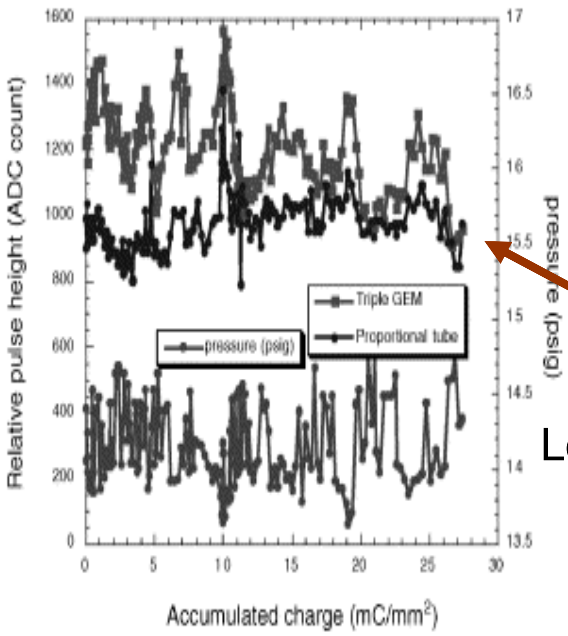

Long term aging test for triple GEM
No degradation after 2.7 C/cm²
NIM A 478 (2002) 263

◆ GEM: Gas Electron Multiplier

F. Sauli, NIM
A 386 (1997) 531

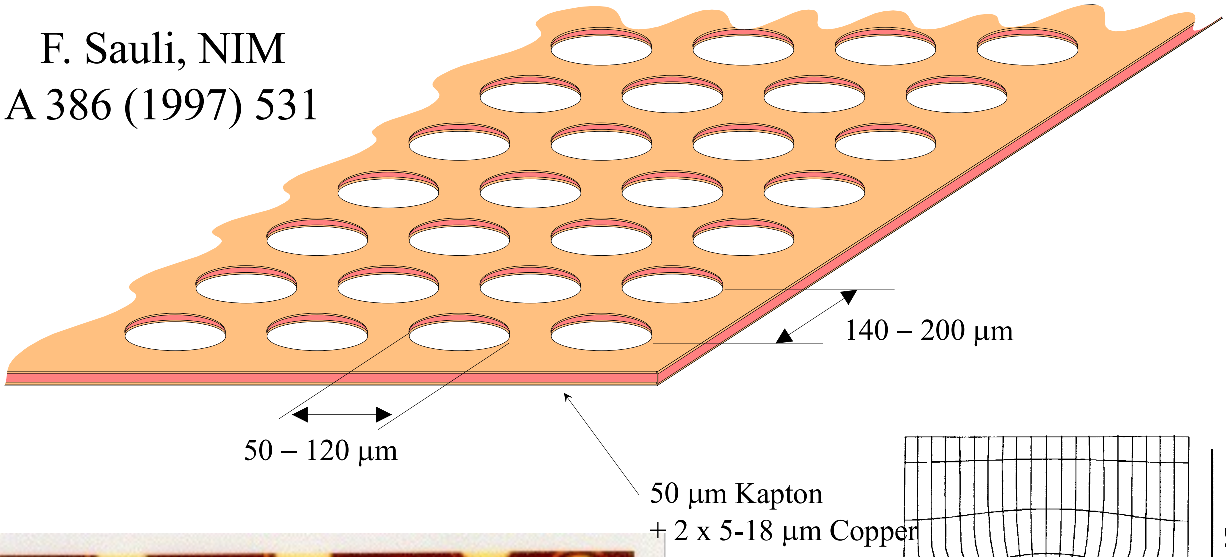

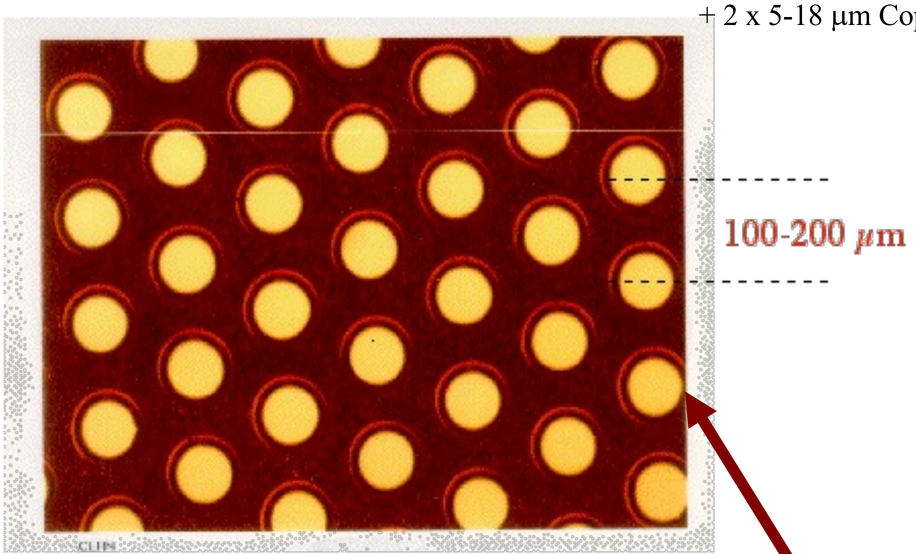

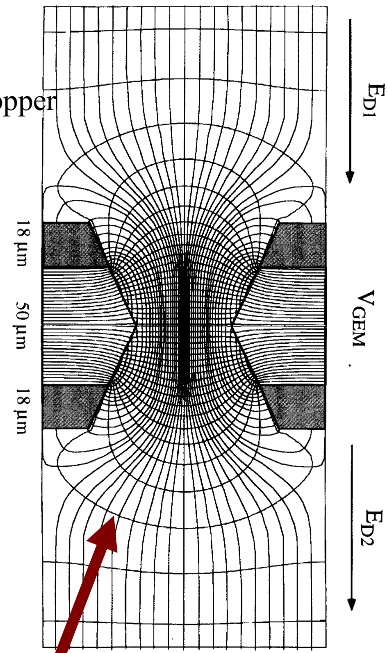

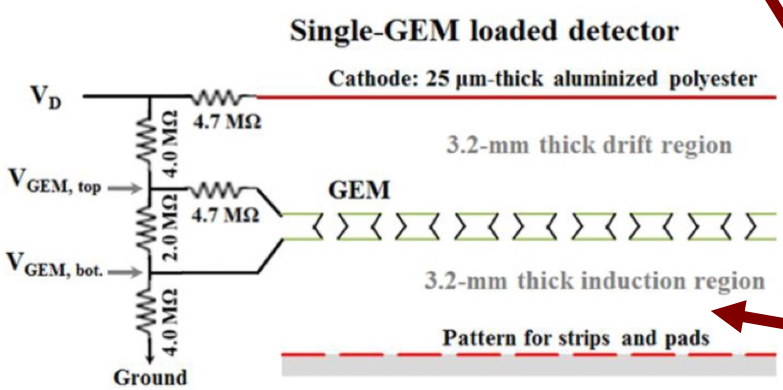

field lines in GEM detector

microphoto of GEM foil

single GEM + readout pads

how avoid aging effects due to radiation? reduce electric field → thicker foils or several layers (foils)

To reduce ageing effects, ion feedback and discharge probability, GEM-amplification is usually done in stacks of foils instead increasing the thickness of the foils. This will also increase the gain of the detector.

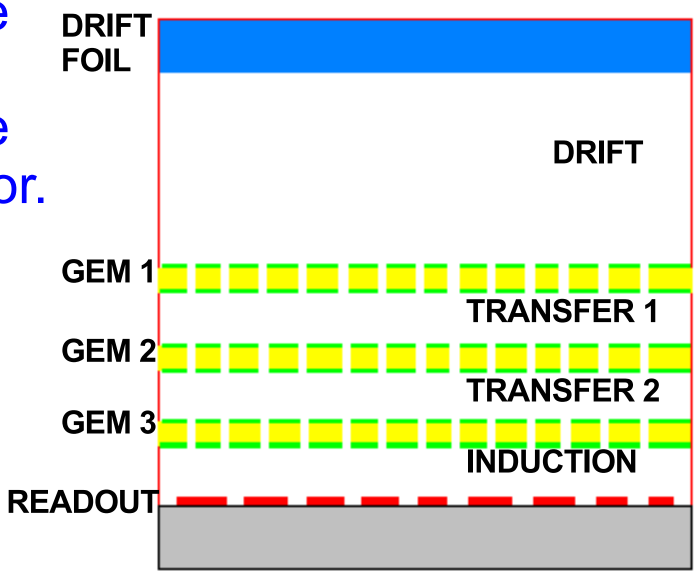

In multiple-GEM detectors the drift is set to few mm with electric fields ~few hundred volts/cm

Distances between foils set to be 2 mm & electric field between foils ~ 2-4 kV/cm

To achieve the same gain as with single GEM system need over 100V less voltage over the GEM-foils.

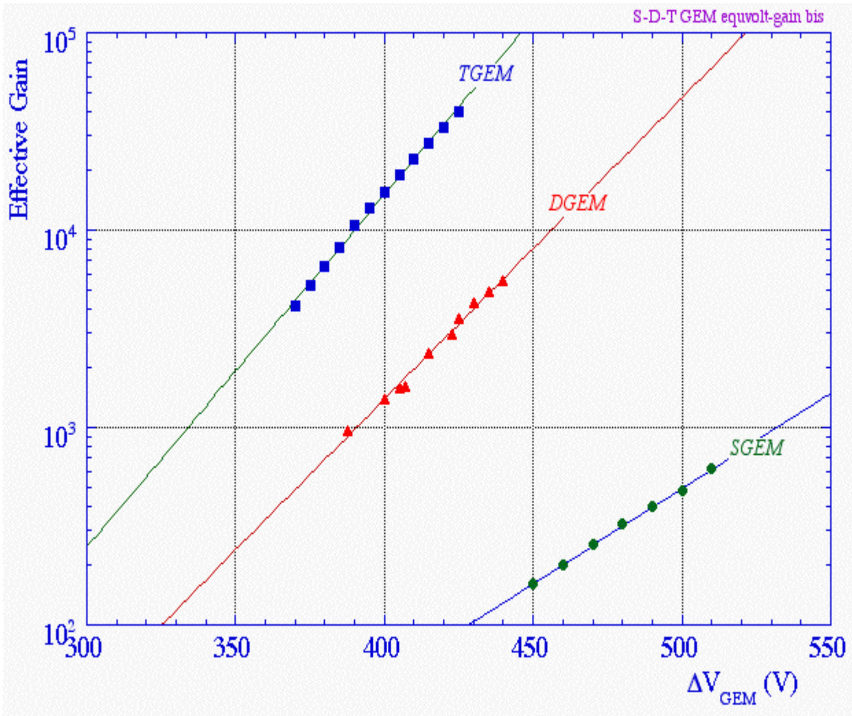

C. Buttner et al, NIM A 409(1998)79;
S. Bachmann et al, NIM A 443(1999)464

- tripple-GEM's (Gas Electron Multiplier)
- resolution: ~ 80 μm (radial), ~ 1° (phi)

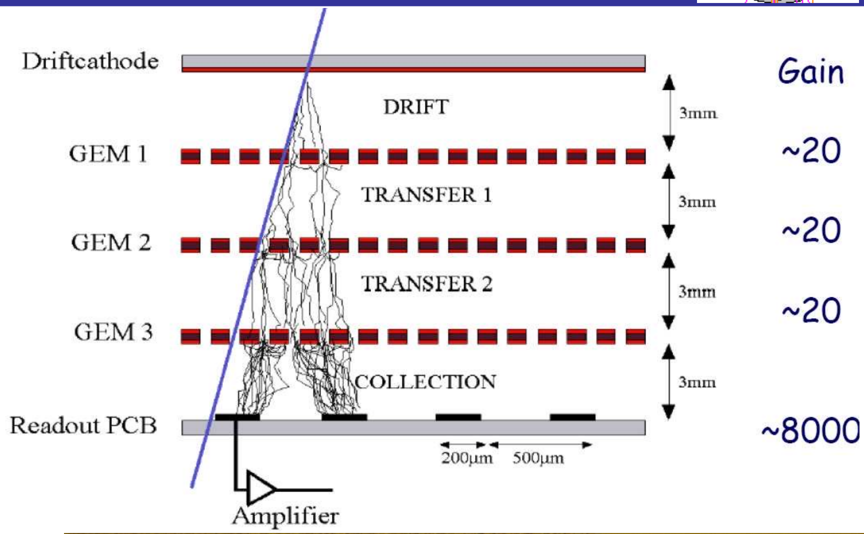

readout board

65(φ) x 24(η) = 1560 pads
pads: Δη x Δφ = 0.06 x 0.015π → 2 x 2 mm^2 — 7 x 7 mm^2

strips: 256 (width /pitch: 80/400 μm)

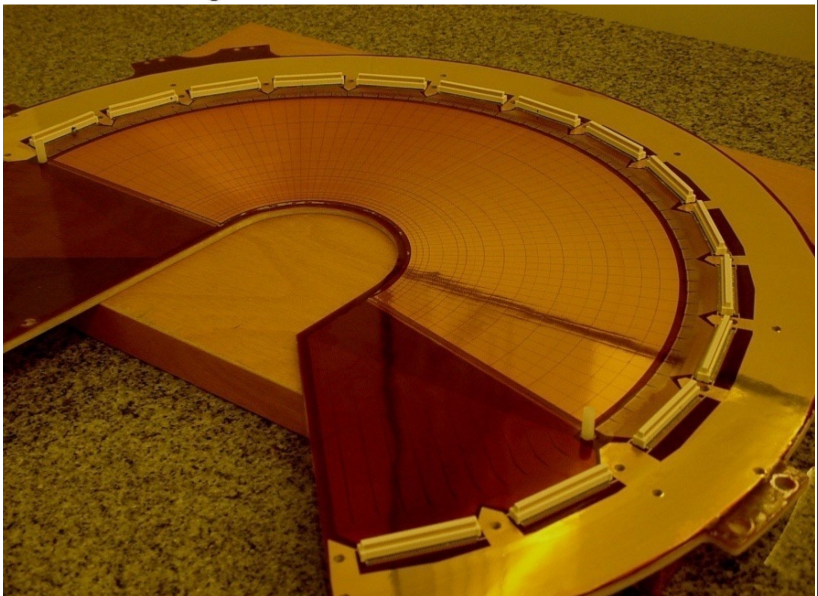

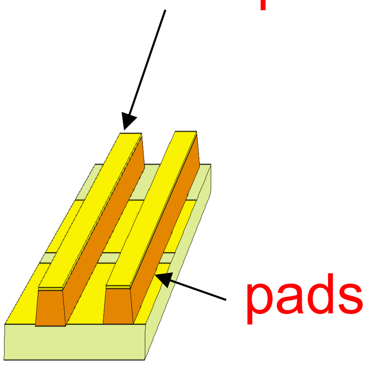

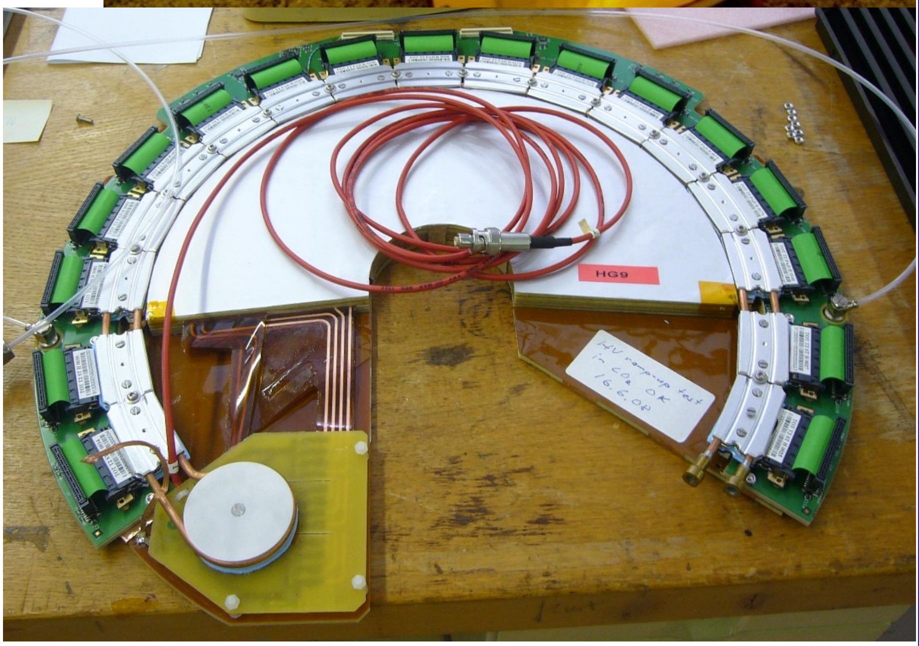

fully equipped tripple-GEM

One T2 quarter assembled & ready at CERN for installation in 2009

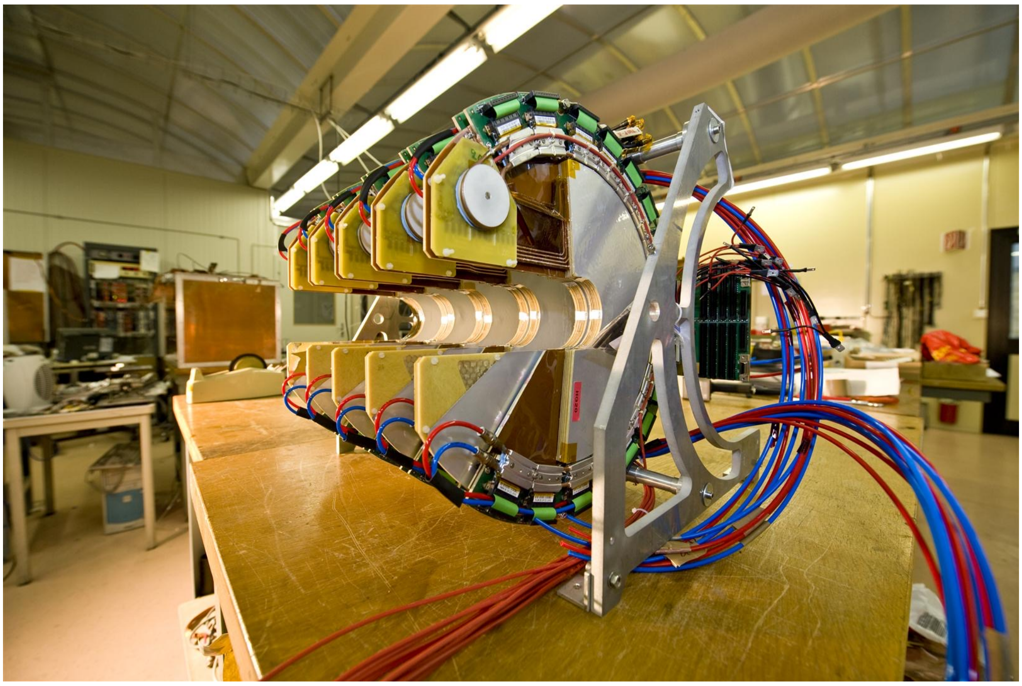

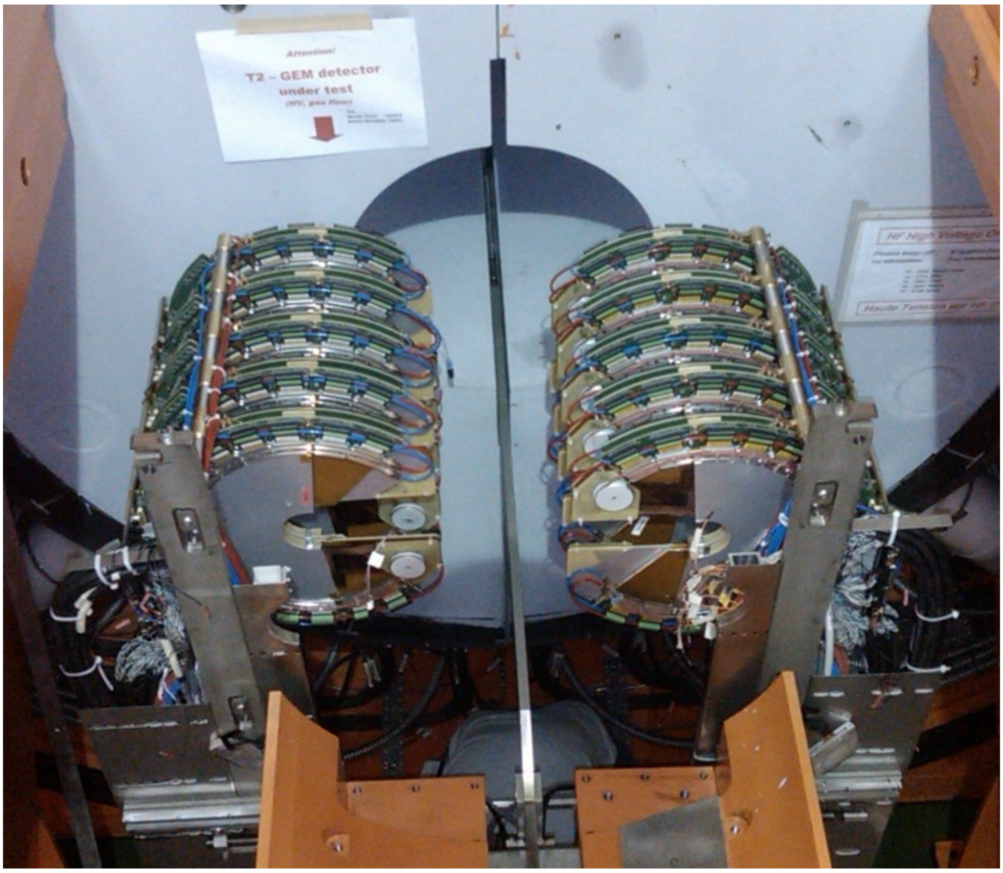

One half of T2 telescope at IP5 before CMS end-cap closure in 2010

Drift chambers

First studies: T. Bressani, G. Charpak, D. Rahm, C. Zupancic, 1969.
First operational chamber: A.H. Walenta, J. Heintze, B. Schürlein, NIM 92 (1971) 373.

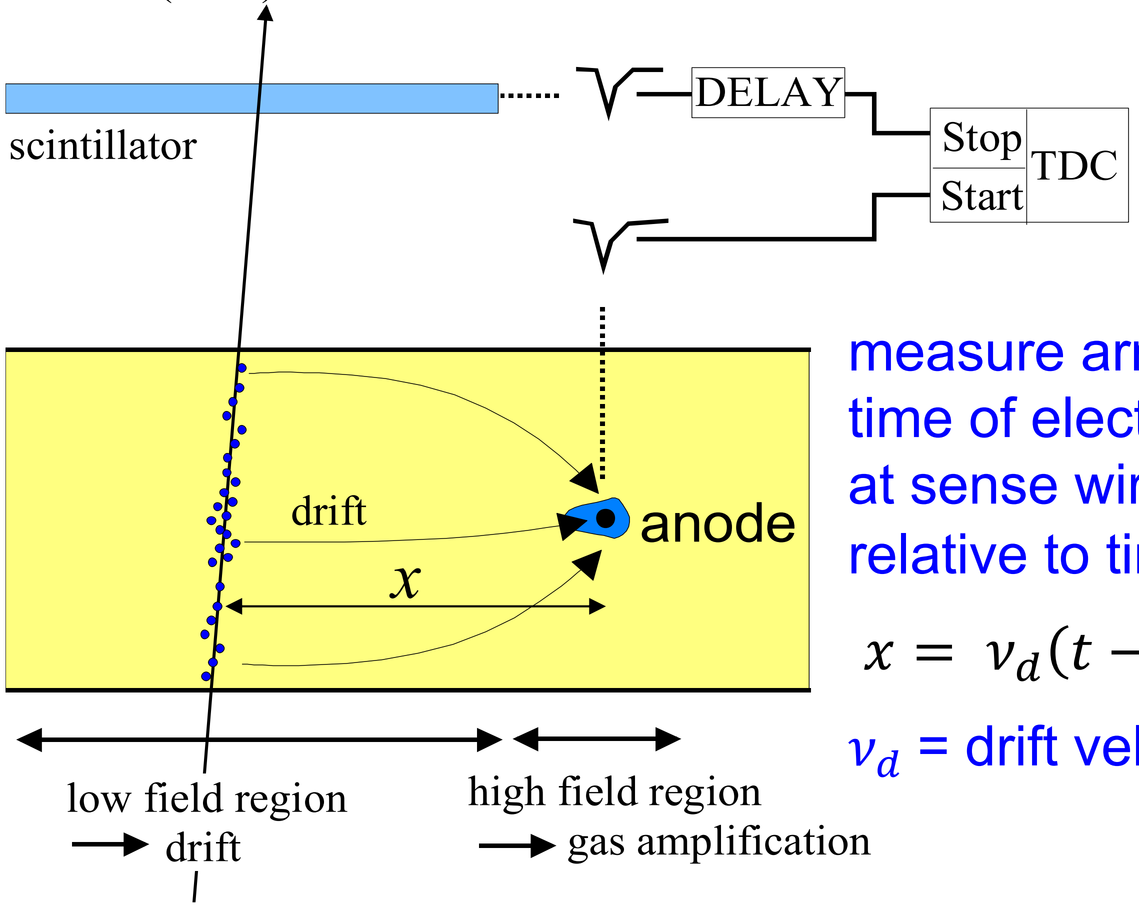

measure arrival time of electrons at sense wire relative to time t_0

$$x = v_d(t - t_0)$$

v_d = drift velocity

what happens during drift towards the anode wire ?

- diffusion ?
- drift velocity ?

Drift & diffusion in gases

No external fields:

Electrons & ions will lose energy due to collisions with gas atoms → thermalization

$$\varepsilon = \frac{3}{2} kT \approx 40 \text{ meV}$$

Undergo multiple collisions, an originally localized ensemble of charges will diffuse along with time t

$$\frac{dN}{N} = e^{-(x^2/4Dt)} dx/\sqrt{4\pi Dt}$$

D: diffusion coefficient

N: number of e⁻–ion pairs

gaussian spread $\sigma_x(t) = \sqrt{2Dt}$ or $D = \sigma_x^2(t)/2t$

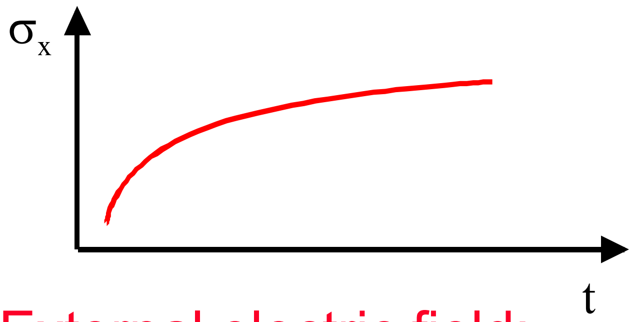

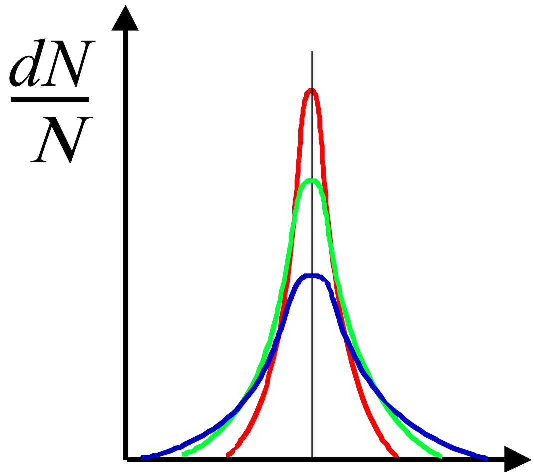

External electric field:

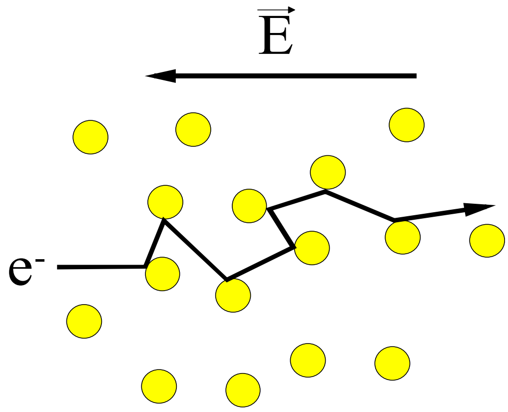

"stop & go" traffic due to scattering from gas atoms → drift velocity ∝ electric field:

$$\vec{v}_D = \mu \vec{E}$$

$\mu = e\tau/m$ (mobility)

$\tau\ (\nu, \epsilon, N_{\text{gas}})$ mean time between collisions,

$\nu\ (\epsilon)$ = velocity (kinetic energy) of electron/ion,

N_{gas} = number of gas molecules per unit volume

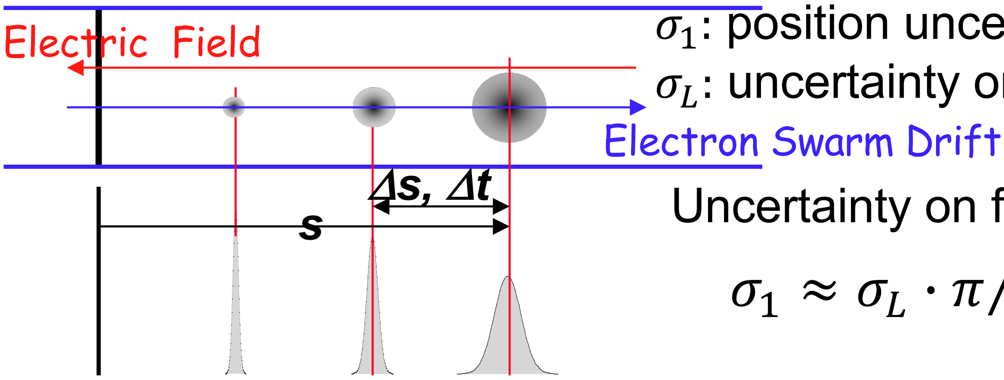

σ_1: position uncertainty first e^-
σ_L: uncertainty on drift length

Uncertainty on first electron:

$$\sigma_1 \approx \sigma_L \cdot \pi / 2\sqrt{3 lnN}$$

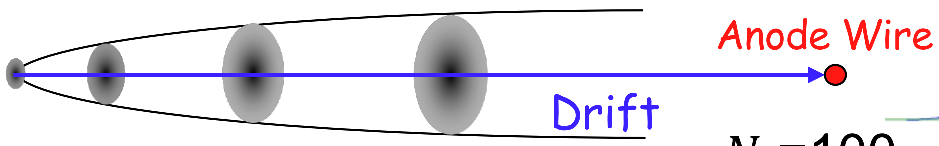

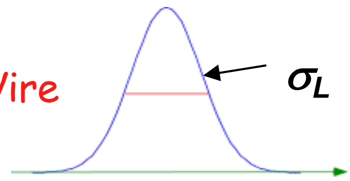

$N = 100 \Rightarrow \sigma_1 \approx 0.4\,\sigma_L$

Single electron Several electrons Many electrons

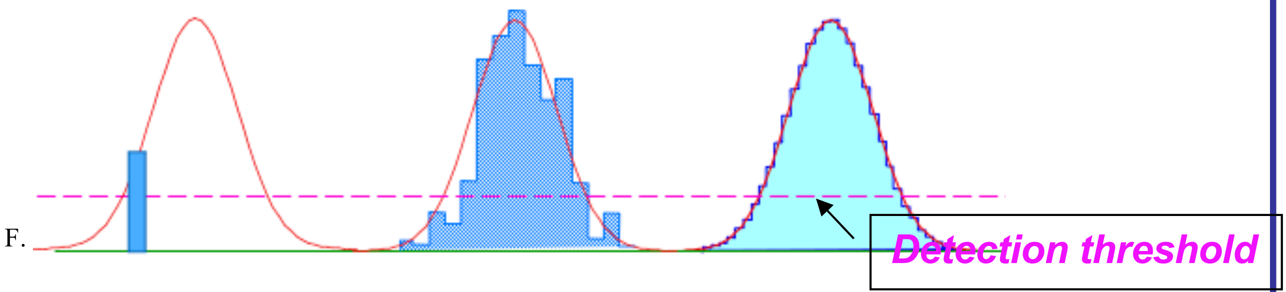

$$\tau = \frac{1}{N_{gas}\sigma(\epsilon)v} = \frac{\lambda}{v}$$

v: instantaneous velocity
N_{gas}: # of molecules/unit volume
σ: collision cross section
λ: average mean free path

σ depends strongly on electron energy ϵ due to interference effects with molecules ("Ramsauer")

typical electron drift velocity: **few cm/µs**

ion drift velocities: ≈ 1000 times smaller

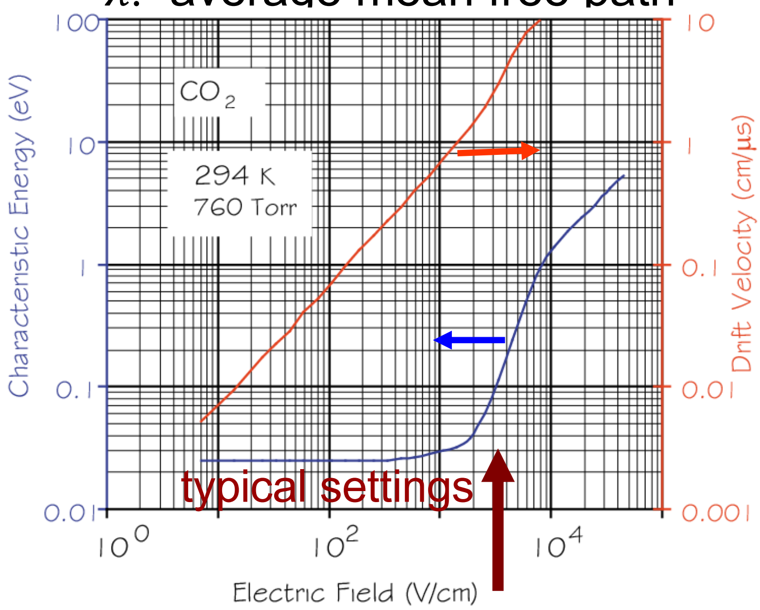

Drift Tubes (DT)

$$E(r) = \frac{U_0}{\ln(r_a/r_i)} \cdot \frac{1}{r}$$

Radiales E-Feld

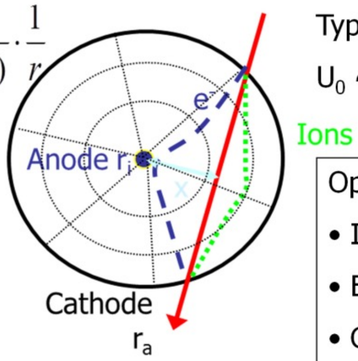

Typical parameters:

$U_0 \sim 2$ kV ; $r_a/r_i \sim$ cm/µm $\sim 10^{-5}$

Operational principle:

- Ionization along the particle's track
- Electrons drift to anode wire
- Gas amplification near the wire, $G \sim 10^3 \ldots 10^5$
- Charge collection, signal creation

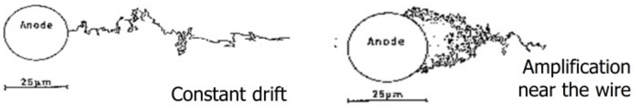

Applet

Resolution can be improved by:

Recording the drift time, Operation at overpressure

Improving the Resolution

1) Measurement of drift time Δt of electrons from location x (where particle passed) to the anode wire

Constant drift velocity v_D wanted (typically ~50 mum/ns, gas dependent)

Used by all exeriments these days

$x = v_D \Delta t$

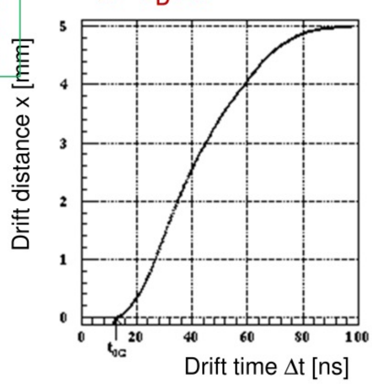

2) Application of overpressure

$$Diffusion\ \sqrt{D} \sim 1/\sqrt{p}$$

Only implemented by ATLAS

Resolution as a function of pressure

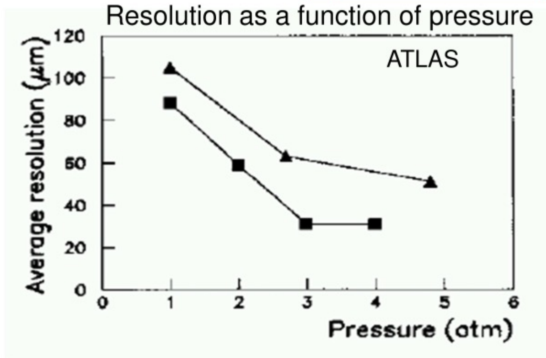

▲ ArC_2H_6 (70/30)%, d=3 cm, D_{Draht}=100 µm
■ $ArCO_2CH_4$ (45/45/10)%, d=2 cm, D_{Draht}= 50 µm

Resolution per cell (R-dependent) → ~ 100 µm → < 100 µm

K.Hoepfner, RWTH Aachen   Cern ACT Lecture: Muon Systems, May 2011   26

In presence of electric & magnetic fields, drift & diffusion are driven by $\vec{E}\times\vec{B}$ effects

Look at 2 special cases:

Special case: $\vec{E} \perp \vec{B}$

$$\tan \alpha_L = \omega\tau$$

α_L: Lorentz angle

$$\omega = e\vec{B}/m :$$

cyclotron frequency

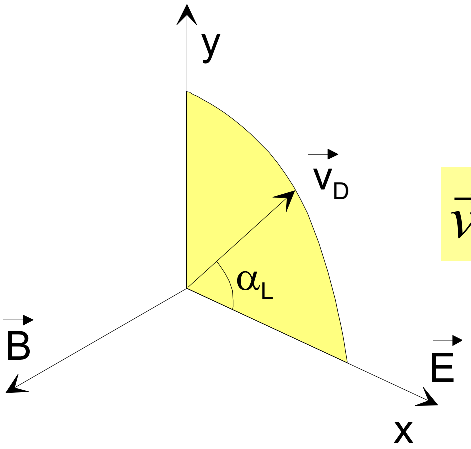

$\vec{v}_D \not\parallel \vec{E}$

Special case: $\vec{E} \parallel \vec{B}$

longitudinal diffusion (along B-field) unchanged. In transverse projection electrons forced on circle segments with radius v_T/ω transverse diffusion coefficient appears reduced

$$D_T(B) = D_{\text{no}\,\vec{B}}/(1+\omega^2\tau^2)$$

very useful … see TPC's !

Transverse diffusion (μm) for a 15 cm drift in different Ar/CH_4 mixtures

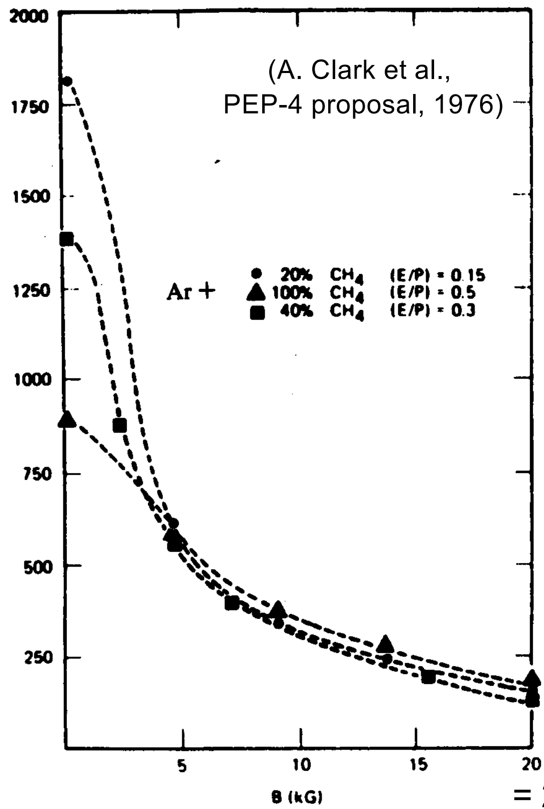

= 2 T

Time Projection Chamber (TPC) → full 3-D tracking

- xy from end plate gaseous detector (MWPC, GEM..)
- z from drift time
- in addition: dE/dx information

transverse diffusion significantly reduced by B-field.

PEP-4 TPC

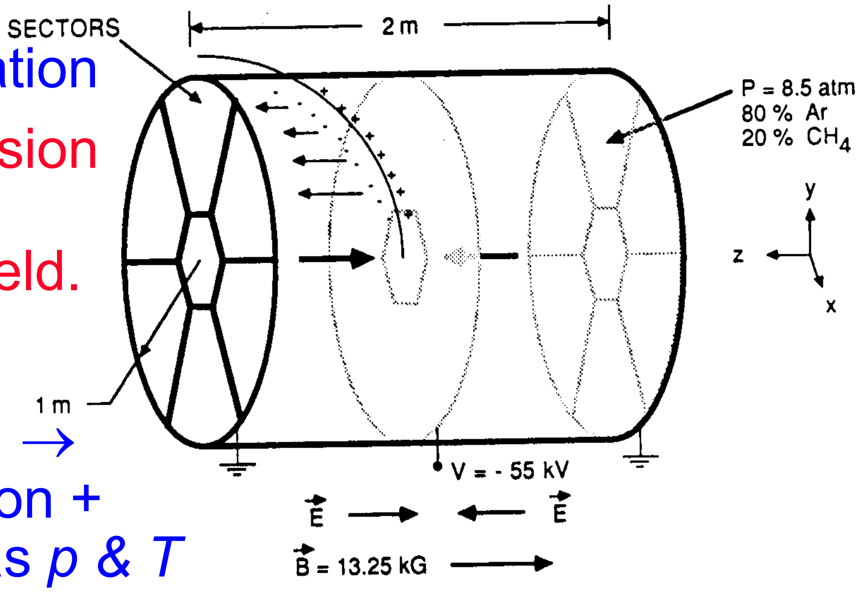

requires precise knowledge of v_D → LASER calibration + correction for gas *p* & *T*

drift over long distances → good gas quality required & not able to handle high rates (drift times μs – ms)

space charge problem from positive ions, drifting back to midwall → gating

drift region
gate
anode plane

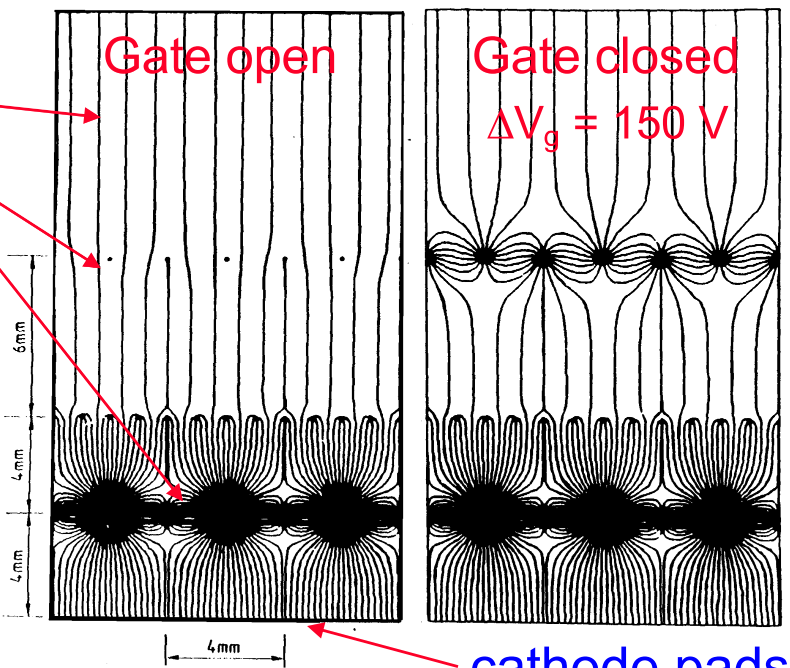

cathode pads

ALEPH TPC

(ALEPH coll., NIM A 294 (1990) 121,W. Atwood et. Al, NIM A 306 (1991) 446)

Ø = 3.6 m, L = 4.4 m

$\sigma_{R\phi} = 173\ \mu m$

$\sigma_z = 740\ \mu m$

(isolated leptons)

Because of MWPC limitations (rate, resolution…), new generation of TPC's use GEM's or Micromegas

This can enable continuous readout TPC and increase the granularity of the whole system

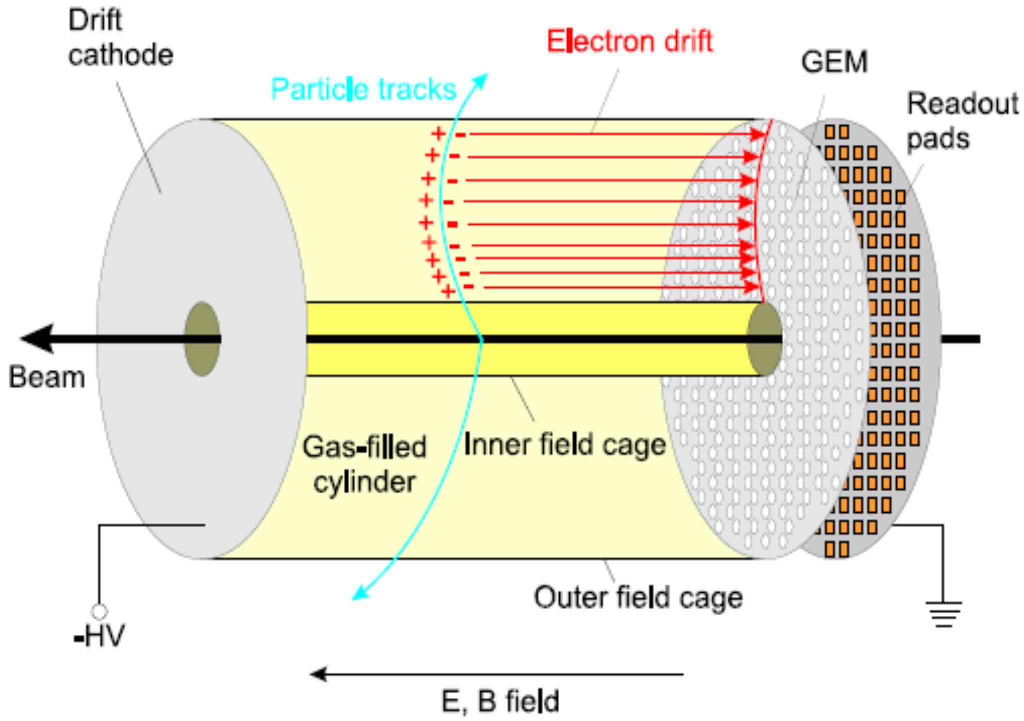

ALICE GEM TPC @ LHC

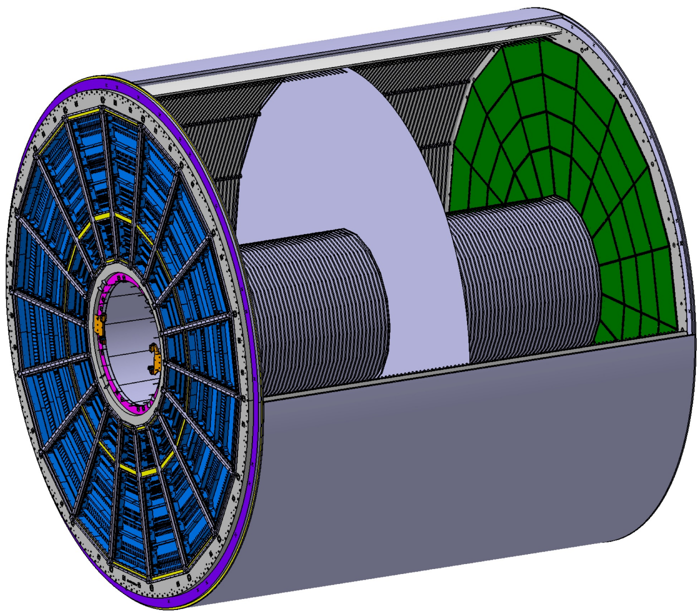

Gas Electron Multiplier

Standard GEM foil

- Copper-polymide-copper sandwich foil (5-50-5 μm).
- Geometrical pattern of etched holes with 140 μm pitch.
- Outer/inner hole $\varnothing \approx 70/50\mu$m.

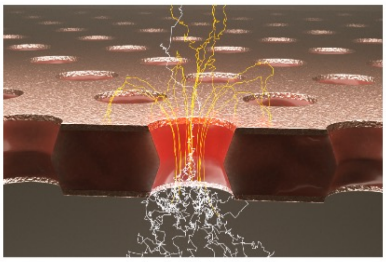

New design

- Stack of four GEM foils (S–LP–LP–S).
- Gain 2000 in $Ne/CO_2/N_2$ (90/10/5) gas mixture.

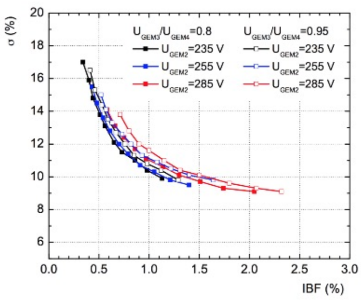

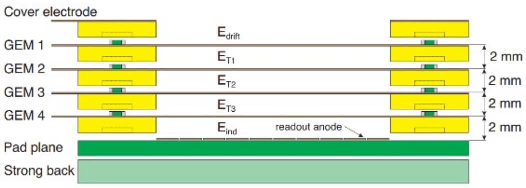

High Definition Optical Scanning
for quality assurance of GEMs

Hardware and tools

- X-Y-Z table with LED background illumination.
- CMOS Camera with telecentric optics and inline lighting.
- Ring-light option.
- Custom robot control-software based on Labview.
- Data storage.
- Computer for image analysis with custom software.

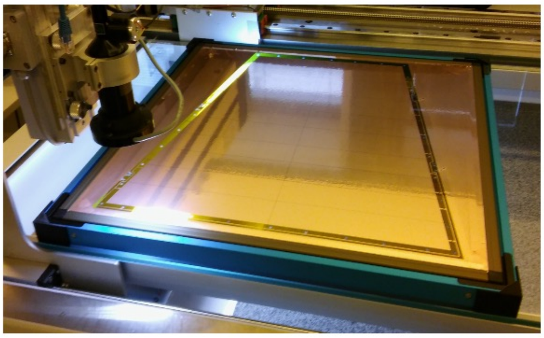

UH & HIP

TEV collaboration 8/ 10

High Definition Optical Scanning (iii) for quality assurance of GEMs

Results (all measured values in μm)

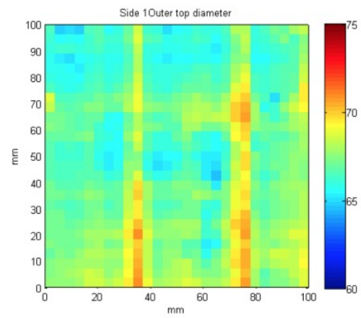

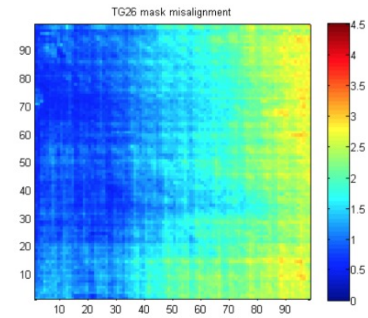

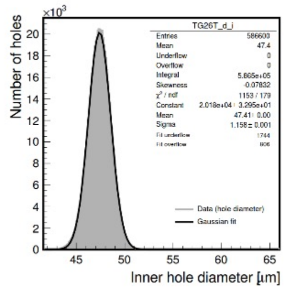

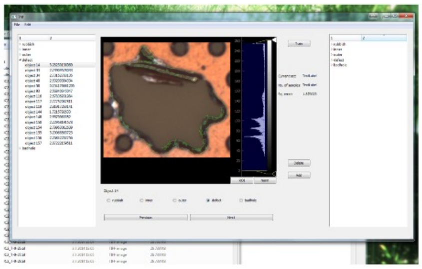

10/ 10

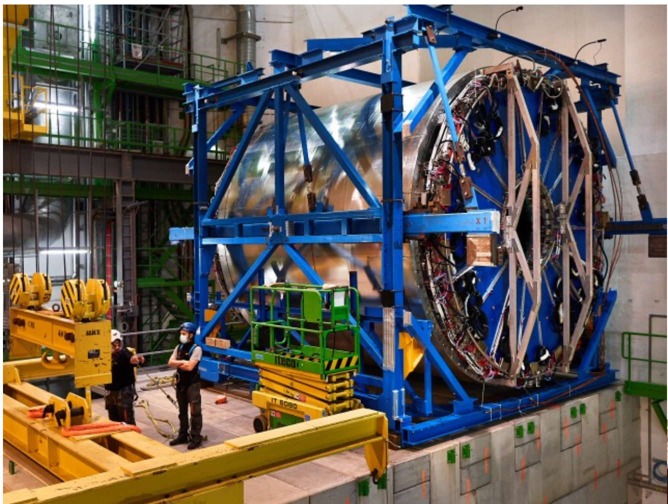

Preparation of new GEM TPC installation

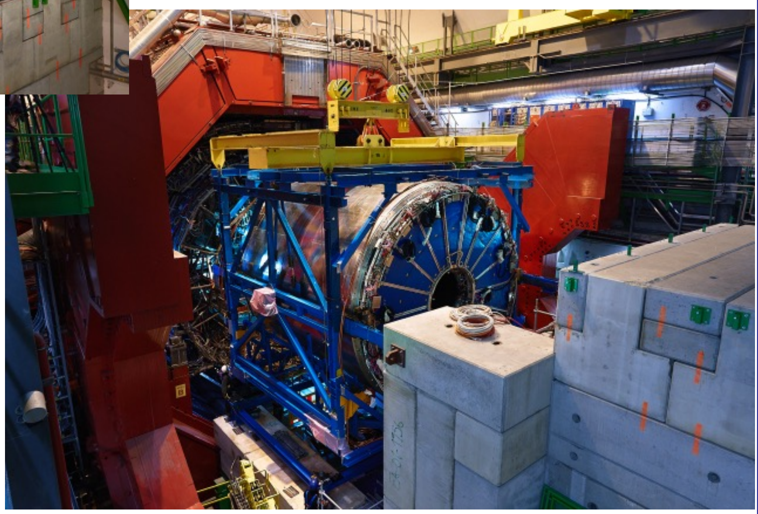

Installation of new GEM TPC into ALICE in August 2020

FAIR (Facility for Antiproton and Ion Research) under construction @ GSI in Darmstadt, Germany. One of five scientific projects: NUSTAR studying radioactive ion beams with Super-FRS (fragment separator) beam line

NUSTAR collaboration (Nuclear Structure, Astrophysics, and Reactions) has more than 700 members in total.

Part of the Finnish Contribution will be in the superconducting in-flight separator (Super-FRS) Diagnostic systems

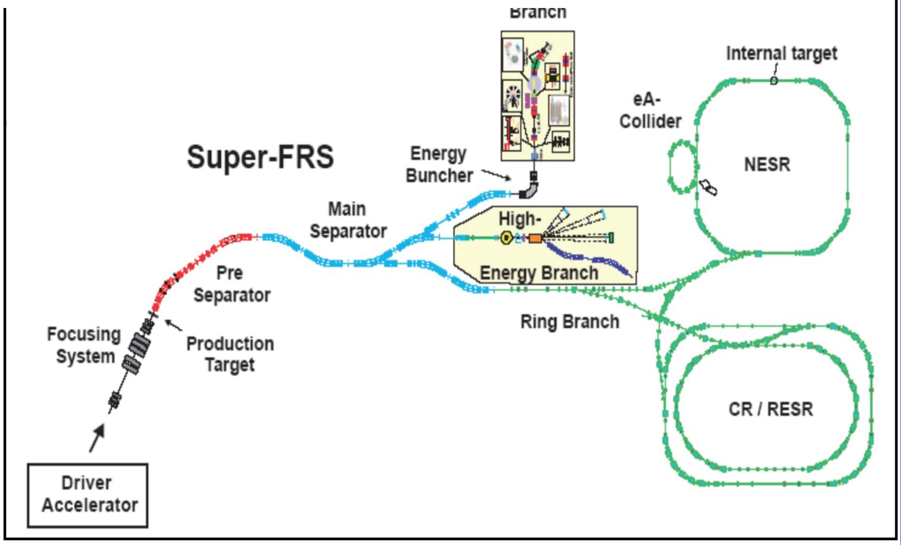

GEM-TPC Development for tracking at Super-FRS

INTRODUCTION & MOTIVATION

Projectile:
Elements p – U
Energy up to 1.5 GeV/u
Intensity up to 10^{12} /spill

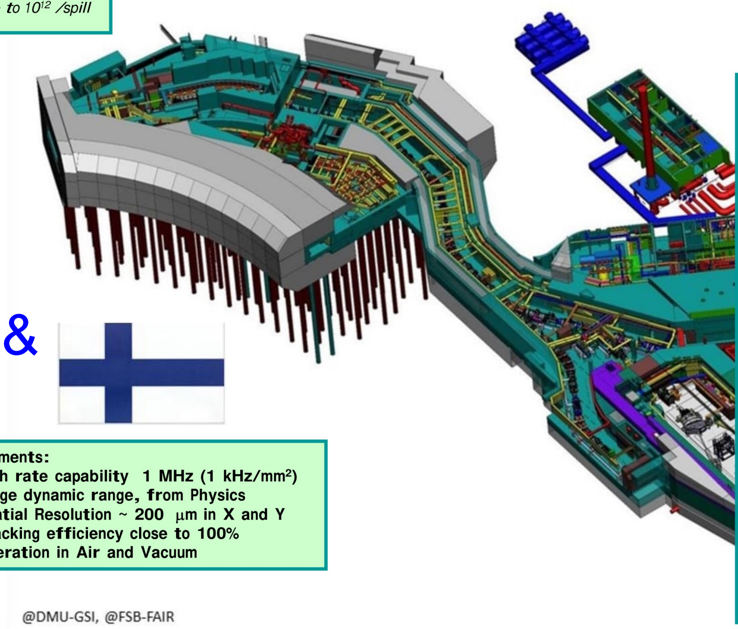

UH & HIP

THE PROJECT TIMELINE

The R&D and Design can be finalized by:

Q4/2024

Mass production:

Q1/2025 – Q1/2026

Part of the Finnish Contribution will be in Diagnostic systems, which is a work package dedicated to provide 14 GEM-TPC detectors.

Requirements:
1.- High rate capability 1 MHz (1 kHz/mm^2)
2.- Large dynamic range, from Physics
3.- Spatial Resolution ~ 200 μm in X and Y
4.- Tracking efficiency close to 100%
5.- Operation in Air and Vacuum

@DMU-GSI, @FSB-FAIR

GEM-TPC Development for tracking at Super-FRS

THE GEM-TPC PROTYPE in TWIN CONFIGURATION – HGB4

Lateral view

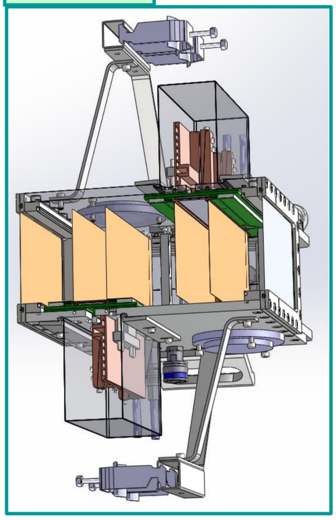

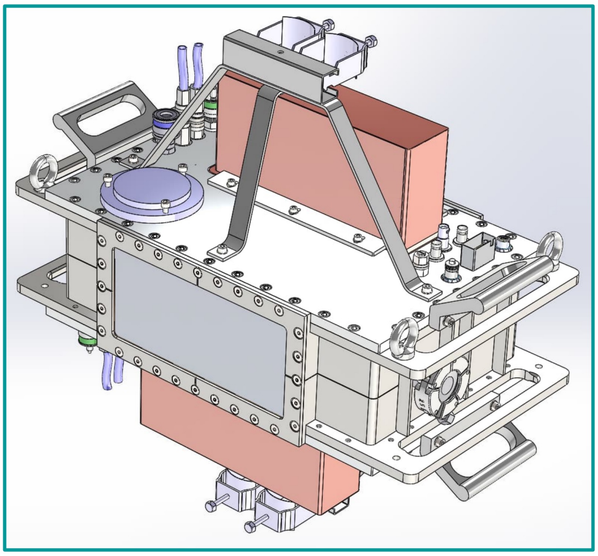

View beam downstream

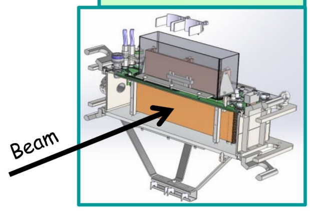

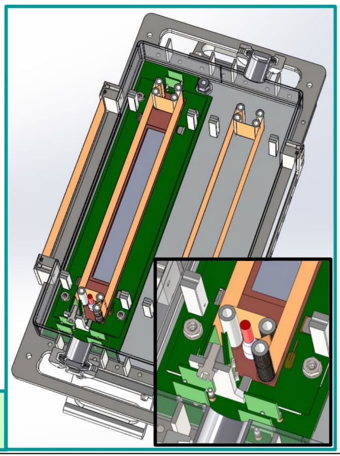

This GEM-TPC has a twin configuration, which means that two GEM-TPC are positioned back to back. This will allow us to increase the tracking efficiency in high rate environment.

View from the top

GEM-TPC Development for tracking at Super-FRS

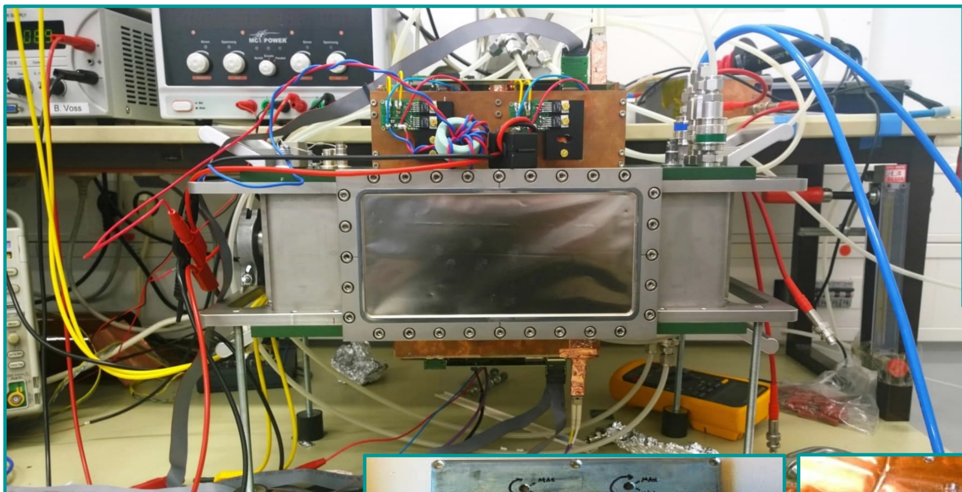

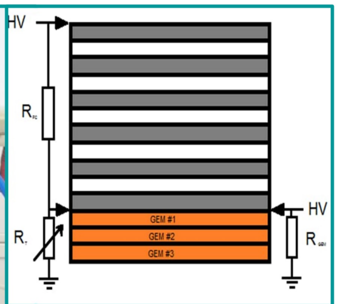

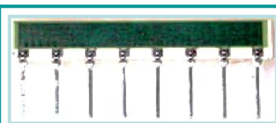

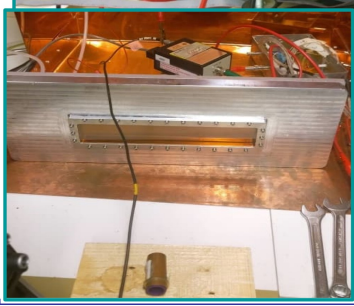

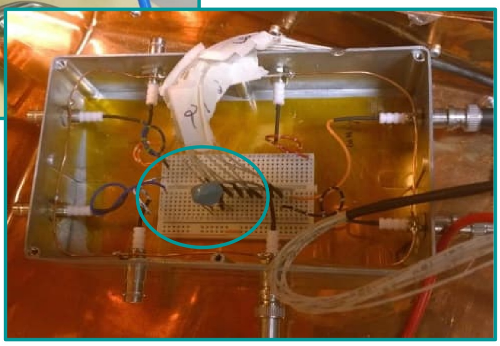

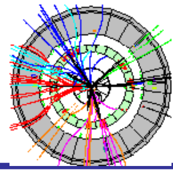

Silicon detectors

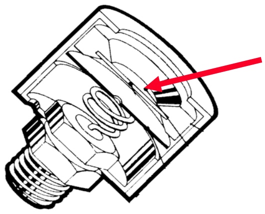

Si sensor

Solid state detectors have a long tradition in measurement of energy (Si, Ge, Ge(Li)).

Interested in their use as precision trackers !

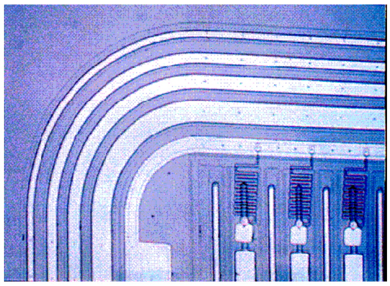

ATLAS SCT

Some characteristic numbers for silicon

- band gap energy: E_{gap} = 1.12 eV.
- $E_{creation}$(electron-hole pair) = 3.6 eV (~ 30 eV in gas) → large number of charge carriers per unit energy loss → good energy resolution
- high specific density (ρ = 2.33 g/cm^3) → compact
- high mobility: $\mu_{electron}$ = ~1400 cm^2/Vs, μ_{holes} = ~ 450 cm^2/Vs (depends somewhat on doping concentration and temperature) → fast charge collection (< 30 ns)
- detector production by microelectronic techniques → small dimensions → high spatial resolution
- rigidity of silicon allows thin self supporting structures. typical thickness 250–300 μm → ~ 24 000 – 32 000 e^--hole pairs (average)
- But no charge multiplication mechanism!!

Semiconductor: valence band (nearly) filled & conduction (conductance) band (nearly) empty

How to obtain a signal ?

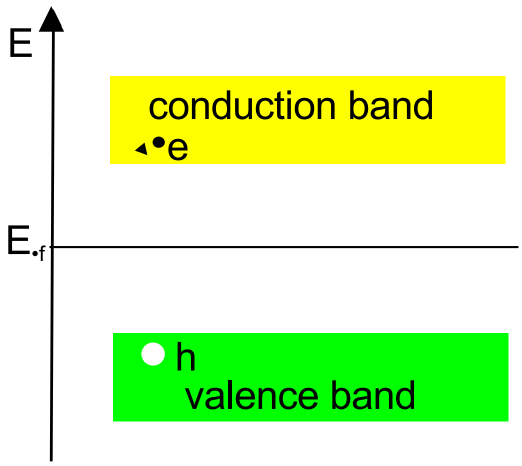

In a pure intrinsic (undoped) material electron density n & hole density p equal. $n = p = n_i$

$$n_i \propto T^{3/2} e^{-E_{\text{gap}}/2k_B T}$$

Silicon: $n_i \approx 1.45 \cdot 10^{10}$ cm^{-3}

This volume has $4.35 \cdot 10^{8}$ free charge carriers, but only $3.2 \cdot 10^{4}$ e-hole pairs produced by a MIP.

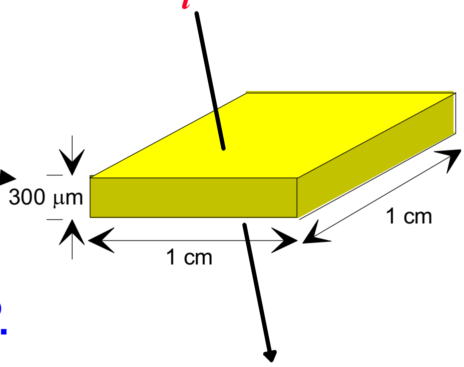

For semiconductors $n \cdot p = n_i^2$ = constant

$\rightarrow$ Reduce number of free charge carriers, i.e. first dope & then deplete the detector

Most detectors make use of reverse biased p-n junctions

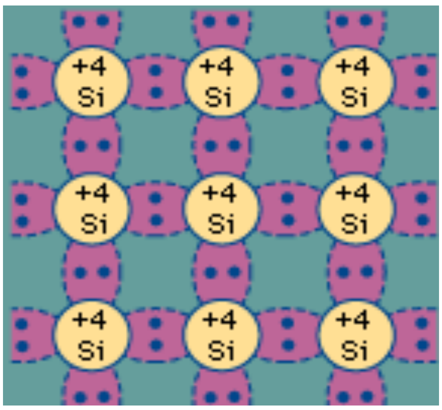

Electron Configuration for Si:

K	2
L	8
M	4 + 4 by bonding $\rightarrow$ 8 group

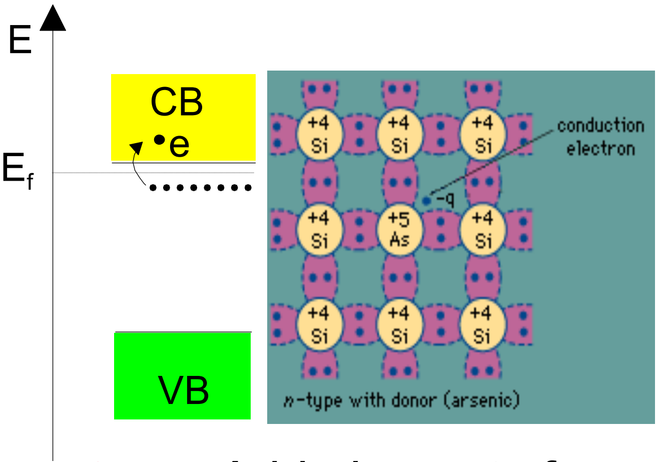

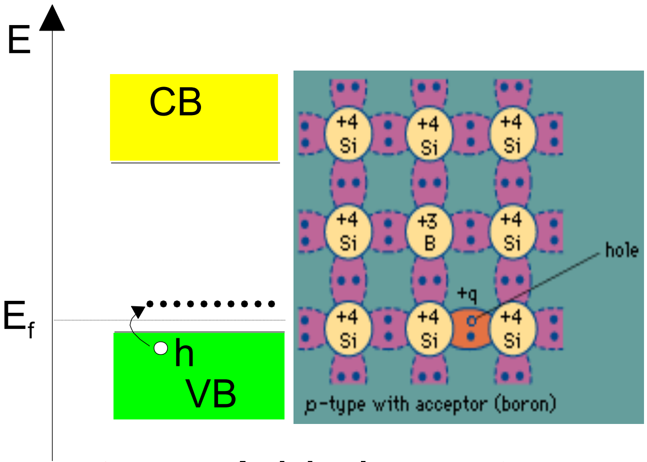

n-type: Add elements from Vth group, donors, e.g. P, As. Free electrons ⇒ electrons majority carriers.

p-type: Add elements from IIIrd group, acceptors, e.g. B, Ga. Free holes ⇒ holes majority carriers.

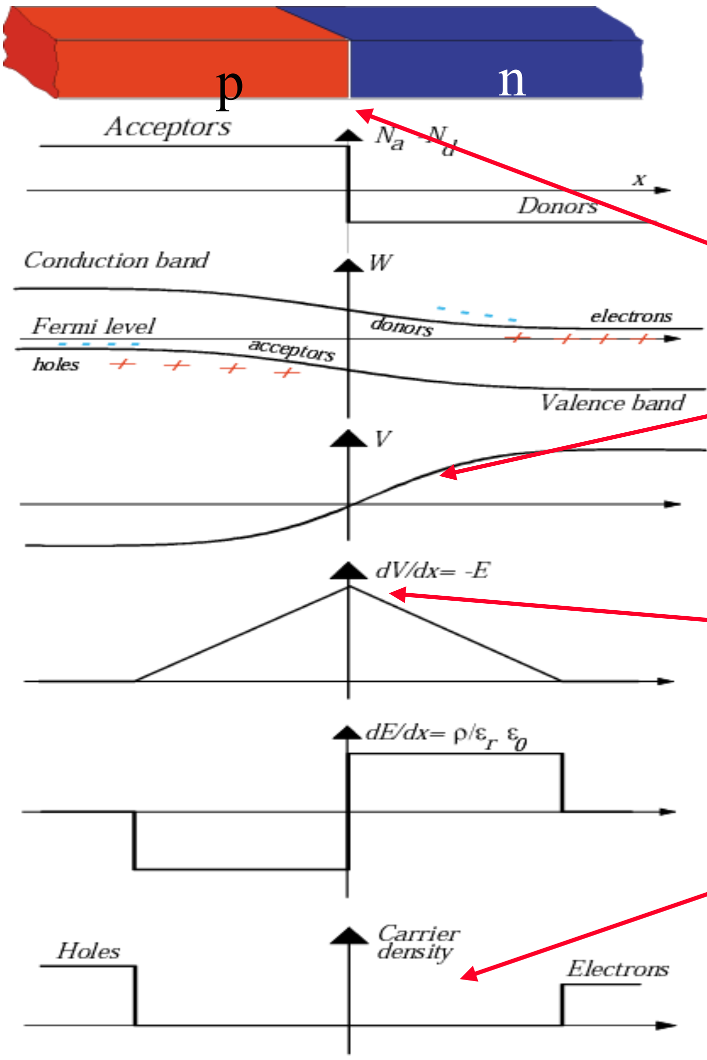

pn junction (= diode) (without bias)

diffusion of e⁻ into p–zone, holes into n–zone → potential difference stopping diffusion → thin depletion layer

peak electric field at boundary between p– & n–zone

no free charge carriers in depletion zone

D. A. Fraser, the physics of semiconductor devices

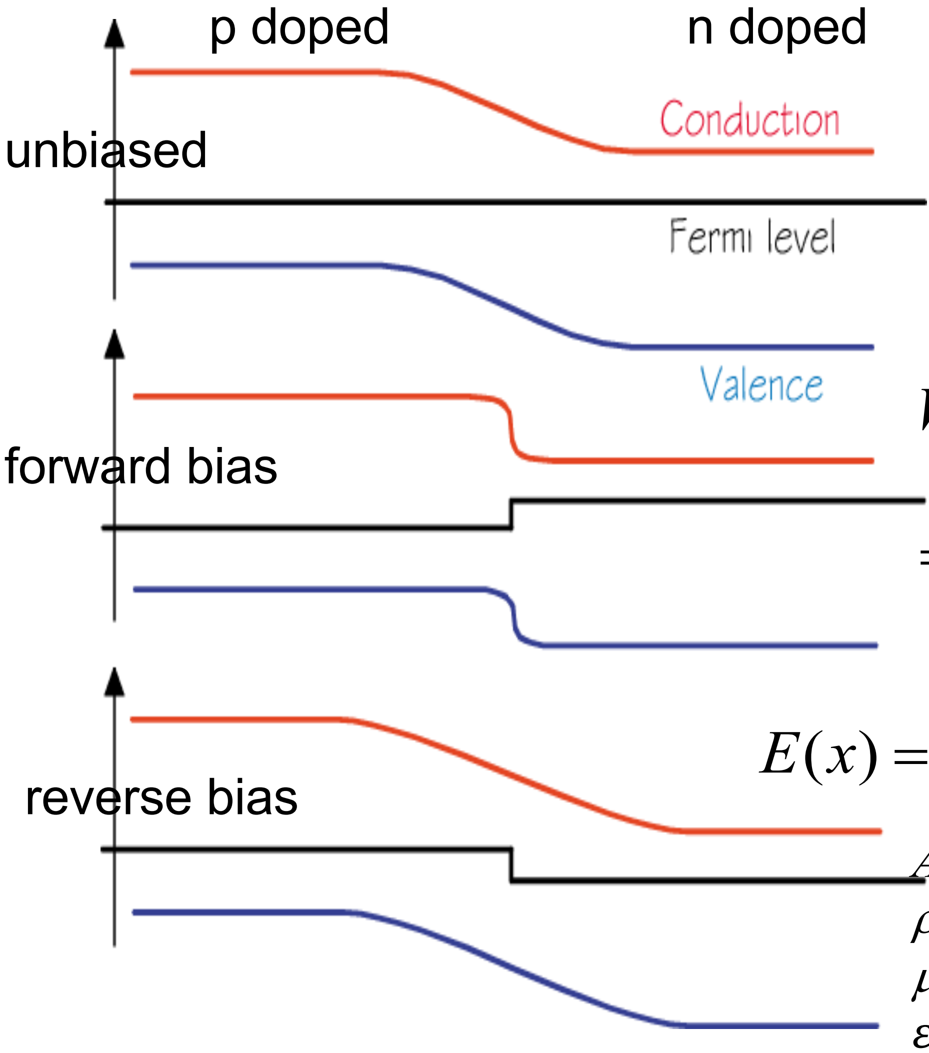

capacitance:

$$C(V) = \frac{\varepsilon A}{W_D}$$

depletion layer thickness:

$$W_D \approx \sqrt{\frac{2\varepsilon V_{\text{bias}}}{eN}} = \sqrt{2\mu\rho\varepsilon V_{\text{bias}}}$$

electric field:

$$E(x) = \frac{2V_{\text{bias}}}{W_D^2}(W - x)$$

A : diode area
ρ : resistivity
μ : mobility
ε : permittivity
V_{bias}: bias voltage

reverse bias voltage applied (~ 100V) → thin depletion zone extended over full junction → fully depleted detector. energy deposited in depletion layer, due to e.g. charged particles, creates free e⁻–hole pairs. In field, e⁻'s drift towards n–side, holes towards p–side → detectable current

	detector grade	electronics grade
doping concentration	10^{12} cm^{-3} (n) – 10^{15} cm^{-3} (p$^+$)	$10^{17(18)}$ cm^{-3}
resistivity	~ 4 kΩ·cm	~ 1 Ω·cm

Spatial information by segmenting p doped layer →
single sided microstrip detector. schematically !

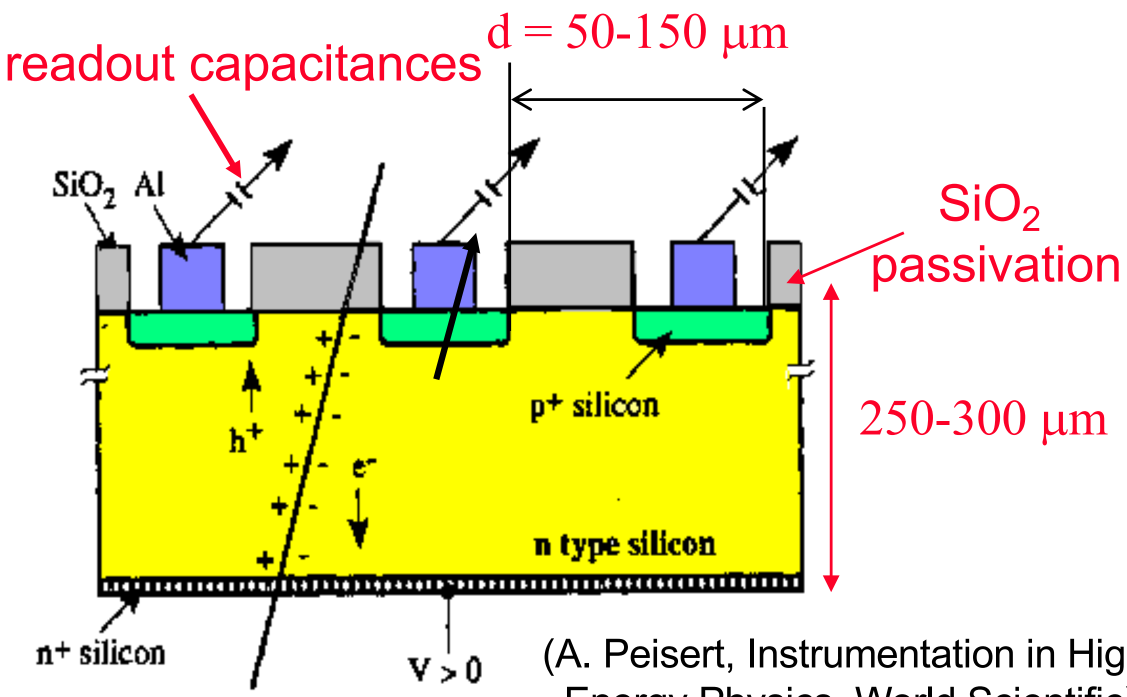

(A. Peisert, Instrumentation in High Energy Physics, World Scientific)

defines end of depletion zone + good ohmic contact

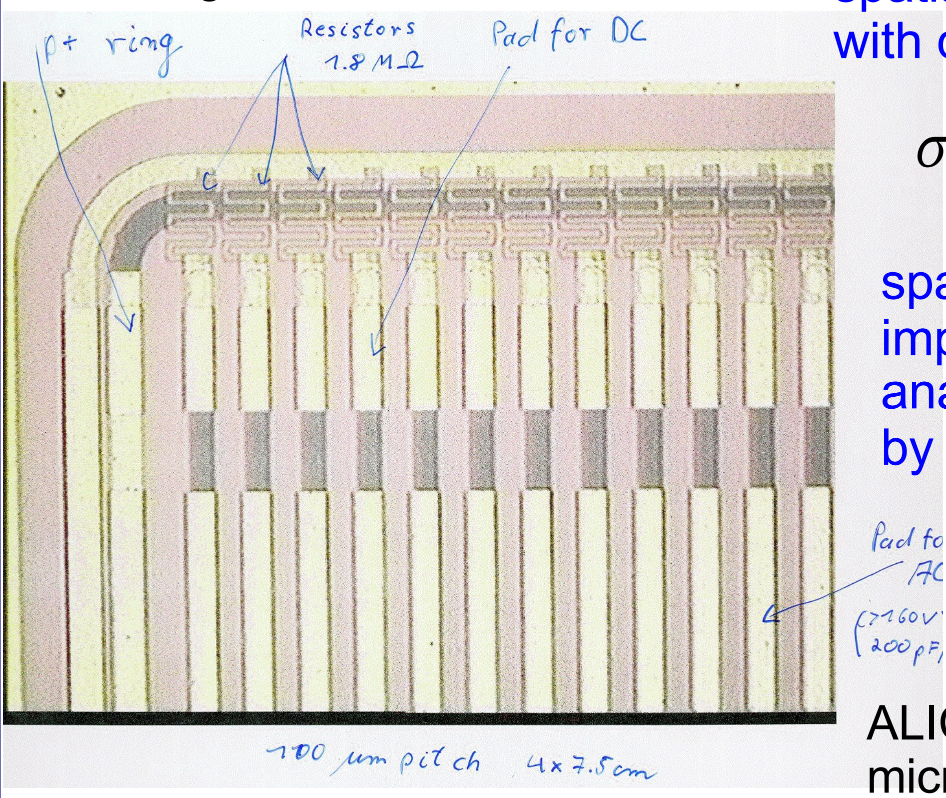

spatial resolution with digital readout:

$$\sigma_x \approx \frac{d}{\sqrt{12}}$$

spatial resolution improves with analog readout by up to a factor 2

ALICE: single sided micro strip prototype

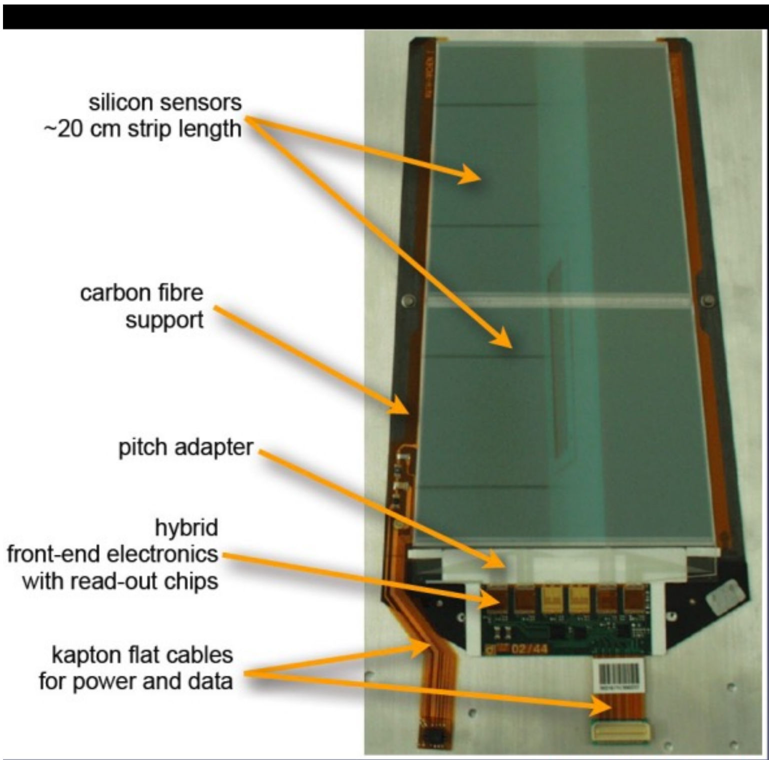

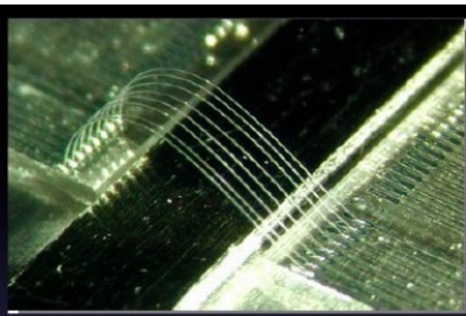

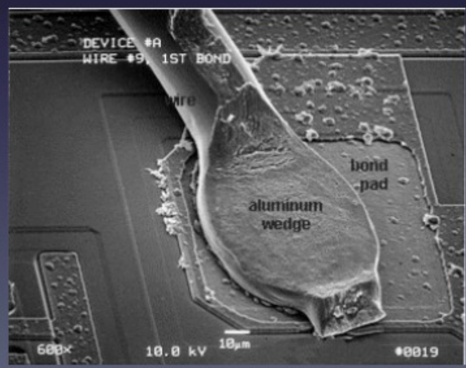

D. Bortoletto Lecture 4 24

Second coordinate: Double sided strip detectors

- **Advantages:**
  - More elegant for measuring 2 coordinates than using stereo modules
  - Saves material
- **Disadvantages:**
  - Needs special strip insulation of n-side (p-stop, p-spray techniques) also ALD
  - Complicated manufacturing and handling procedures
- Expensive
- Ghost hits possible

ALD = atomic layer deposition

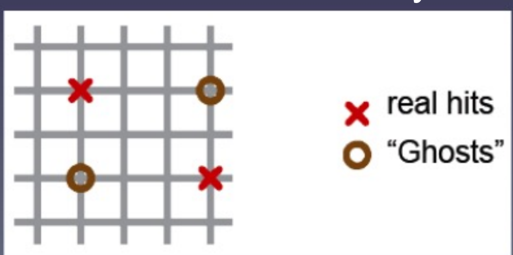

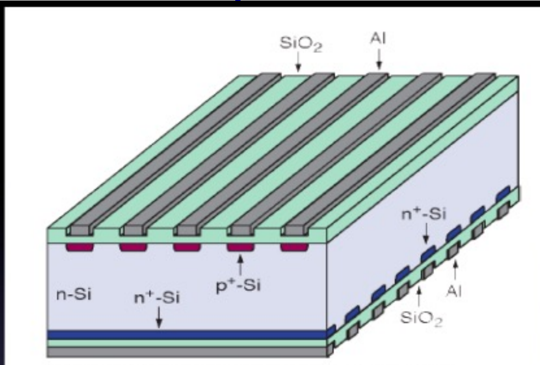

Scheme of a double sided strip detector (biasing structures not shown)

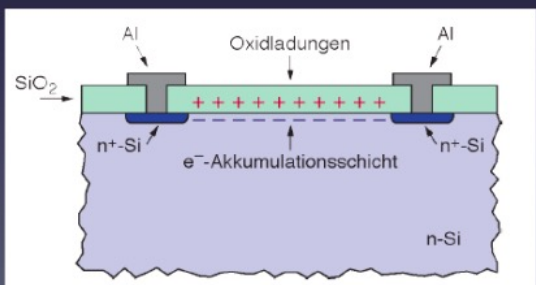

Positive oxide charges cause electron accumulation layer.

25

Second coordinate: square segmentation →

- **Hybrid Active Pixel Sensors (HAPS)**
  - segment silicon to diode matrix
  - also readout electronic with same geometry
  - connection by bump bonding techniques

Flip-chip assembly:

pixel detector bump-bonded to readout electronics

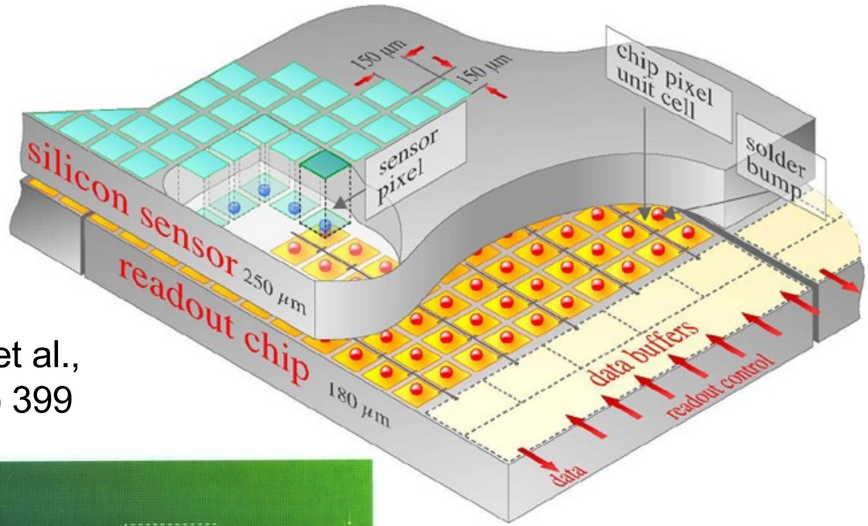

RD 19, E. Heijne et al., NIM A 384 (1994) 399

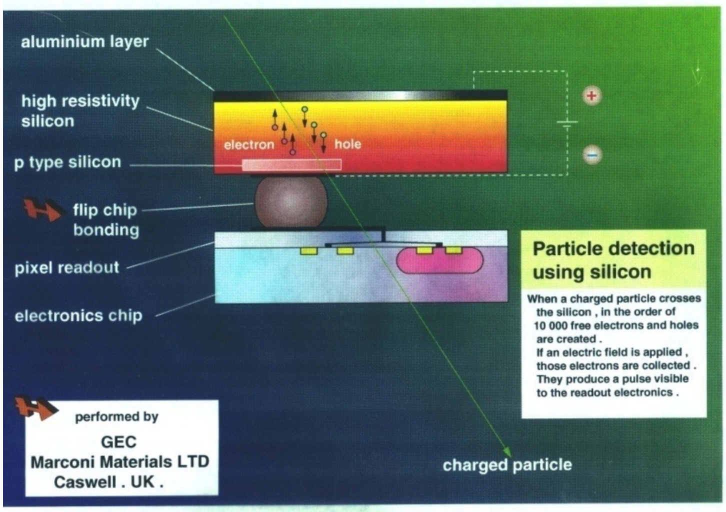

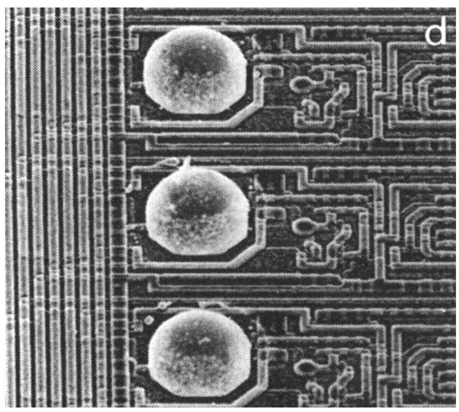

- First experiment WA94 (1991), WA97 (“Omega”)
- HAPS detectors extensively used at LHC (ATLAS, ALICE & CMS) due their good ability to do tracking in high multiplicity environment with a high precision.

Important features

- Macroscopic features of a good semiconductor sensor are
  - ✔ Low capacitive load → low noise in readout electronics
  - ✔ Low leakage current → low noise in readout electronics
  - ✔ Good charge collection
  - ✔ High speed

current density J vs current I: $I = J \cdot A$

Characteristics of the diode structure

- **Capacitance (C-V)**

The capacitance of the diode influences the noise of the readout electronics by loading the amplifier

The capacitance of the pn-junction is given by

$$C_j = \frac{\epsilon_R \epsilon_0}{W_D} \cdot A$$

The capacitance of the junction will decrease when reverse bias voltage is applied until full depletion is reached.

WE WANT LOW CAPACITANCE!

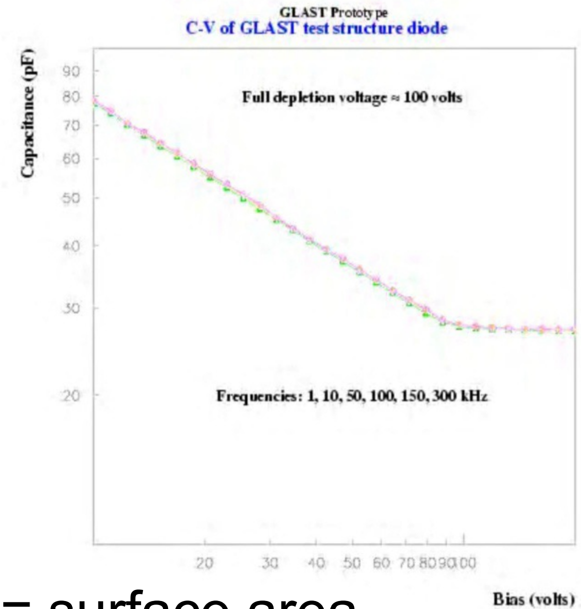

A = surface area of pn-junction

Characteristics of the diode structure

$\tau_g \propto T^{-0.5}\, e^{+|\Delta t|/kT}$ *

- **Leakage current (I-V)**

✔ diffusion current

Electrons generated in the p+ region and holes generated in the n+ region diffuse to the junction and are collected by electrodes. Small effect for Si but large for Ge at room temperature. ⇒ Ge detectors must be cooled !!

$$J_s = q\sqrt{\frac{D_P}{\tau_P}}\frac{n_i^2}{N_D}$$

where D_P is the diffusion constant for electrons in the p+ region and τ_P is the lifetime of the electron

✔ generating current

This is the dominated current in a good sensor. The current is due to generation-recombination in the depleted region.

$$J_g = q\, g W_D$$ (current per area)

g is the generation rate dependent of the intrinsic carrier concentration, n_i. τ_g = charge carrier generation life time (~10^{-3} s)

$$g = \frac{n_i}{\tau_g}$$

- **Leakage current (I-V)**

✔ generating current(cont.)

The current is also sensitive to temperature. 7 K decrease in T halves current. Lower T ⇒ increase generation life time τ_g ⇒ Si detector cooled !!

✔ surface current

Surface current is a contribution on complex effects happening in the boarder between the semiconductor and surface oxide. The current level is very dependent on processing quality and handling.

Δt = energy difference between trap and intrinsic Fermi levels

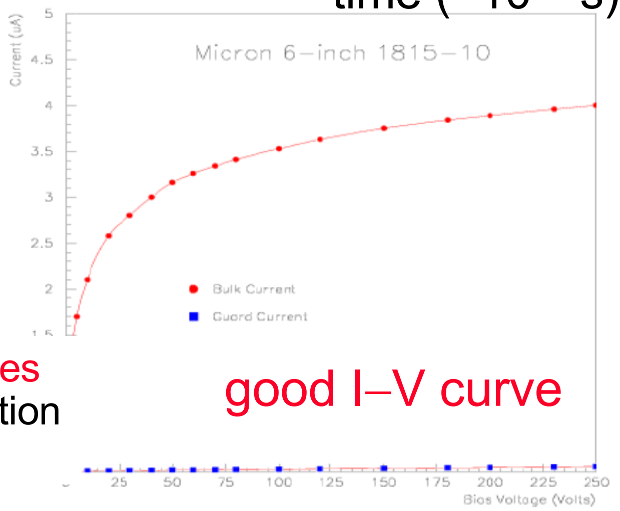

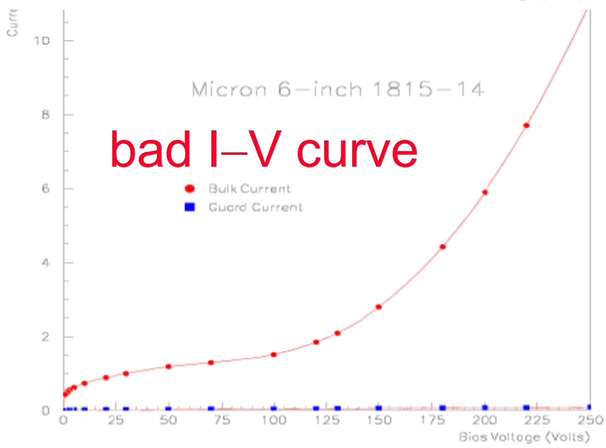

* see e.g. A. Chilingarov, JINST 8 (2013) P10003

Pixel detectors that combine separate sensor and electronics, fabricated with different processes, are a hybrid technology.

The *hybrid* geometry of the detector *introduces substantial material into the detection volume.*

This can be traced to the demands this design makes on the power budget through: sensor bias, analog and digital architecture, and data transmission.

This translates to copper conductors and cooling systems, and reduced positional resolution.

Initiatives to reduce power consumption in hybrid detectors:
- reduce material per detector layer
- integrate power conductors in mechanical support
- introduce special powering systems including DC-DC converters and serial powering of modules.

A different solution: *monolithic detectors*....

Most promising technology: MAPS

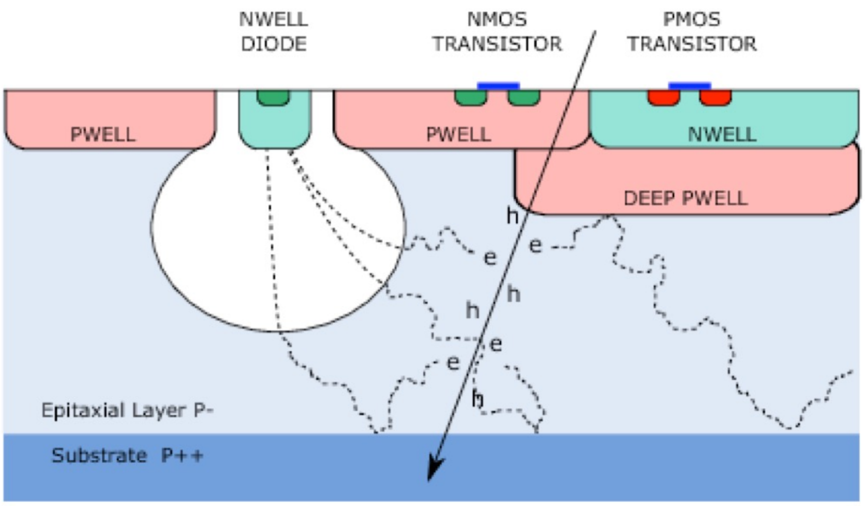

Monolithic Active Pixel Sensors[1,2] (MAPS) use an n-channel MOSFET transistor (NMOS) embedded in an *epitaxial* p-layer (thickness 15 microns) similar to standard CMOS chips. The n-well of the transistor collects the electrons generated by charged particles from a thin depletion layer through diffusion only.

[1] R.Turchetta, et al., Nucl. Instr. and Meth. in Phys. Res. A 458: 677-689, 2001.
[2] I. Peric, Nucl. Instr. and Meth. in Phys. Res. A 582: 876-885, 2007.

ALICE ITS installed 2021 for LHC Run 3

- Based on the Alpide chip in TJ 180 nm

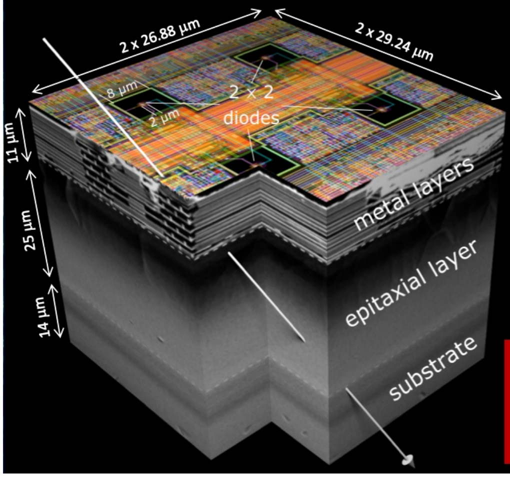

- Tremendous progress in CMOS pixel designs
  - Pixel pitch: 29 μm x 27 μm
  - Power < 40 mW/cm^2
  - Integration time <10 μs

(not fast enough for CMS & ATLAS)

All monolithic silicon pixel tracking becoming possible

- ALICE MAPS-CMOS Tracker
  - 7-layers, 12.5 Giga pixels, 10m^2
  - R coverage: 23 – 400 mm
- Material/layer:
  - 0.3% X_0 (IB)
  - 1.0% X_0 (OB)

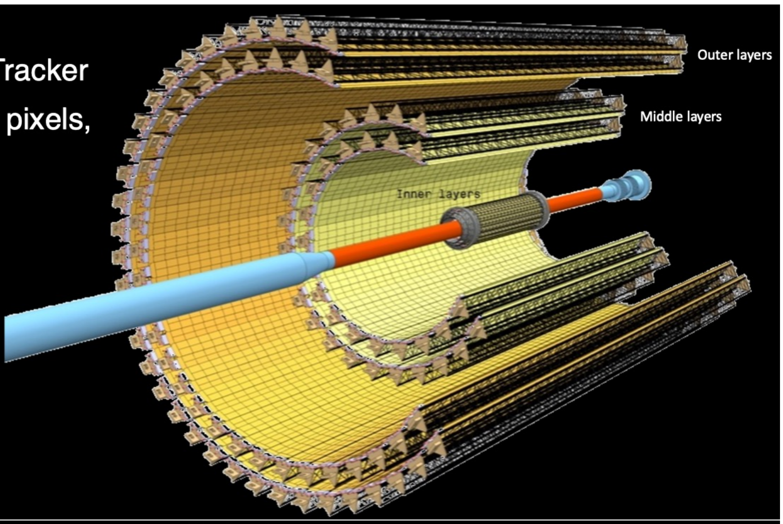

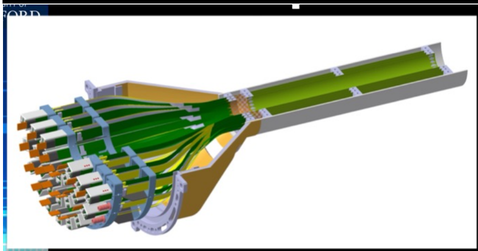

Technology advances:

- 300 mm wafer-scale chips fabricated with stitching
- thinned down to 20-40 µm bent to the target radii
- held in place by carbon foam ribs

Key benefits:

- extremely low material budget: 0.02-0.04% X_0 (beampipe: 500 µm Be: 0.14% X_0)
- homogeneous material distribution leading to smaller systematic error

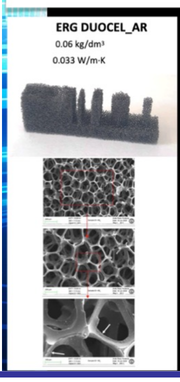

D. Bortoletto, MT-

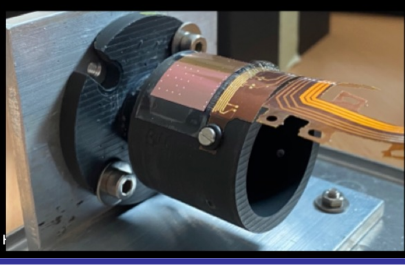

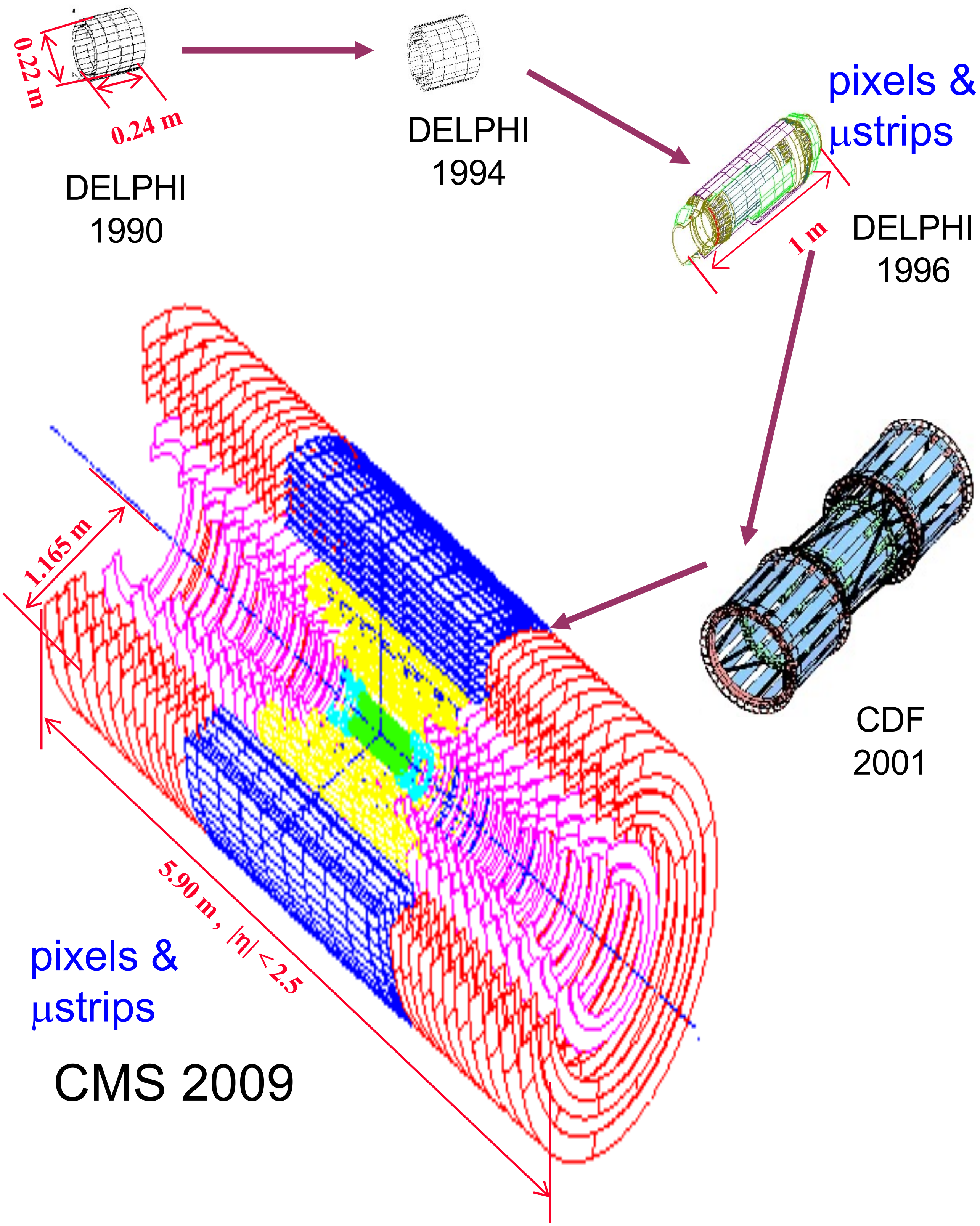
0.22 m
0.24 m
DELPHI 1990
DELPHI 1994
pixels &
µstrips
1 m
DELPHI 1996
CDF 2001
1.165 m
5.90 m , |η| < 2.5
pixels &
µstrips
CMS 2009

Purpose of silicon trackers

The role of the tracking detector is to image with the highest possible precision the trajectories of charged particles.

Their many applications in a particle physics experiment:

1. **Reconstruct vertices**: identify cases where 2 or more tracks emerge from a common point. The primary vertex indicates the initial hard interaction. The secondary vertex signals that a particle decay occurred at that vertex – typically a heavy particle: c, b, τ.

2. **Reconstruct the curvature of tracks** in a known magnetic field – to infer their momentum p. The sign of the curvature gives the particle's electric charge.

3. **Measure track impact parameter:** gaps between vertices, or events where the momentum emerging from a secondary vertex does not point to the primary vertex – these indicate intermediate particles.

4. **Measure finite particle lifetimes** – to identify production of b-hadrons or tau leptons.

5. **Provide a trigger** for events of special interest.

CMS high pileup event with 78 reconstructed vertices

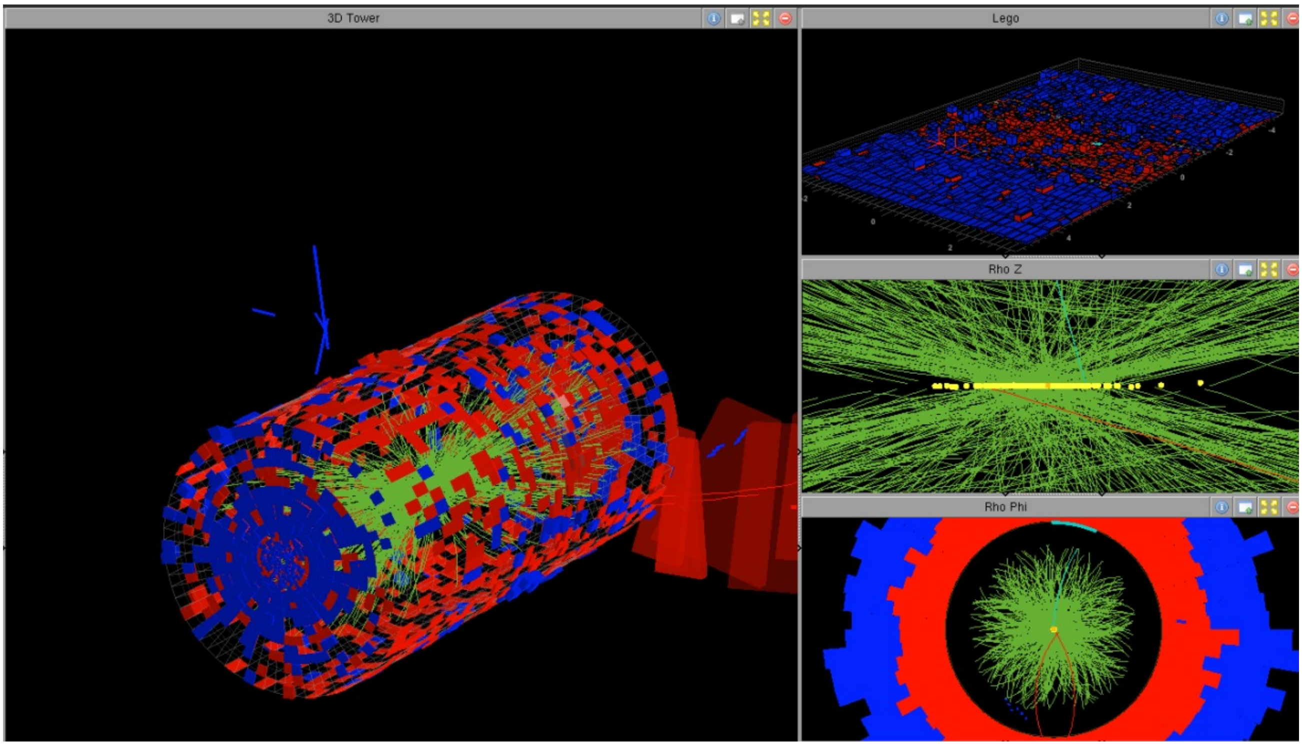

Motivation: distinguish decay products of b hadrons or τ leptons (flying few 100 μm to few cm before decay) from particles coming from initial collision point (= "primary vertex").

two methods: a) signed impact parameter (= distance of closed approach from particle trajectory to primary vertex)

$\alpha < \pi/2 \rightarrow \delta = +|\delta|$ $\qquad$ $\alpha > \pi/2 \rightarrow \delta = -|\delta|$

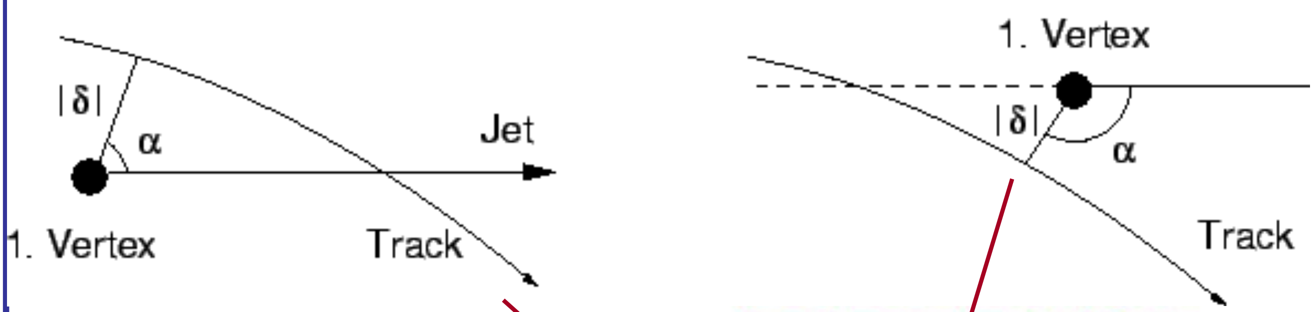

negative part of distribution used for obtaining resolution (no lifetime effect expected):

usually use impact parameter significance

$$S = (|\delta| / \sigma_\delta) \cdot \text{lifetime sign}$$

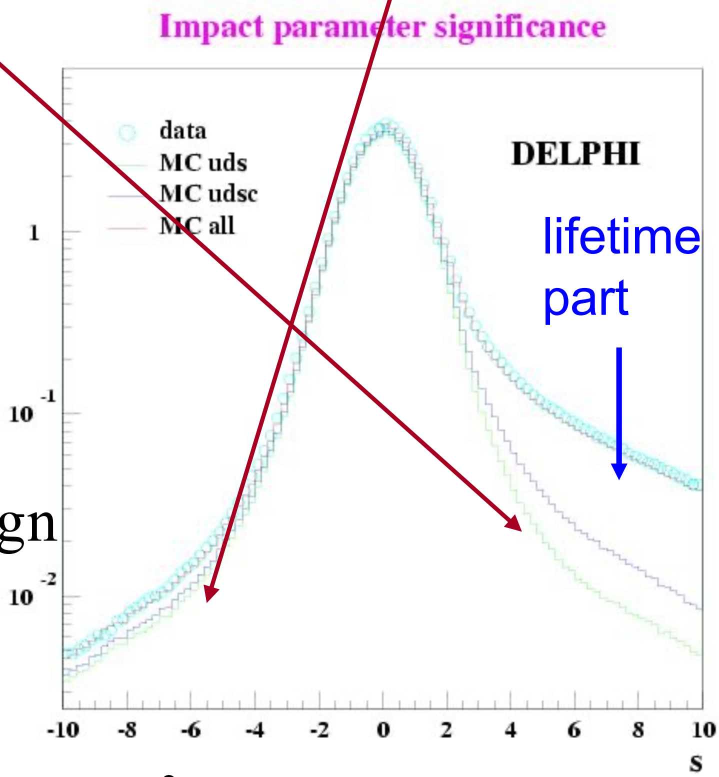

impact parameter resolution:

$$\sigma_\delta^2 = \sigma_{\text{extrapol}}^2 + \sigma_{\text{mult scatt}}^2 + \sigma_{\text{prim vertex}}^2$$

primary vertex contr. depends on beam size: mostly small

$$\sigma_{\text{extrapol}} = \sigma_s \sqrt{r_1^2 + r_2^2} \,/\, d$$

primary vertex

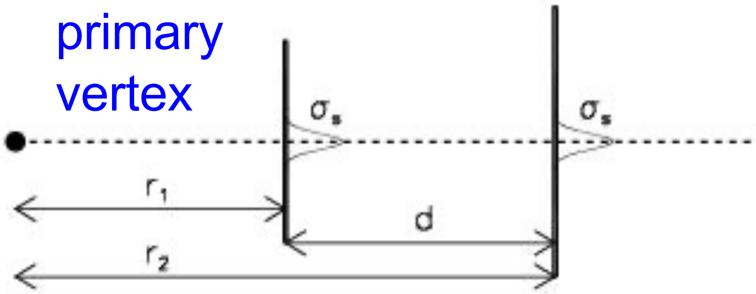

extrapolation error to primary vertex optimised by having
1. first measurement as close as possible,
2. lever arm d large
3. spatial resolution σ_s as good as possible

$$\sigma_{\text{mult scatt}} = \frac{\alpha_{\text{mult scatt}}}{p \sin^{3/2}\theta}, \quad \text{where} \quad \alpha_{\text{mult scatt}} \propto \sqrt{\Sigma^{\text{all traversed}}_{\text{material}} (x / X_0)}$$

(multiple scattering $\propto 1 / p_T = 1 / p \sin\theta$ & $\sqrt{x}$ length of traversed material; for a barrel geometry $\propto \sqrt{x} / \sin\theta$)

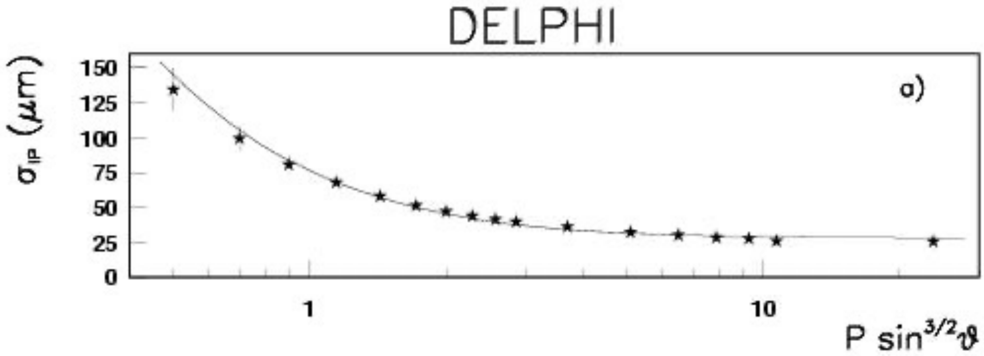

b) Decay length $= c\beta\gamma\tau$ as distance between primary and a separately reconstructed "secondary vertex"

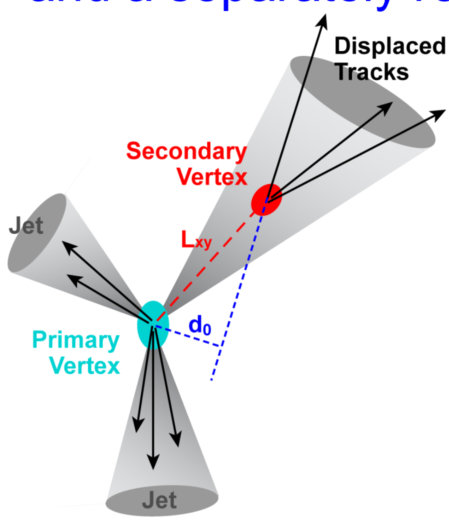

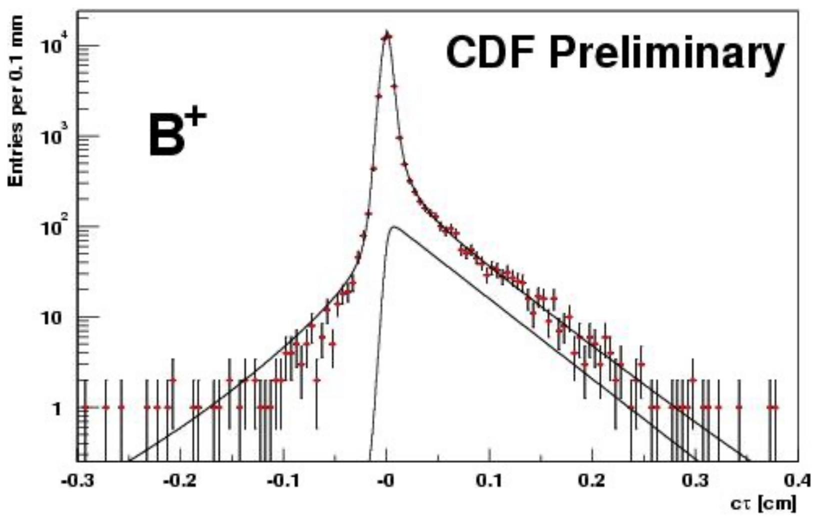

- **ATLAS** Strips: 61 m^2 of silicon, 4088 modules, $6x10^6$ channels Pixels: 1744 modules, 80 x 10^6 channels 2014 new innnermost pixel layer: +12 x 10^6 channels
- **CMS** the world largest silicon tracker 200 m^2 of strip sensors (single sided) 11 x 10^6 readout channels ~1m^2 of pixel sensors, $60x10^6$ channels 2017 new pixel detector: 1856 modules, 124 x 10^6 channels
- **ALICE** Pixel sensors Drift detectors Double sided strip detectors

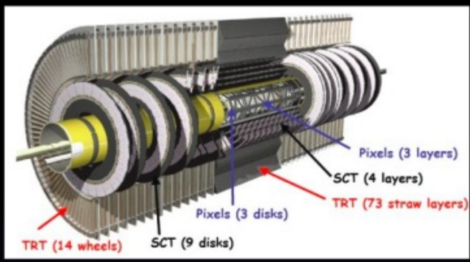

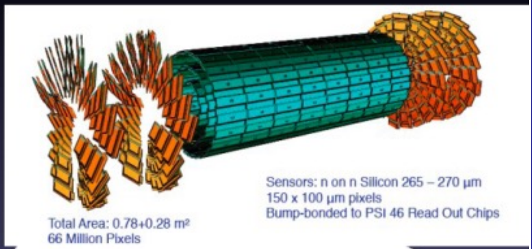

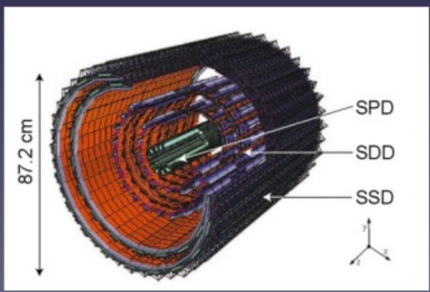

- **LHCb** VELO: Si Strips

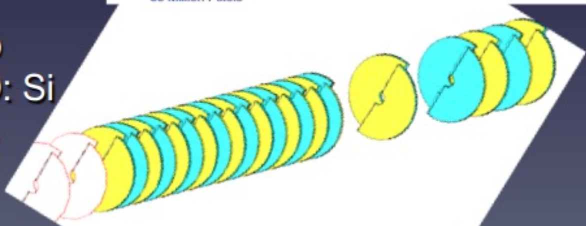

D. Bortoletto Lecture 4 7

Tracker material

- Reconstruction of photon conversions ($\gamma \rightarrow e^+e^-$) can provide precise map of the material
  - The number of photon conversion in a volume ≈ amount of material x reconstruction efficiency
  - The reconstructed vertices can be used to build detailed maps of the Tracker material

DATA

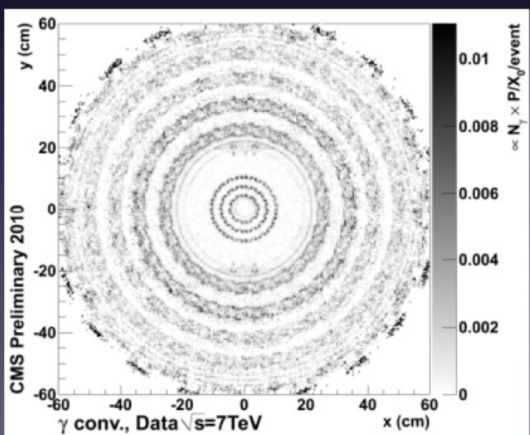

MC

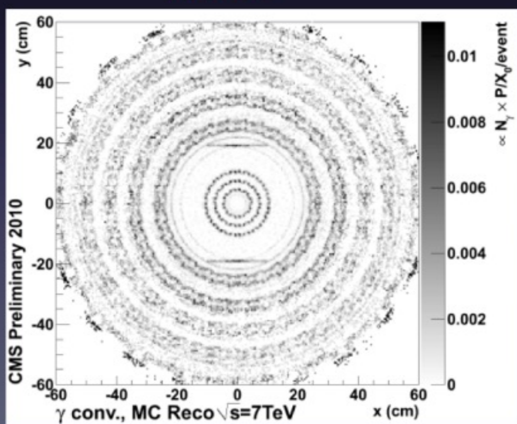

D. Bortoletto Lecture 4 33

Radiation damage in silicon sensors

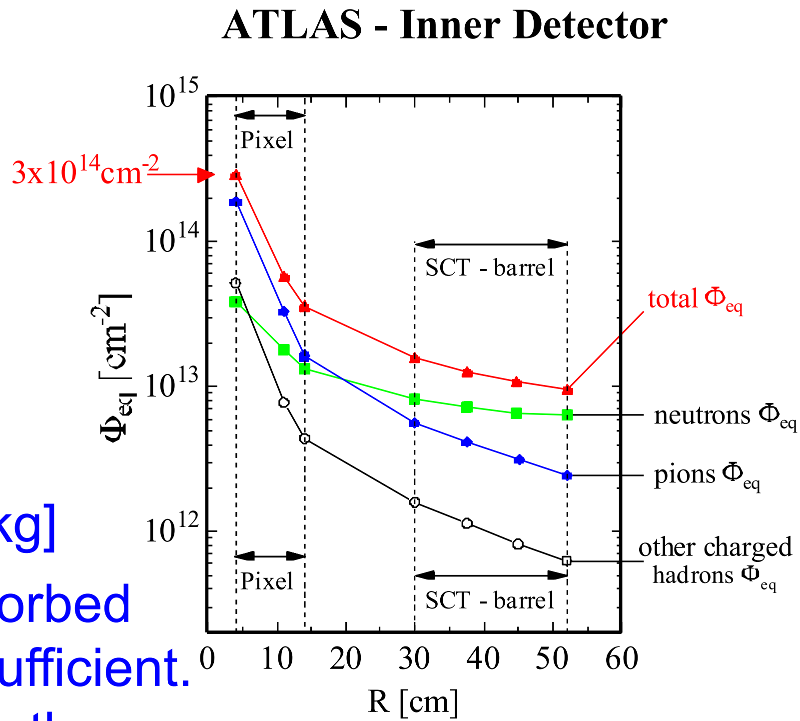

A major issue for LHC detectors !

Some definitions

- fluence:

Φ = dN/dA [cm^{-2}]

- dose:

D = dE/dm [Gy = J/kg]

Specification of absorbed dose / fluence not sufficient. Damage depends both on particle type (e,π,n,p,γ...) & energy ! Many effects & parameters involved (not all well understood)!

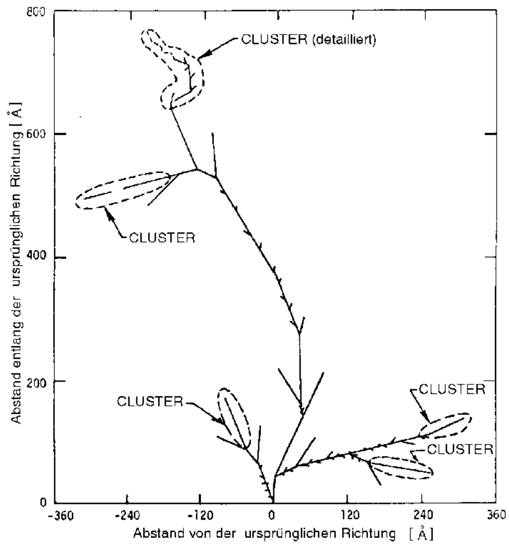

Damage caused mainly by non ionising energy loss

Bulk effects: Lattice damage, vacancies & interstitials.

Crystallographic defects:

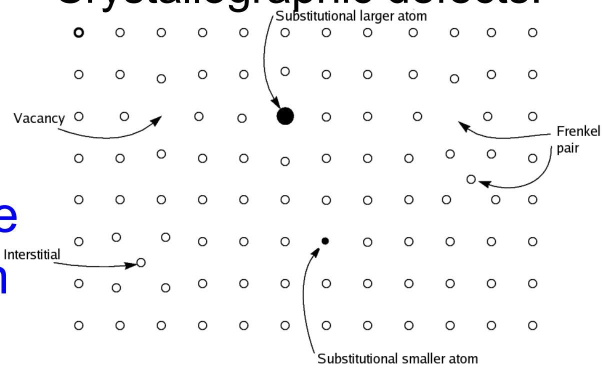

Surface effects: Charge build-up, increased surface leakage currents (controllable by careful fabrication & design e.g. multiple guard rings).

NIEL hypothesis (a good enough approximation!): damage ∝ energy deposition in collisions which displaces atoms

Relative damage (normalized to damage caused by 1 MeV neutrons)

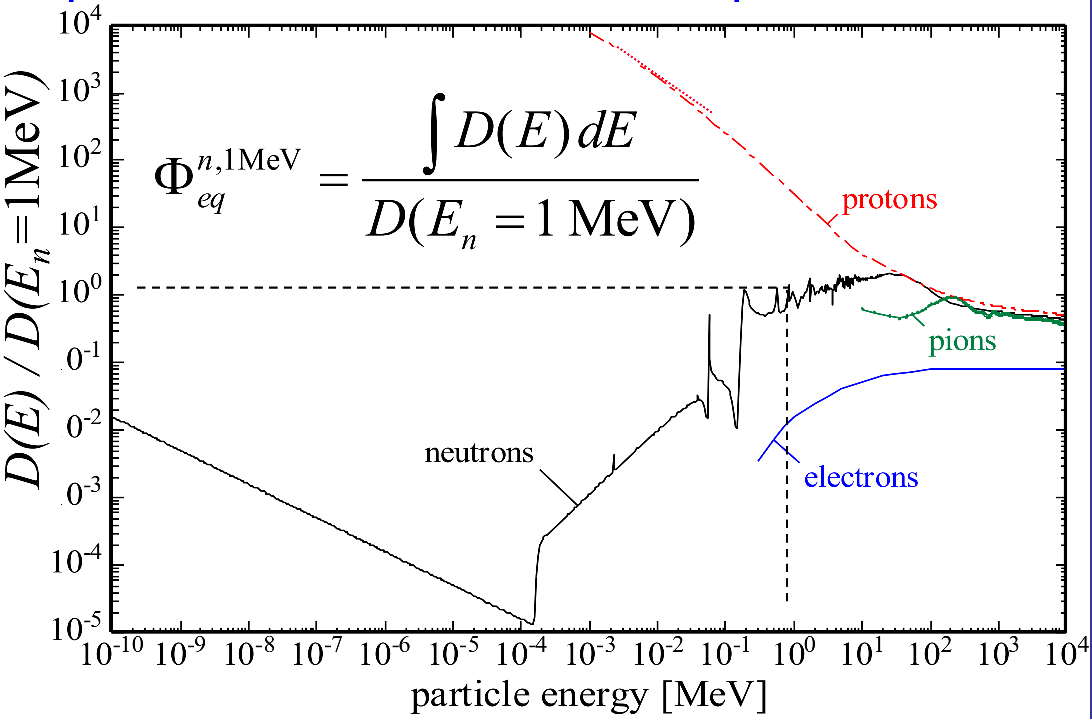

Main radiation induced macroscopic changes:

1. Sensor leakage current increase (∝ junction volume)

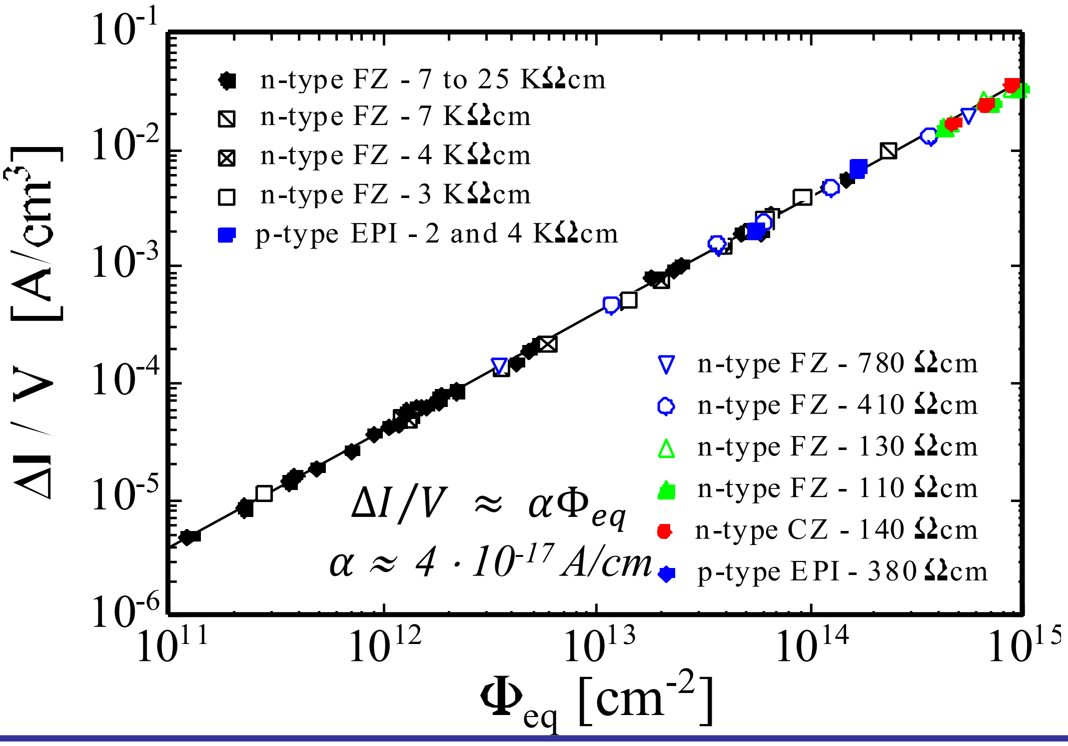

shows strong temperature dependence (without even considering radiation damage)

2. Depletion voltage change & type inversion. Tricky.

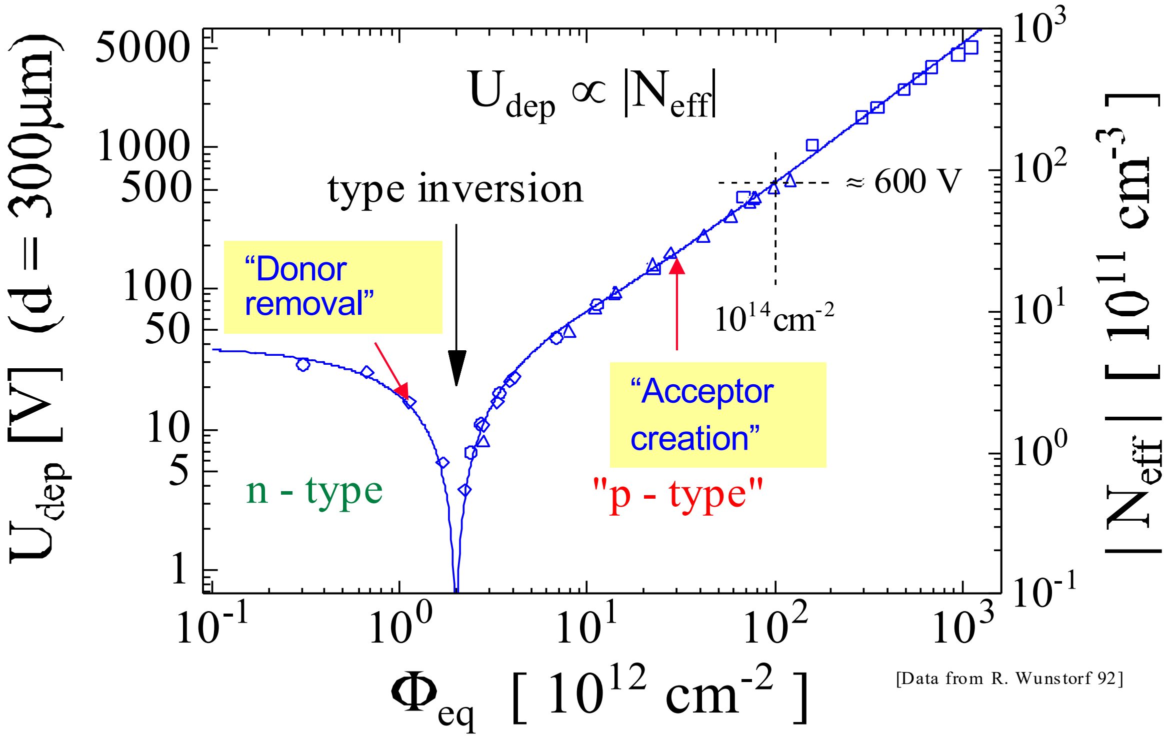

$$N_{eff} \approx N_0 e^{-\delta\Phi} - \beta\Phi$$

N_{eff}: space-charge concentration
$\delta \approx 6 \cdot 10^{-14}\ cm^2$ *(donor removal)*
$\beta \approx 0.03\ cm^{-1}$ *(acceptor creation)*

3. Charge collection efficiency decrease (& in case of underdepletion get larger charge spread → worse resolution)

Charge trapping in defects

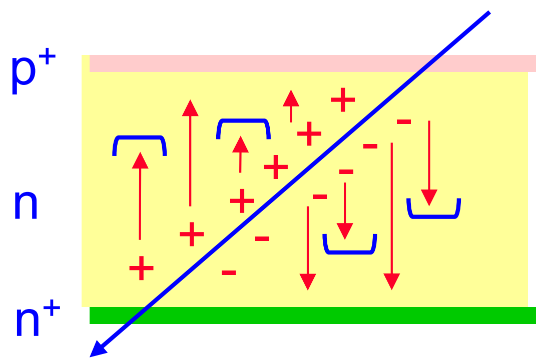

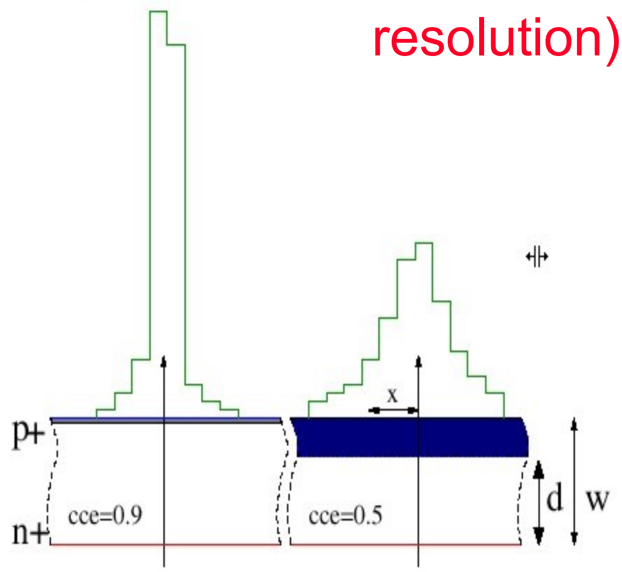

How to cope with the radiation damage ?
Possible strategies (utilized by LHC collaborations):

- Geometrical: build sensors such that they stand high depletion voltage (up to 1000 V)
- Environmental: sensors at low temperature (–20ºC).

→ Slower reverse annealing. Lower leakage current.

- Defect engineering. RD50 http://rd50.web.cern.ch/RD50/

Introduce specific impurities in silicon, to influence defect formation. Example Oxygen

Diffusion Float Zone Oxygenated (DOFZ) silicon generally used in LHC detectors. Gain a factor 3.

Development still going on with e.g. Czochralski silicon that naturally contain more oxygen.

- New detector concepts

3D detectors → "horizontal" biasing. Lower depletion voltage, faster charge collection & better radiation hardness

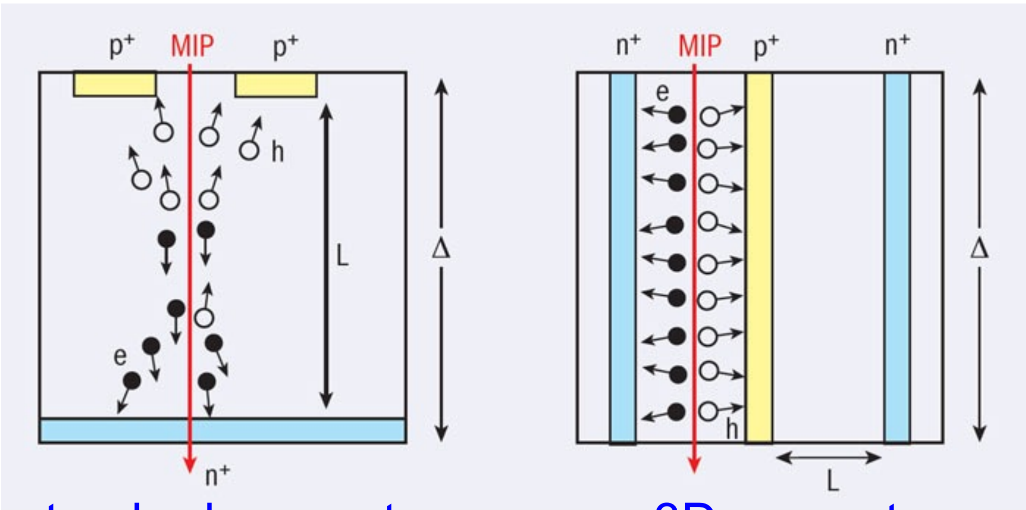

standard geometry 3D geometry

ATLAS & CMS use 3D detectors for their pixel detectors

More advanced methods (cont.)

RD42
http://cern.ch/rd42

- New materials

Diamond. Grown by Chemical Vapor Deposition. Bandgap large (~6 eV). No doping required! Naturally radiation hard

ATLAS & CMS use diamond detectors as luminosity monitors

comparable resolutions & S/N ratios with silicon… but become polarized @ large particle fluxes

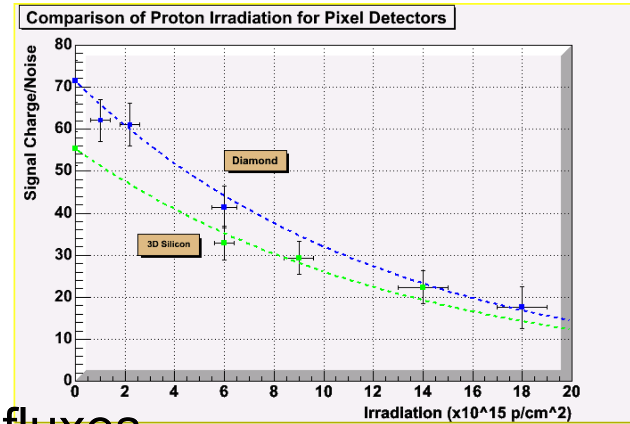

S/N-ratio vs irradiation for diamond & 3D pixel detector with same electronics

Latest development: use solid state detectors also for time-of-flight (TOF) ("4D-vertexing") due to their compactness, reliability & variable segmentation

Timing resolution proportional to capacitance (low capacitance → diamond) & inversely proportional to signal-to-noise ratio (high signal-to-noise ratio → low gain avalanche silicon detectors, LGADs)

LGAD (gain ~ 5–20) achieved by adding extra highly doped layer